UNIVERSITÀ DEGLI STUDI DI FOGGIA

Dipartimento di Medicina Clinica e Sperimentale

PhD Course

"Experimental and Regenerative Medicine"

XXXI Cycle

PhD Thesis

Title

"KEAP1/NRF2 PATHWAY PROFILING: UNCOVERS MOLECULAR INTERSECTION WITH NOTCH PATHWAY IN SMALL CELL LUNG CANCER"

Tutor

Prof. Fazio Vito Michele

PhD Student

Dott. Fabrizio Federico Pio

Supervisor

Dott.ssa Muscarella Lucia Anna

A. A. 2017-2018

INDEX

“Il mondo è nelle mani di coloro

che hanno il coraggio di sognare

e di correre il rischio di vivere i propri sogni”

(Paulo Coelho)

CHAPTER I

1. ETIOPATHOLOGY OF LUNG CANCER

1.1 INCIDENCE AND EPIDEMIOLOGY

Lung cancer represents the leading cause of cancer incidence and mortality, with about two million of new lung cancer cases and 1.8 million of predicted deaths within the current year with a 5-year survival rate of less than 18% [1]. Approximately one-half of the cases and over one-half of the cancer deaths in the world will be estimated in Asia by the end of this year, in contrast to Europe that accounts for 23.4% of the total cancer cases and 20.3% of all cancer deaths (**Figure 1**). By sex, lung cancer is the most commonly diagnosed cancer and the leading cause of cancer death in males, followed by prostate and colorectal cancer for incidence, and liver and stomach cancer when we talk about mortality **(Figure 2)**, [2].

Since the differential trends by sex and rates between men and women involve several European countries (**Figure 3**), it is postulated that this difference comes from sex-specific distribution of histologic subtypes as well as smoking prevalence [3].

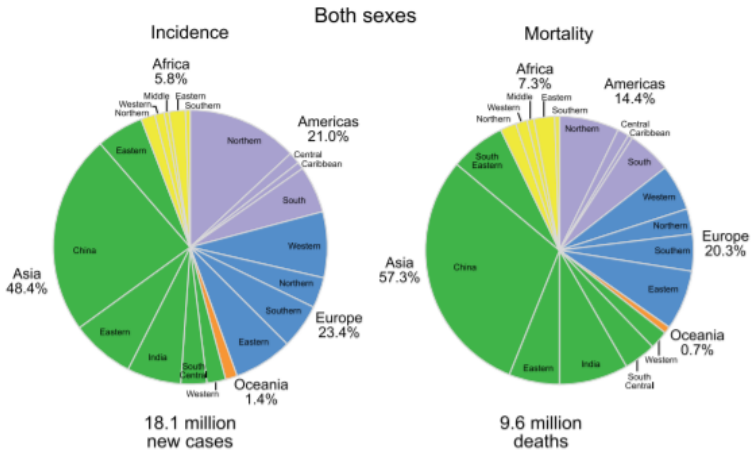

Figure 1. Pie charts based on the distribution of cases and deaths by globe area in 2018 for both sexes. For each sex, the area of the pie chart reflects the proportion of the total number of cases or deaths [4].

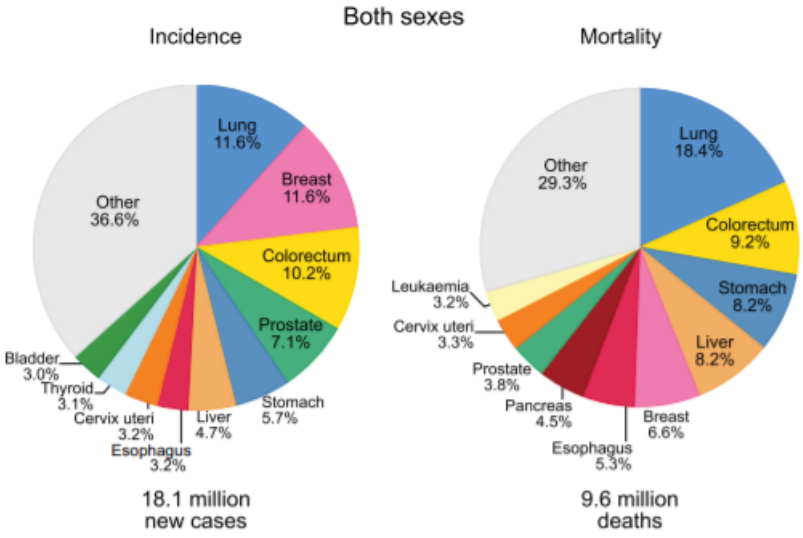

Figure 2. Pie charts show the distribution of cases and deaths for the 10 most common cancers in 2018 for both sexes. For each sex, the area of the pie chart reflects the proportion of the total number of cases or deaths [4].

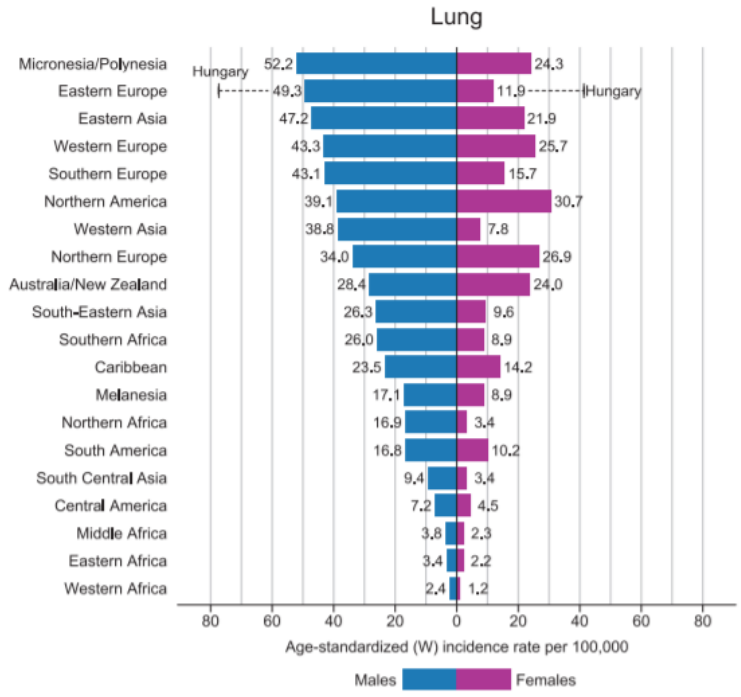

Figure 3. Bar chart of region-specific incidence age-standardized rates by sex for cancers of the lung in 2018. Rates are shown in descending order of the world (W) age-standardized rate between men and females [4].

1.2 ETIOLOGY AND PATHOGENESIS OF LUNG CANCER

The regional variations in common cancer types are linked to societal, economic, environmental and lifestyle changes which lead to differentially impact on the profile of this most complex group of diseases, including lung cancer [5].

Many of factors may increase the risk of lung cancer onset. Some of these are well-known and highly related to significant risk as environmental factors, mainly cigarette smoking and second-hand smoke exposure.

The incidence and contribution of cigarette smoking play an important role in lung carcinogenesis [6]. As the smoke moves more deeply into the respiratory tract, many hundreds of chemical components and particles are deposited on the airway and alveolar surfaces. The balance between metabolic activation and detoxification of potential carcinogens in people who smoke is linked to cancer susceptibility. The potency of carcinogens comes from covalent DNA binding that induces the production of "DNA adducts" in which the carcinogen metabolite is bound to one of the DNA bases or phosphate group and finally chemically modified [7]. If the DNA adducts persist unrepaired, they can cause miscoding during DNA replication with incorrect nucleotide incorporation as a result of permanent mutation. If these mutations in DNA sequence affect critical regions of oncogenes or tumor suppressor genes (i.e. TP53; G:C > T:A mutations are probably caused by benzo[a]pyrene), the alteration of the normal growth control mechanisms and uncontrolled proliferation may occur in tumor cells. Approximately 20 potential carcinogens of 3,500 chemical substances have been revealed in a burning cigarette which may indirectly promote pulmonary neoplastic transformation by oxidative damage or play a key role in single-strand DNA breaks induced by the release of free radicals (**Figure 4**), [8]. Therefore, the second-hand smoke should be not underestimated. In fact, passive smoking is a mixture of side stream smoke that derives from the end of a lighted source, leading to an estimated 50,000 deaths in adult non-smokers [9].

However, other factors that could contribute to the lung cancer which must not be neglected i.e. unhealthy diet, occupational carcinogens, viral infection, genetic predisposition and family history.

Unlike the dietary factors contribute to the onset of approximately 30% of all cancers. Consumption of vegetables, such as broccoli and cabbage, which are rich in

isothiocyanates, give some protective effects versus lung cancer promotion. In contrast dietary items, including red meat, dairy products, saturated fats, and lipids, have been linked to an increased risk of developing lung cancer [10].

It has been estimated that about 25% of cancers are related to viral infections. This is quite plausible since it is well established and ascertained the association between infection, inflammation and cancer risk. In a study conducted on Asian population in 2001, the association between lung cancer and concomitant Human papillomavirus (HPV) 16 and 18 types, especially in the subject non-smokers and older than 60 years was reported [11]. Several studies also have demonstrated that infection with Mycobacterium tuberculosis is commonly associated with a higher risk of lung cancer (RR = 1.74 [95% CI = 1:48 to 2:03]), independently of smoking habits [12].

Although the causes of lung cancer are almost exclusively environmental, it is likely that there is consistent individual variation in the lung cancer susceptibility due to occupational factors such as the exposition to asbestos and silica fibers, radon and its decay products, ionizing radiation, and air pollution are clearly correlated to lung cancer [13]. For example, the alpha-particles of radon, emitted by decay products, induce DNA damage in respiratory epithelial cells and can lead to the inactivation of p16 tumor suppressor gene via methylation processes [14]. As opposed to radon, asbestos is a well-known carcinogen that enhances the risk of lung cancer in people exposed to airborne fibers, especially in smokers in a dose-dependent manner. The relative risk for lung cancer with asbestos exposure alone is 5-fold, with cigarette smoking alone 10-fold, but considering both asbestos and cigarette smoke, a higher level will have occurred to 29-fold [15].

Last but not least, the genetic predisposition in occasional familiar clustering is considered the most important variable risk in lung cancer development. To date, the genes ascribable to lung susceptibility remain elusive. An inherited genetic susceptibility has an important role in predisposition to lung cancer is now a well-established fact, especially in the modulation of biological processes regarding the bioactivation or degradation of carcinogens or response to DNA repair and cell-cycle control [16]. Genetic polymorphisms as risk factors in the onset of lung cancer have been described in genes codifying for the enzymes involved in xenobiotic

metabolism in phase I and II. The link is mainly due to the correlation between the exposure to carcinogens (especially tobacco smoke) and the development of this tumor. The major classes of carcinogens in tobacco and tobacco smoke are converted into DNA-reactive metabolites by cytochrome P450 (CVP)-related enzymes such as CYP1A1 (Cytochrome P450 Family 1 Subfamily A Member 1) and GSTM1 (Glutathione S-transferase mu1), that contribute to metabolic activation and play a central role in elimination of electrophilic species, respectively [17]. Many genes and gene families affect the activation and detoxification of PAHs (polycyclic aromatic hydrocarbons). Germline mutations in TP53 inherited in a recessive manner is likely to increase the risk of lung cancer. The induction of CYP1A1 is promoted by the specific binding of aromatic inducer compounds to the aromatic hydrocarbon (Ah) receptor. An Ah receptor nuclear translocator (ARNT) gene is also involved in the CYP1A1 induction pathway [18]. Therefore, individuals lacking the GSTM1 activity (Glutathione S-transferase mu1) seems to have a slightly increased risk of lung cancer occurrence [19].

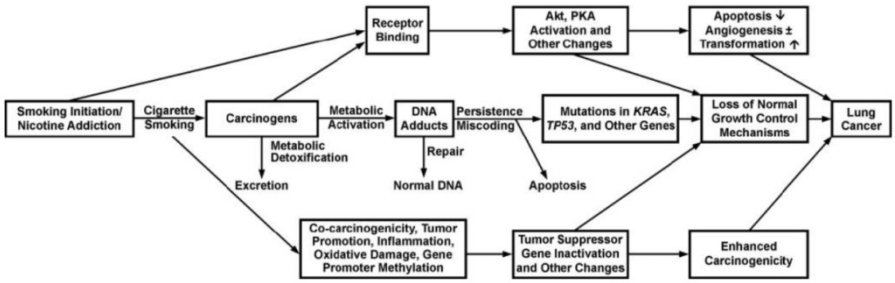

Figure 4. Mechanistic framework for understanding how cigarette smoking causes dynamically genetic and epigenetic events of lung cancer development [20].

1.3 HISTOLOGICAL CLASSIFICATION OF LUNG CANCER

The World Health Organization (WHO) provides to a complete histopathological classification of lung tumors (**Table 1**), [21]. More than 95% of lung cancers are classified as four main histological types: squamous cell carcinoma (SqCC), adenocarcinoma (ADC), large cell carcinoma (LCC) and small cell carcinoma (SCLC). The histological definition is performed through a careful evaluation of the

conventional morphological criteria of hematoxylin-eosin staining. Immunohistochemistry (IHC) technique is fundamental in the definition of NSCLC when the tumor is presented poorly differentiated or not otherwise specified (NOS).

The ADC histological type shows a typical positivity for TTF-1 (Thyroid Transcription Factor-1) expression, cytokeratin 7 and napsin. The SqCC expresses p63, p40, high molecular weight cytokeratin (eg. CK5/6) and desmocollin-3, whereas chromogranin, synaptophysin, CD56 are the current best markers for neuroendocrine tumors [22]. In the differential diagnosis between ADC and SqCC the use of TTF-1 and p40 it is currently the best approach, also in view of preserving the neoplastic tissue for molecular studies [*AIOM, linee guida neoplasie del polmone, 2018*].

Table 1. The 2015 World Health Organization (WHO) classification of Tumors of the Lung distinguished for Histologic Type and Subtypes [21].

Malignant epithelial tumours	
Squamous cell carcinoma	8070/3
Papillary	8052/3
Clear cell	8084/3
Small cell	8073/3
Basaloid	8083/3
Small cell carcinoma	8041/3
Combined small cell carcinoma	8045/3
Adenocarcinoma	8140/3
Adenocarcinoma, mixed subtype	8255/3
Acinar adenocarcinoma	8550/3
Papillary adenocarcinoma	8260/3
Bronchioloalveolar carcinoma	8250/3
Nonmucinous	8252/3
Mucinous	8253/3
Mixed nonmucinous and mucinous or indeterminate	8254/3
Solid adenocarcinoma with mucin production	8230/3
Fetal adenocarcinoma	8333/3
Mucinous ("colloid") carcinoma	8480/3
Mucinous cystadenocarcinoma	8470/3
Signet ring adenocarcinoma	8490/3
Clear cell adenocarcinoma	8310/3
Large cell carcinoma	8012/3
Large cell neuroendocrine carcinoma	8013/3
Combined large cell neuroendocrine carcinoma	8013/3
Basaloid carcinoma	8123/3
Lymphoepithelioma-like carcinoma	8082/3
Clear cell carcinoma	8310/3
Large cell carcinoma with rhabdoid phenotype	8014/3
Adenosquamous carcinoma	8560/3
Sarcomatoid carcinoma	8033/3
Pleomorphic carcinoma	8022/3
Spindle cell carcinoma	8032/3
Giant cell carcinoma	8031/3
Carcinosarcoma	8980/3
Pulmonary blastoma	8972/3
Carcinoid tumour	8240/3
Typical carcinoid	8240/3
Atypical carcinoid	8249/3
Salivary gland tumours	
Mucoepidermoid carcinoma	8430/3
Adenoid cystic carcinoma	8200/3
Epithelial-myoepithelial carcinoma	8562/3
Preinvasive lesions	
Squamous carcinoma *in situ*	8070/2
Atypical adenomatous hyperplasia	
Diffuse idiopathic pulmonary neuroendocrine cell hyperplasia	
Mesenchymal tumours	
Epithelioid haemangioendothelioma	9133/1
Angiosarcoma	9120/3
Pleuropulmonary blastoma	8973/3
Chondroma	9220/0
Congenial peribronchial myofibroblastic tumour	8827/1
Diffuse pulmonary lymphangiomatosis	
Inflammatory myofibroblastic tumour	8825/1
Lymphangioleiomyomatosis	9174/1
Synovial sarcoma	9040/3
Monophasic	9041/3
Biphasic	9043/3
Pulmonary artery sarcoma	8800/3
Pulmonary vein sarcoma	8800/3
Benign epithelial tumours	
Papillomas	
Squamous cell papilloma	8052/0
Exophytic	8052/0
Inverted	8053/0
Glandular papilloma	8260/0
Mixed squamous cell and glandular papilloma	8560/0
Adenomas	
Alveolar adenoma	8251/0
Papillary adenoma	8260/0
Adenomas of the salivary gland type	
Mucous gland adenoma	8140/0
Pleomorphic adenoma	8940/0
Others	
Mucinous cystadenoma	8470/0
Lymphoproliferative tumours	
Marginal zone B-cell lymphoma of the MALT type	9699/3
Diffuse large B-cell lymphoma	9680/3
Lymphomatoid granulomatosis	9766/1
Langerhans cell histiocytosis	9751/1
Miscellaneous tumours	
Harmatoma	
Sclerosing hemangioma	8832/0
Clear cell tumour	8005/0
Germ cell tumours	
Teratoma, mature	9080/0
Immature	9080/3
Other germ cell tumours	
Intrapulmonary thymoma	8580/1
Melanoma	8720/3
Metastatic tumours	

1.3.1 ADENOCARCINOMA AND SQUAMOUS CELL CARCINOMA OF THE LUNG

ADC has a predominantly peripheral tumor development, with frequent pleural involvement and neoplastic effusion. In this histological type, a loco-regional lymph node spread is frequently observed, in addition to intra-parenchymal blood and airborne spread as well as the occurrence of early distant metastases. By cytology analysis, adenocarcinoma cells may be single or arranged in three-dimensional morulae, acini, pseudopapillae, true papillae with fibrovascular cores and/or sheets of cells. About the mixed histological variants, the pathological diagnosis of ADC is made by plotting the percentages of each component. Cytoplasm volume undergoes a series of changes but is usually relatively abundant. It is typically cyanophilic and more translucent in comparison with squamous cell carcinoma. Nuclei are usually single, eccentric and round to oval with relatively smooth contours and minimal nuclear irregularity [23].

SqCC affects predominantly the hilum of the lung and is based on different variants that may be classified into four subtypes: papillary, clear cell, small cell, basaloid. Squamous cell carcinoma can be divided into subtypes: keratinizing squamous cell carcinoma, non-keratinizing squamous cell carcinoma, and basaloid squamous cell carcinoma. The main morphological features of squamous differentiation can be attributed to intercellular bridges, keratinization and squamous cell pearlescent formations. In well-differentiated tumors, these peculiarities are immediately evident, while in poorly differentiated are complex to identify. In a background of necrosis and cellular debris, large tumor cells display central, irregular hyperchromatic nuclei exhibiting one or more small nucleoli with abundant cytoplasm. Tumor cells are usually isolated and can show bizarre shapes [24].

1.3.2 NEUROENDOCRINE TUMORS OF THE LUNG (NET)

Neuroendocrine tumors (NETs) is a heterogeneous group of malignancies arising from neuroendocrine cells of the lung. Lung NETs can be distinguished into four subtypes: well-differentiated, low-grade typical carcinoids (TCs), (2% of

primary lung neoplasms); well-differentiated, intermediate-grade atypical carcinoids (ACs), (<1%); poorly differentiated, high-grade large cell neuroendocrine carcinoma (LCNECs), (3%); and poorly differentiated, high-grade SCLCs (20%), (**Figure 5**). Recent data from WHO classification of lung tumors introduced new diagnostic criteria for lung NETs on the basis of histopathologic features, including cell size, cell morphologic features, mitotic index, architectural growth patterns, and presence of necrosis. Ki67/MIB-1 marker is required to distinguish the small biopsies and cytological specimens (carcinoid tumors and high-grade neuroendocrine carcinomas) by differential diagnosis [25]. With regard to lung NETs grading, the therapy is very helpful to define as the distinction between grade 1 (TCs), grade 2 (ACs), and grade 3 (SCLCs and LCNECs). Patients with grade 1 or 2 tumors are generally treated with somatostatin analogs (SSAs), whereas patients with grade 3 tumors are treated with chemotherapy. Both TCs and ACs are able to affect regional lymph node or distant metastasis with ACs being more aggressive than TCs. ACs have higher rates of lymph node involvement at diagnosis (36%) and distant metastases (26%) than TCs (9% and 4%, respectively). Furthermore, a poorer 5 and 10-year survival rates are associated with ACs rather than TCs [26].

LCNEC is a high-grade non-small cell neuroendocrine carcinoma that follows the morphologic criteria: organoid, trabecular or rosette-like growth patterns; large size, polygonal shape, low nuclear/cytoplasmatic (N/C) ratio, coarse or vesicular nuclear chromatin and frequent nucleoli; high mitotic rate with a mean of 60 mitoses per 2 mm^2; frequent necrosis and at least one positive neuroendocrine immunohistochemical marker or neuroendocrine granules studied by electron microscopy. Patients affected by LCNEC are generally heavy smokers with a poor prognosis and a survival rate at 5 years and 10 years of 27% and 11%, respectively. The large cell carcinoma is usually diagnosed by exclusion when under the optical microscope should be kept out from the presence of adenocarcinoma or squamous cell carcinoma. LCNEC consists of a heterogeneous group of poorly differentiated tumors that sometimes show the morphological, immunohistochemical and molecular features of adenocarcinomas (TTF1-positive and *KRAS*-mutated), other cases of squamous (p63-positive), other times they appear totally undifferentiated [27].

Carcinoid tumors account for 1 to 2% of all invasive lung malignancies. Carcinoids are more common in 55-year-old patients, of which 40% are defined non-smokers. Central carcinoids often demonstrate radiological evidence of an endo-bronchial obstructive component. Unlike, they are more often of the spindle-cell type when peripheral carcinoids occur. Both TC and AC are characterized histologically by endocrine, organoid growth pattern and uniform cytologic features, consisting of a nucleus with fine, granular chromatin and moderate eosinophilic, finely granular cytoplasm. A histological distinction between typical and atypical carcinoid is based on the mitotic count and the presence or absence of necrosis. Typical carcinoids show less than 2 mitoses per 2 mm^2 areas of viable tumor (10 high power field) and without positivity to necrosis. The presence of mitosis between 2 to 10 per 2 mm^2 or the presence of necrosis defines the diagnosis of atypical carcinoids. Initial treatment for carcinoid tumors remains surgical resection, if possible. Patients with typical carcinoid (TC) have a good prognosis and rarely die from their tumors. Compared with TC, AC shows a larger tumor size, a higher rate of metastases and significantly short-term survival. Both typical and atypical carcinoid tumors are histologically lower-grade tumors than SCLC and LCNEC and their tumor mitotic rates are the reflection of the proliferation rates [28]. Mitotic rates are high in SCLC and LCNEC, where necrosis tends to be very extensive. The markers used for the identification of carcinoids are those used for all neuroendocrine tumors, such as chromogranin, synaptophysin, and CD56. In small biopsies, Ki-67 staining can be useful to distinguish TC or AC from high-grade LCNEC or SCLC, and show high proliferation rates. The value of Ki-67 is very low in the typical carcinoid (less than or equal to 5%) and between 5 and 20% in atypical carcinoid [26, 29].

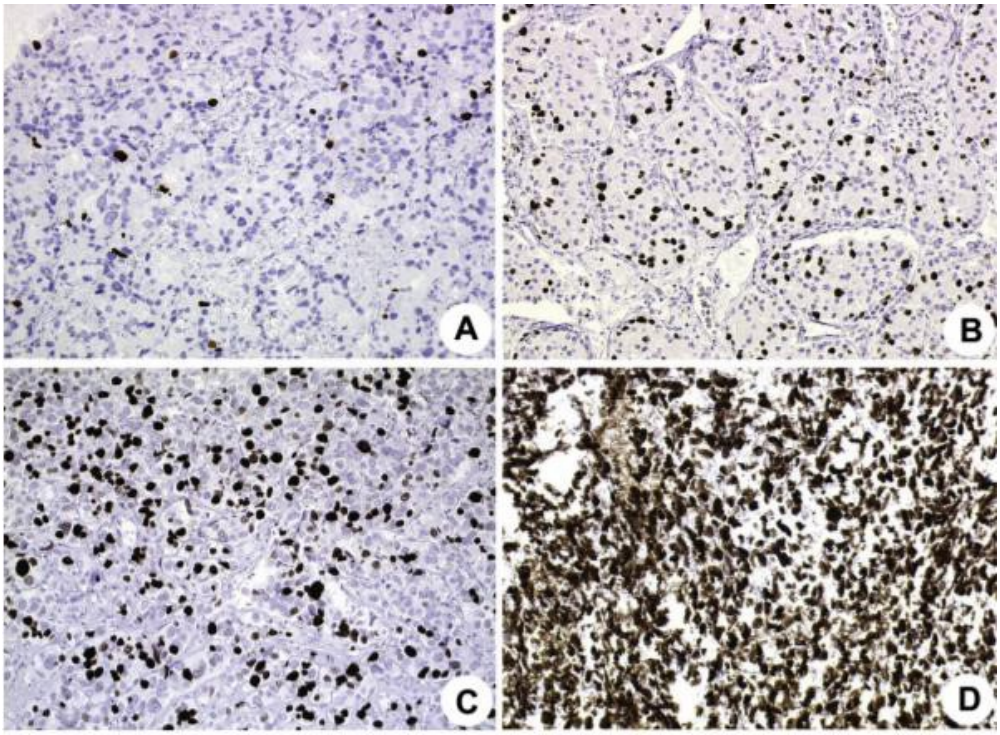

Figure 5. Ki-67 labeling index distribution in the four subtypes of lung neuroendocrine tumors: typical carcinoid **(A)**, atypical carcinoid **(B)**, large cell neuroendocrine carcinoma **(C)**, and SCLC **(D)**, [26, 29].

1.3.3 SMALL CELL LUNG CANCER (SCLC)

Small Cell Lung Cancer (SCLC) includes approximately 20% of all lung cancer which is diagnosed annually and up to a maximum of 25% of lung cancer deaths/year. The etiology of SCLC is heavily related to tobacco use since about 98% of patients with SCLC have a smoking history. Most SCLCs have a central localization and a loco-regional spread, although the metastatic lesions of SCLC cells are spreading up to bone marrow and liver [30]. Histologically, SCLC is defined as malignant epithelial tumor consisting of small cells with scant cytoplasm, ill-defined cell borders, finely granular nuclear chromatin, and absent or inconspicuous nucleoli (**Figure 6**). It was called “oat cell carcinoma” for the round, oval and spindle-shaped cells. High mitotic count and extensive necrosis are features of this type of tumor. Diagnosis is necessary by the use of bronchoscopy and cytology but often the

primary tumor is not detectable on radiographic methods. The diagnosis can be carried out through H&E-stained sections without using immunostaining in the majority of cases. The combined SCLC histology was found in 4-6% of cases as a mixture between SCLC and large cell carcinoma, 1-3% of the cases as SCLC mixed with adenocarcinoma or squamous cell carcinoma, while in other cases it may be associated with giant cell carcinoma and sarcomatoid carcinoma [21, 31].

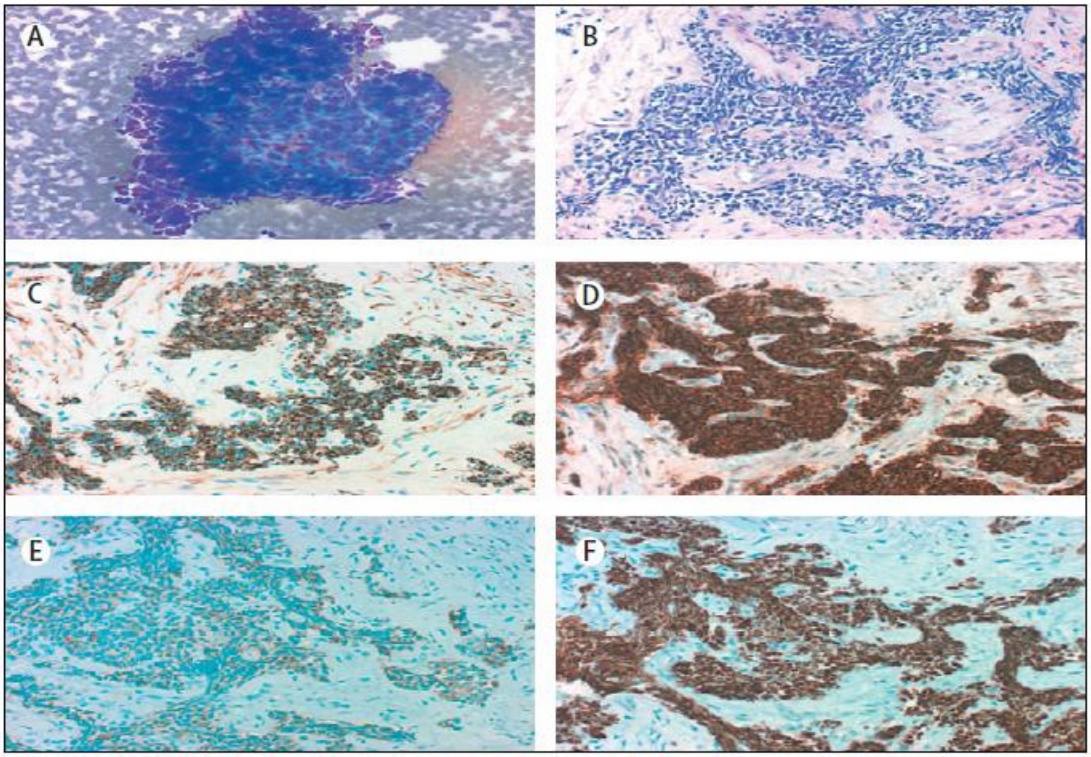

Figure 6. Microscopic features of SCLC. **(A)** In typical SCLC, cells are small (generally less than the size of three small resting lymphocytes) with scant cytoplasm, nuclear molding, and finely granular nuclei with inconspicuous nucleoli. **(B)** Cells can be round, oval, or spindle-shaped and cell borders are rarely seen. Architectural patterns include nesting, trabeculae, peripheral palisading, and rosette formation, as seen in other neuroendocrine-tumor cells. Immunohistochemistry shows strongly positive results for **(C)** CK-7, the neuroendocrine markers **(D)** CD56 and **(E)** synaptophysin, and **(F)** TTF-1 along plasma membranes and in the nuclei [32].

1.4 LUNG CANCER STAGING

Lung cancers are classified according to four stages of the TNM System based on increasing severity, indicated by the sequence from 1 to 4 numbers. The TNM System is the international classification of the tumor evolution (staging) that considers three main parameters: the size of the primary tumor (T), the involvement of regional lymph nodes adjacent to the tumor (N) and the presence of distant metastasis (M). Each of these categories is divided into subgroups, depending on the size of the progressively growing tumor, the number of lymph nodes, and the presence or absence of distant metastases (**Figure 7 and Table 2**). Regarding the lymph nodes, N0 has defined a condition where the regional lymph nodes are not affected, and by a growing marking N1 to N3, the progressive involvement of a greater number of lymph node stations. The presence of metastases is characterized by an indication M1, while M0 indicates their absence. Overall, cancer is considered the more advanced the more massive and extended beyond the body concerned. As well as for the formulation of prognosis, the staging of tumors is crucial to determine the most effective treatment strategy [33]. Stage I: tumor confined to the lung without lymph node involvement. Stage II: lung cancer with pulmonary hilum lymph node involvement. Stage III: • A) tumor with extension to the chest wall or ipsilateral mediastinal lymph node involvement; • B) tumor with extension to vessels and organs intrathoracic or with the involvement of contralateral mediastinal lymph nodes. Stage IV: lung cancer with distant metastases [34].

Table 2. T, N, and M symbols in the Eighth edition of Lung Cancer classification established by The Union for International Cancer Control/ American Joint Committee on Cancer/International Association for the Study of Lung Cancer (UICC/AJCC/IASLC), [34].

T (Primary Tumor)		**Label**
T0	No primary tumor	
Tis	Carcinoma in situ (Squamous or Adenocarcinoma)	Tis
T1	Tumor ≤3 cm,	
T1a(mi)	Minimally Invasive Adenocarcinoma	T1a*(mi)*
T1a	Superficial spreading tumor in central airways[a]	T1a *SS*
T1a	Tumor ≤1 cm	T1a *≤1*
T1b	Tumor >1 but ≤2 cm	T1b *>1-2*
T1c	Tumor >2 but ≤3 cm	T1c *>2-3*
T2	Tumor >3 but ≤5 cm or tumor involving:	
	visceral pleura[b],	T2 *Visc Pl*
	main bronchus (not carina), atelectasis to hilum[b]	T2 *Centr*
T2a	Tumor >3 but ≤4 cm	T2a *>3-4*
T2b	Tumor >4 but ≤5 cm	T2b *>4-5*
T3	Tumor >5 but ≤7 cm	T3 *>5--7*
	or invading chest wall, pericardium, phrenic nerve	T3 *Inv*
	or separate tumor nodule(s) in the same lobe	T3 *Satell*
T4	Tumor >7 cm	T4 *>7*
	or tumor invading: mediastinum, diaphragm, heart, great vessels, recurrent laryngeal nerve, carina, trachea, esophagus, spine;	T4 *Inv*
	or tumor nodule(s) in a different ipsilateral lobe	T4 *Ipsi Nod*
N (Regional Lymph Nodes)		
N0	No regional node metastasis	
N1	Metastasis in ipsilateral pulmonary or hilar nodes	
N2	Metastasis in ipsilateral mediastinal/subcarinal nodes	
N3	Metastasis in contralateral mediastinal/hilar, or supraclavicular nodes	
M (Distant Metastasis)		
M0	No distant metastasis	
M1a	Malignant pleural/pericardial effusion[c] or pleural /pericardial nodules	M1a *Pl Dissem*
	or separate tumor nodule(s) in a contralateral lobe;	M1a *Contr Nod*
M1b	Single extrathoracic metastasis	M1b *Single*
M1c	Multiple extrathoracic metastases (1 or >1 organ)	M1c *Multi*

TX, NX: T or N status not able to be assessed

[a] Superficial spreading tumor of any size but confined to the tracheal or bronchial wall
[b] such tumors are classified as T2a if >3≤4 cm, T2b if >4≤5 cm.
[c] Pleural effusions are excluded that are cytologically negative, non-bloody, transudative, and clinically judged not to be due to cancer.

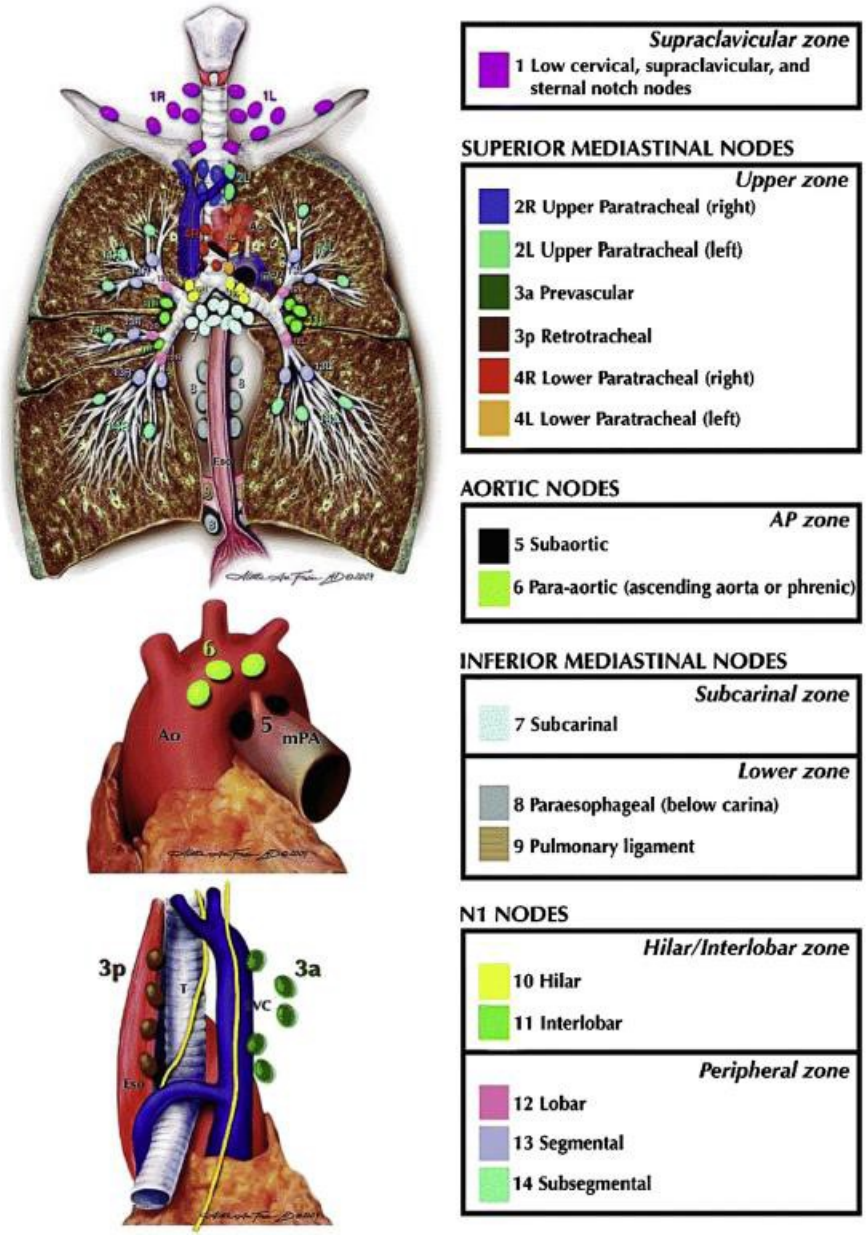

Figure 7. The International Association for the Study of Lung Cancer node map for lung cancer [35].

The classification underlying the Anatomic Stage/Prognostic Groups of SCLC consists of two stages as Limited-stage (LS) and Extensive-stage (ES) and reflects the highest importance in radiation therapy and allows to a better selection of patients for this kind of treatment (**Table 3**). This system defines limited stage (LS) as a condition which includes contralateral supraclavicular nodes, laryngeal nerve involvement and superior vena cava obstruction (Stage I-III; T any, N any, M0) and

excludes T3-T4 due to multiple lung nodules that are too extensive or have tumor/nodal volume that is too large to be encompassed in a tolerable radiation plan. Extensive stage (ES) includes a disease that cannot be classified as limited, such as malignant pleural or pericardial effusions and hematogenous metastases (Stage IV; T any, N any, M 1a/b), [36]. This recommendation is found on the conclusion that the primary tumor (T), node (N), metastasis (M) classification, in addition to the stage I through IV groupings, are suitable as a predictor for the overall survival in SCLC. Nevertheless, the prognostic discrimination for the TNM system is less impressive in SCLC than non-SCLC [33, 37].

Table 3. Anatomic Stage/Prognostic Groups for 8th edition of TNM for SCLC and Lung Neuroendocrine tumors (changes to the 7th edition are highlighted in bold and underlined), [33, 37].

Occult carcinoma	TX	N0	M0
Stage 0	Tis	N0	M0
Stage IA1	**T1(mi)**	**N0**	**M0**
	T1a	**N0**	**M0**
Stage IA2	**T1b**	**N0**	**M0**
Stage IA3	**T1c**	**N0**	**M0**
Stage IB	T2a	N0	M0
Stage IIA	T2b	N0	M0
Stage IIB	**T1a-c**	**N1**	**M0**
	T2a	**N1**	**M0**
	T2b	N1	M0
	T3	N0	M0
Stage IIIA	**T1a-c**	**N2**	**M0**
	T2a-b	N2	M0
	T3	N1	M0
	T4	N0	M0
	T4	N1	M0
Stage IIIB	**T1a-c**	**N3**	**M0**
	T2a-b	N3	M0
	T3	**N2**	**M0**
	T4	N2	M0
Stage IIIC	**T3**	**N3**	**M0**
	T4	**N3**	**M0**
Stage IVA	**Any T**	**Any N**	**M1a**
	Any T	**Any N**	**M1b**
Stage IVB	**Any T**	**Any N**	**M1c**

1.5 GENETIC AND EPIGENETIC ABNORMALITIES AND THERAPEUTIC TARGETS IN SCLC

SCLC is featured by genomic instability and very high mutation burden with regard to the potential effect of long-term treatment with carcinogens in tobacco smoke [38]. Genomic characterizations of SCLC have been considered very complex in relation to aggressive cancer behavior which is usually diagnosed at unresectable stages in small biopsies or cytology specimens. The typical molecular and cytogenetic alterations in SCLC show the common loss of function of tumor suppressor *TP53* (75-90%) and *RB1*, recurrent amplification of *MYC* family genes and deletions in chromosome 3p. About 6% of tumors carrying amplified *FGFR1* and *PTEN* inactivation [39,40]. The phosphatidylinositol-3-kinase(PI3K)/AKT/mTOR signaling pathway has been implicated in new frontiers of cancer drug development and has been shown constitutively activated in a significant percentage of SCLC cases as a consequence of alterations, such as deletions of *PTEN*, *PIK3CA* mutations, or mTOR overexpression. In surgically resected SCLCs, genetic alterations in the PI3K/AKT/mTOR pathway were found at the prevalence of 36%. The individual changes in this pathway are mutually exclusive, suggesting the key driving role of each of the genes [41]. Up-regulation of anti-apoptotic signaling pathways may also occur in SCLC. Specifically, the anti-apoptotic protein BCL-2 results in an overexpression of SCLC cell lines and represses the pro-apoptotic multi-domains of BAX and BAK proteins [42]. Instead, inactivating mutations in *NOTCH* genes have been discovered by whole-genome sequencing in a range of 25% SCLC tumors, suggesting that these alterations may represent a major feature of SCLC (**Figure 8**), [43, 44]. In high-grade neuroendocrine tumors, including SCLC, related ligand delta-like 3 (DLL3), one of NOTCH ligands, is highly up-regulated and aberrantly expressed on the cell surface, making it a potential therapeutic target probably associated with the neuroendocrine phenotype tumorigenesis [45].

Aberrations in epigenetic regulators have been also found to be a major hallmark of SCLC. Recurrent mutations in genes encoding histone modifiers such as the histone acetyltransferases (HATs) CREBBP and EP300 and the histone methyltransferases MLL, MLL2 and EZH2 are recently reported in SCLC [40]. In this epigenetic key, loss of *RB1* has been also associated with overexpression of

enhancer of zeste 2 (EZH2), a histone methyltransferase which participates in histone methylation and promotes the transcriptional repression by silencing of this tumor suppressor gene. SCLCs showed significant increases in the levels of EZH2, thymidylate synthase, apoptosis mediators, and DNA repair proteins, including the PARP1, a DNA repair protein and E2F1 co-activator that has been highly expressed at the mRNA and protein levels [46]. Lastly, RNA-sequencing data have identified multiple fusion transcripts in primary SCLC specimens, including a recurrent *RLF–MYCL1* fusion [47]. The aim is to understand how individual genomic alterations occur, improve the prognosis and therapeutic target development in SCLC patients.

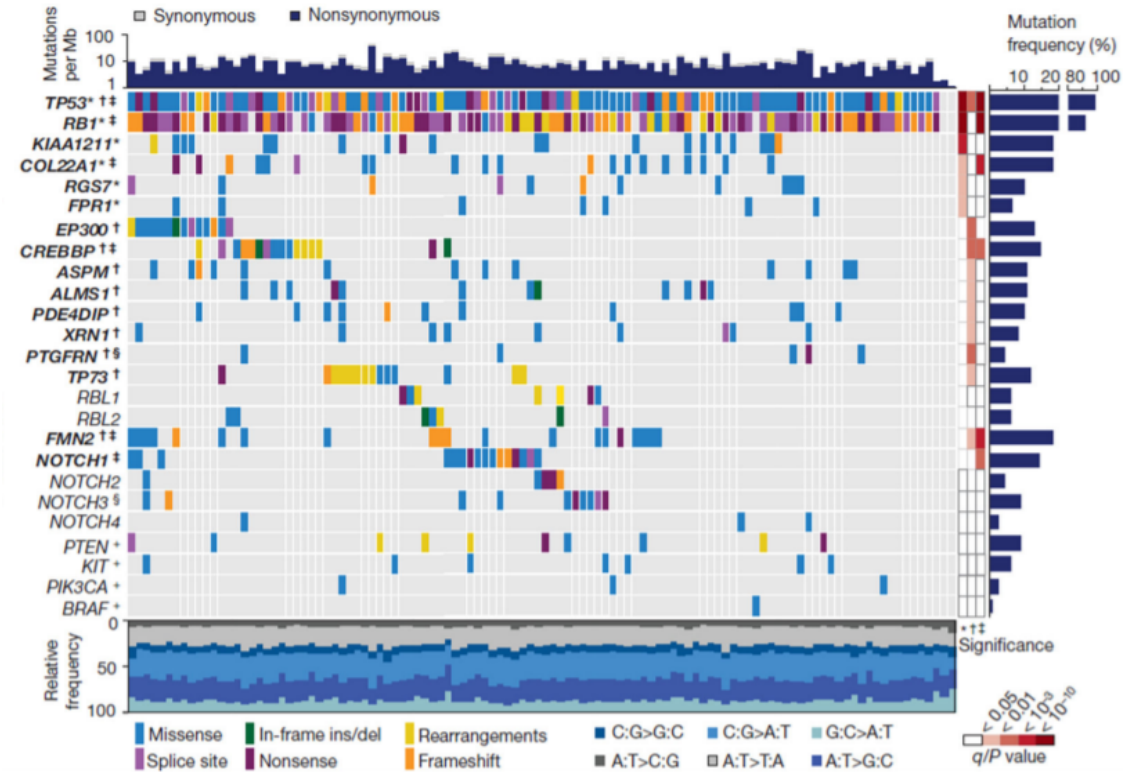

Figure 8. Genomic alterations in SCLC. Tumor samples are arranged from left to right. Alterations of SCLC candidate genes are annotated for each sample according to the color panel below the image. The somatic mutation frequencies for each candidate gene are plotted on the right panel. Mutation rates and type of base-pair substitution are displayed in the top and bottom panel, respectively [43].

In the epigenetic context, recent findings provided insights into the mechanisms by which DNA methylation events could impair the extrinsic apoptosis pathway and

suggested early evidence of the potential for pharmacological reversibility of such events in SCLC cells. Methylated gene promoters were enriched in binding sites for the neurogenic transcription factors NEUROD1, heart and neural crest derivatives-expressed protein 1 (HAND1), zinc finger protein 423 (ZNF423), and RE1-silencing transcription factor (REST), which the authors interpreted as being indicative of a defect in neuroendocrine differentiation [48]. According to the functional role of hypermethylation in cancer-specific gene silencing, *Poirier JT et al.* demonstrated that an increased promoter methylation occurred in a major subgroup of SCLC in a manner similar to what has been described in other tumor types as the 'CpG-island methylator phenotype' (CIMP), [49] which has been associated with unfavorable prognosis across multiple tumor types [50]. In an ensuing study, however, SCLC samples could be similarly stratified according to CIMP status, and patients with CIMP-positive tumors had a poorer prognosis than those with CIMP-negative disease, consistent with observations among lung carcinoma epi-types [51].

1.6 THERAPEUTIC APPROACHES IN SCLC

The high mutational burden of SCLC might provide opportunities for therapeutic intervention. As previously reported, SCLC is staged as limited-stage (LS-SCLC) or extensive-stage (ES-SCLC) disease and these distinctions are both prognostic and lead to the drug treatment in terms of effectiveness and availability. The initial strong response of SCLC to conventional chemotherapy (approximately 60%–70% response rates) and to radiation is clearly counteracted by its resistance to second-line and subsequent therapies developed after cancer recurrence. The current treatment for LS-SCLC has recently been reviewed and typically includes cisplatin-etoposide chemotherapy in combination with radiation therapy (RT), [52]. Chemo-radiotherapy with cisplatin and etoposide has been responding to an objective response rate (ORR) of 70–90% and has been associated with 44% survival at 2 years and 23% survival at 5 years. The first-line treatment of ES-SCLC generally consists of 4–6 cycles of chemotherapy plus platinum-based agent (either cisplatin or carboplatin) and etoposide. Most patients undergo rapid disease relapse within 6 months [53]. After

relapse, topotecan is provided as the only second-line drug after the US Food and Drug Administration (FDA) approvation. As regards other options after front-line therapy, taxanes, (docetaxel and paclitaxel) irinotecan, vinorelbine, and gemcitabine are still used. To date, temozolomide (TMZ) was approved for the second-line setting, in the light of its oral dosing and activity in central nervous system lesions (a 38% response rate was observed in patients who had brain metastasis in a phase II study), [54]. An evolution of therapeutic options for SCLC patients over the past three decades is shown in **Figure 9**. Finally, in the third-line setting, responses to chemotherapy are less frequent, and there is no authorization on treatment beyond first and second-line therapy.

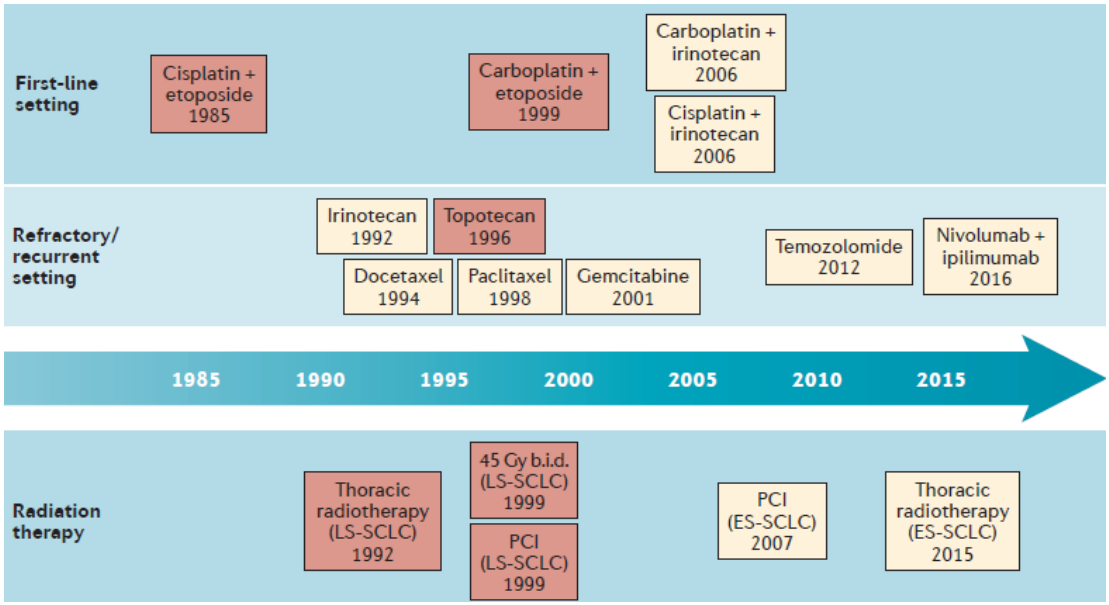

Figure 9. Timeline of therapeutic advances for SCLC. The red-shaded boxes represent standard-of-care therapies that have been approved by the FDA; the yellow-shaded boxes show the therapies that have been recommended by the National Comprehensive Cancer Network (NCCN), [53].

Many of the new insights into the biology of SCLC are being actively translated into clinical trials of novel treatments for SCLC patients [55]. The introduction of targeted therapy suggested the importance of tumor cell reliance on biological pathways to which drugs inhibiting these pathways could be applied. Understanding the molecular basis of SCLC has established that some of pathways target receptor

tyrosine kinases (RTK) and their downstream signaling mediators such as RAS and PI3K/mTOR as relevant in therapeutic application. It has been well-known how SCLC therapies have activity against multiple molecular targets as represented in **Figure 10**. As regards the class of Receptor tyrosine kinases, which consists of essential components of signal transduction mediating cell-to-cell communication, it can be distinguished different molecular ligand such as v-kit Hardy-Zuckerman 4 feline sarcoma viral oncogene homolog (c-Kit), c-Met (mesenchymal-epithelial transition factor), epidermal growth factor receptor (EGFR), fibroblast growth factor receptors (FGFRs), insulin-like growth factor-1 receptor (IGF-1R) and vascular endothelial growth factor receptors (VEGFRs), [56]. Different hypothesis concerning high level of expression of c-Kit and its ligand, stem cell factor (SCF) has been found in SCLC and imatinib, a small molecule tyrosine kinase inhibitor has been evaluated in pre-clinical in SCLC models [40]. However, subsequent clinical trials failed to show any activity of imatinib as a single agent or in combination with chemotherapeutic drugs. Likewise, gefitinib is a synthetic small organic molecule targeting intra-cytoplasmatic domain of *EGFR* that blocks its growth-promoting effects and previously tested for evaluating chemosensitive SCLC patients with phase II trial. There was no improvement in response rate or survival since *EGFR* was not expressed [57].

mTOR is expressed in approximately 50% of SCLC tumors, suggesting that the phosphatidylinositol 3-kinase (PI3K)/AKT/mTOR pathway is frequently activated in SCLC. mTOR inhibitors act on intracellular serine/threonine protein kinases that regulate cell growth, cell survival, and transcription. Two mTOR inhibitors that have been evaluated in SCLC are temsirolimus (CCI-779) and everolimus (RAD001). Temsirolimus is a synthetic rapamycin ester and it is being used as consolidation treatment in patients with extensive-stage SCLC in complete remission; instead everolimus represents a specific mammalian target of rapamycin inhibitor which acts as a second-line therapy for SCLC in phase II study [56].

Cancer cells often adopt anti-apoptotic defense mechanisms in response to oncogenic stress or anti-cancer therapy [58]. The “direct” apoptosis promoters are those that inhibit the mechanism of BCL-2 proteins also described in SCLC cell lines and in xenograft models. The overexpression of BCL-2 is related to both malignant

transformation and chemotherapeutic resistance. BCL-2 overexpression occurs in 75-95% of SCLC, and it is associated with gene amplification of the *BCL-2* locus on chromosome 18q21 [59]. Oblimersen, the first BCL-2 inhibitor, combined with carboplatin/etoposide was well-tolerated in a phase I trial in patients with extensive stage SCLC but a combination with carboplatin/etoposide in phase II clinical trial did not improve clinical outcome. It has been defined as an agent that might enhance the efficacy of standard cytotoxic chemotherapy [56].

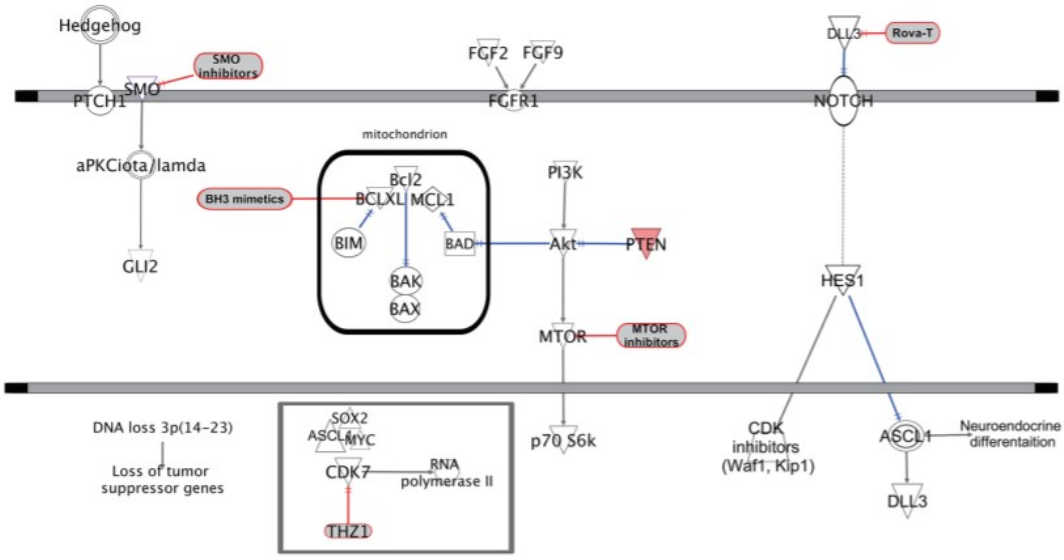

Figure 10. Molecular and therapeutic targets in SCLC. The figure simplifies the complex network of plasma membrane (PM) receptors, intracellular signaling pathways and cellular functions that have been implicated in SCLC development and progression [60].

A recent report showed that targeting the enzyme Poly-(ADP-ribose) polymerase (PARP1), a DNA repair protein, has proved to be efficacious in pre-clinical models of SCLC. Due to the fact that several tumors are dependent on PARP-mediated DNA repair for their survival, the inhibition of PARP is related to stop the proliferation of those cells. PARP protein levels are up-regulated in SCLC relative to other lung cancers. Upon administration, PARP1/2 inhibitor (E7449) selectively binds to PARP1 and PARP2, thereby preventing the repair of damaged DNA via base excision repair (BER) pathway [61].

With regard to an antibody-drug conjugate which is intended to decrease toxicity and improve the therapeutic index, Rovalpituzumab tesirine (Rova-T) may play an important role in the recognition of DLL3. Preclinical findings demonstrated *in vivo* efficacy of Rova-T in patient-derived xenograft models of SCLC, with a strong correlation between the level of DLL3 expression and therapeutic activity [62].

Among the novel target therapeutic approaches, the stimulation of immune response by using Immune Checkpoint Inhibitors (ICIs) are increasing in the treatment of lung cancers. For example, both Nivolumab and Pembrolizumab, two anti-PD-1 (programmed death 1) immunoreceptor antibodies, showed significant antitumor activity in PD-L1 positive SCLC pre-treated patients (KEYNOTE-028 and CheckMate 032 trials), [63]. To date, the uncover aspects of the biology of SCLC and its microenvironment have important implications for exploring a new therapeutic strategy for the management and treatment of SCLC patients.

CHAPTER II

2. THE NRF2/NOTCH PATHWAYS CROSSTALK

2.1 OXIDATIVE STRESS

Oxidative stress is defined as a disturbance in the equilibrium between free radicals (FR), reactive oxygen species (ROS) and endogenous antioxidant defense systems [64]. ROS are considered as host defending molecules released by neutrophil for exogenous pathogens destruction such as bacteria; however, evidence suggests that ROS also play a central role in the determination of cell fate as second messengers and regulating cellular signaling and gene expression [65].

Oxidative stress has been involved in several human diseases including atherosclerosis, rheumatoid arthritis, pulmonary fibrosis, neurodegenerative diseases and aging. This state has been reported and based on exogenous and endogenous (intracellular) origins. As the first site of origin, the term "environmental exposures" generally refers to specific environmental pollutants. The risk of constant exposure to several chemical and physical insults, the use of pharmaceuticals, heavy metals, xenobiotics, and ionizing radiation are included into extrinsic factors that play an important role, as reported in **Figure 11** [66]. On the other side, there are many intrinsic factors derived from metabolic and pathological processes, which encompassing ROS of both free radicals, oxidants, and pro-inflammatory cytokines as a result of oxidative stress [67].

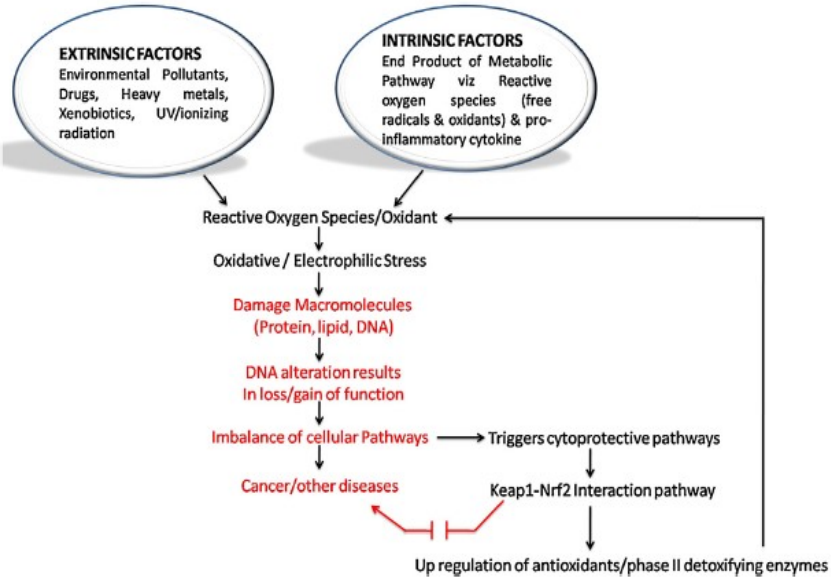

Figure 11. Factors involved in ROS generation and a cascade of events in detoxification [67].

ROS are distinguished in two groups: free-radicals such as superoxide radicals (O2-) and non-radical ROS such as hydrogen peroxide (H2O2). The primary free radicals in cells are related to superoxide (O2-) and nitric oxide (NO) species. Superoxide is produced through either incomplete reduction of molecular oxygen in electron transport systems or as a specific product of an enzymatic process, while NO comes from a series of specific enzymes (as result of nitric oxide synthases). Both superoxide and NO are reactive species and can rapidly react in order to produce series of other ROS and RNS (reactive nitrogen species), [64]. ROS structural changes occur through DNA damage in the double strand, because of the alterations in the purine or pyrimidine bases. The major mechanisms that cells use to repair oxidative damage lesions are due to single strand breaks (SSBs), double-strand breaks (DSBs), or oxidative generated clustered DNA lesions (OCDLs). Incomplete repair or loss of repair of DNA through OS may achieve to mutagenesis and genetic alteration in the apoptotic signaling pathway [68]. When the redox equilibrium is disturbed by the excessive accumulation or depletion of ROS, many cellular

signaling pathways are activated to avoid cellular dysfunction and subsequent development of the several diseases including lung cancer [65].

Among the detoxifying and response to oxidative stress pathways, one of the most important is the activation KEAP1/NRF2 cascade. KEAP1 (Kelch-like ECH associated protein) and (Nuclear factor erythroid 2 [NF-E2]–related factor 2) NRF2 are the main components of this pathway. KEAP1 is the master negative repressor of NRF2 protein in unstressed cells; under exposure of oxidative stress, it releases NRF2 which further transits from the cytoplasm to the nucleus and activates a battery of cytoprotective genes. These genes codify for several Phase II detoxification enzymes, such as glutathione-S transferases (GSTs), NADP (H): quinone oxidoreductase (NQO1), glutathione peroxidases (GPx), catalase, superoxide dismutases (SODs), epoxide hydrolase, heme oxygenase (HO1), UDP-glucuronosyltransferases (UGTs), and gamma-glutamylcysteine synthetase (GCL), [69].

2.2 THE KEAP1/NRF2 AXIS

As described below, cells are constantly exposed to oxidative stress and they fight it using a complex and powerful cellular defense machinery. Central to this cellular defensive machinery is the NRF2 and its negative regulator KEAP1 [70]. The KEAP1 protein was first identified as a binding partner of NRF2 and its name comes from the structural similarities with the Drosophila Kelch protein. KEAP1 is a dimeric protein consisting of 624 amino acids distributed into five domains namely: the amino-terminal region (NTR), the BTB/POZ (Bric-a-brac, tramtrack, broad-complex/poxvirus zinc finger) domain, a cysteine-rich intervening region (IVR), the double-glycine repeat (DGR) or Kelch domain, and the carboxy-terminal(C-terminal) region (CTR), (**Figure 12b**), [66]. The BTB/POZ domains have been found to be as substrate-specific adaptors for Cullin-3 (CUL3) ubiquitin ligase and promote the homodimerization and heterodimerization, making heteromeric multimers of KEAP1 [71]. The DGR domain comprises six repeats of the Kelch motif, which is responsible for the interaction of KEAP1 with the actin cytoskeleton and also

anchors KEAP1 to the cytoplasm [72]. The Neh2 domain of NRF2 contains two binding motifs, called ETGE and DLG, which bind to the DGR/Kelch domain of KEAP1 with different affinities. Instead, the C-terminal region of KEAP1 was also shown to bind to the Neh2 domain of NRF2 [73]. IVR domain acts as a flexible bridge between BTB and the Kelch domain which is necessary for regulation and is also implicated into the nuclear export signal (NES). In addition, both BTB and IVR domains are involved in proteasome-dependent NRF2 degradation. The human KEAP1 consists of 27 cysteines acting as ROS sensors in the regulation of cellular homeostasis. Among the cysteine residues, Cys151, Cys171, Cys273, and Cys288 are highly reactive, which are present in the BTB–IVR domains of KEAP1. Cys-151 is linked to the activation of the NRF2 molecular cascade in presence of certain inducers as Sulforaphane (SFN), Diethyl Maleate (DEM), tert-Butylhydroquinone (t-BHQ), Dimethylformamide (DMF), [74].

The NRF2 has been characterized for the first time in 1994 from a hemin-induced K562 erythroid cell line and showed high sequence homology to the known p45 subunit of NF-E2 (nuclear factor erythroid 2), [75]. It has 605 amino acids distributed among seven highly conserved Neh (NRF2-ECH homologous structure) domains, known as Neh1-Neh7 (**Figure 12a**) and has a molecular weight ranging from 95 to 110 kDa. The Neh1 domain has been shown to heterodimerize with small Maf protein and binds to the ARE within DNA since it contains a CNC-type bZIP DNA-binding motif [76].

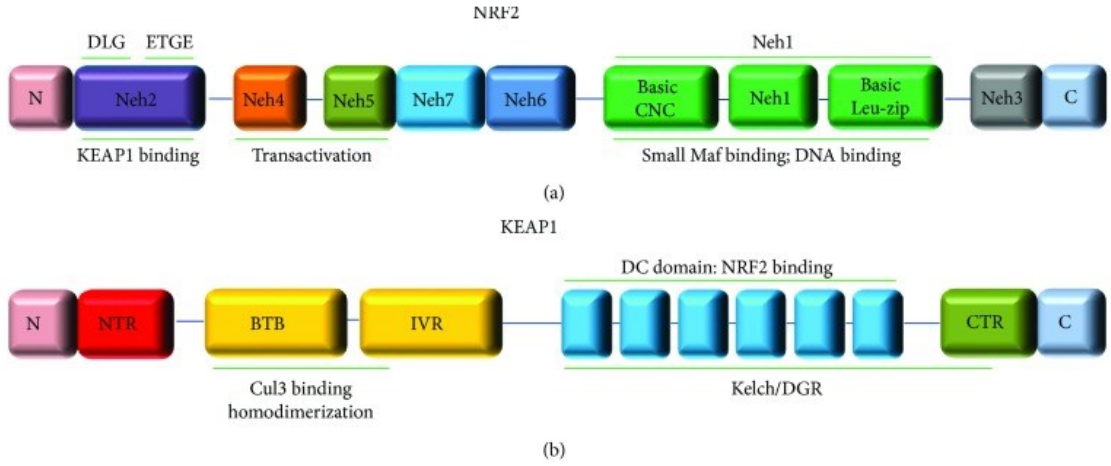

Figure 12. Domains architecture of the NRF2 **(a)** and KEAP1 **(b)** proteins. **(a)** NRF2 protein is divided into seven highly conserved domains, Neh1 to Neh7 (NRF2-ECH homology: Neh). The coordinates of NRF2 protein domains are shown as follows: Neh2 (16-89aa); Neh2 DLG motif (17-32aa), Neh2 ETGE motif (77-82aa), Neh4 (111-134aa), Neh5 (182-209aa), Neh7 (209-316aa), Neh6 (337-394aa), Neh1 (435-568aa), and Neh3 (569-605aa). **(b)** KEAP1 protein contains a number of functional domains including the N-terminal region (NTR; 1-60aa), broad complex, tramtrack and bric-a-brac (BTB; 61-179aa), the intervening linker domain (IVR; 180-314aa), the double glycine/Kelch domain harboring six Kelch-repeat domains (315-359aa; 361-410aa; 412-457aa; 459-504aa; 506-551aa; 553-598aa), and the C-terminal region (CTR; 599-624aa), [77].

The Neh2 domain, positioned in the N-terminal region of NRF2, is crucial for regulating NRF2 stability. It contains two binding sites (DLG and ETGE motifs) that are implicated into KEAP1 binding and seven lysine residues underlying ubiquitin conjugation. The Neh3, Neh4 and Neh5 domains are able to mediate the transcriptional activation of NRF2 target genes. The Neh7 domain is involved into control the interactions with RXRa (retinoic X receptor a), which functions as an NRF2 repressor and its downstream target genes [73]. In neoplastic malignancies, the transcription factor NRF2 acts not only as a tumor suppressor but also an oncogene. It is considered a tumor suppressor because its cytoprotective functions play a key role in the cellular defense mechanism against exogenous and endogenous insults,

including xenobiotics and oxidative stress. However, several recent studies demonstrated that hyperactivation of the NRF2 pathway is able to create an intracellular environment that favors the survival of normal as well as malignant cells, protecting them against oxidative stress, chemotherapeutic agents, and radiotherapy. A schematic representation of the dual role of NRF2 in cancer onset and progression is shown in **Figure 13** [78].

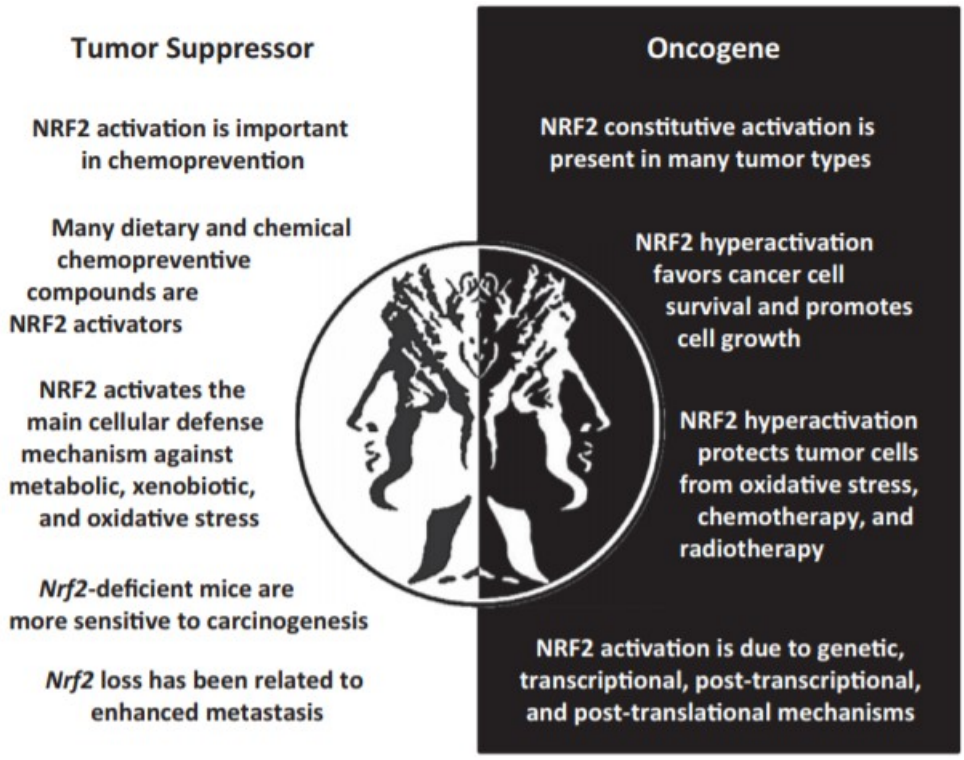

Figure 13. The left side of the figure lists some of the main evidence supporting the tumor-suppressive role of NRF2; the right side of the figure summarizes the evidence to support the oncogenic role of NRF2. The bi-frontal figure represents Janus, the Roman god with two faces [78].

The NRF2 is a master regulator of several redox-sensitive genes implicated in resistance of tumor cells against therapeutic drugs through the interaction with the KEAP1 protein. Therefore, the function of KEAP1 as a negative repressor of NRF2 is mainly focused on the KEAP1-dependent ubiquitination of NRF2. Under basal conditions, KEAP1 acts as an adaptor component for the CUL3. In turn, CUL3 binds

ring-box 1 (RBX1, also called ROC1) to complete and form a core E3 ubiquitin ligase complex. This complex is known as the responsible for NRF2 ubiquitination and degradation through 26S proteasome [79]. The “hinge and latch” model suggested that two KEAP1 molecules in the dimeric interaction with one NRF2 molecule at two binding sites, the high-affinity ETGE (hinge) and the low affinity DLG (latch) motifs [80]. This model does not necessarily promote the release of NRF2 by the KEAP1 dimer, but it seems to favor the idea that the low-affinity interaction between DLG and the Kelch-repeat domain is prevented as a result of dimeric KEAP1 to adopt a conformation that alters the relative steric positions of the two Kelch-repeat domains [81]. Under stressed conditions, it has been proposed that covalent modifications of the critical cysteine residues in the BTB domain of KEAP1 lead to a "steric clash" between KEAP1 and CUL3 since KEAP1 is a thiol-rich protein and it is proved to be more sensitive. It is found that de novo synthesized NRF2 accumulated in the cytoplasm and translocates into the nucleus where it forms a heterodimer with small MAF protein [82]. This complex specifically recognizes enhancer sequences known as Antioxidant Response Elements (AREs), located in the regulatory regions of genes encoding for cellular defense enzymes, and activates their expression through the transcription machinery, as reported in **Figure 14** [83].These results boosted into the dissociation of the KEAP1–CUL3 interaction and, therefore, completed the disruption of KEAP1-CUL3-E3-ligase activity. KEAP1–CUL3 complex is disrupted due to oxidative stress as in the case of modification at Cys151 in BTB domain, which also lead in the reduction of NRF2 degradation [84].Cys273 and Cys288, located in the IVR domain, are also found to be required for KEAP1-dependent ubiquitination of NRF2 under basal conditions. Cys151 in the BTB domain is able to conduct in the de-repression of NRF2 both under basal conditions and upon exposure of cells to NRF2 inducers. Modification of Cys151 probably prevents the KEAP1-CUL3 interaction and the ubiquitination of NRF2, resulting in the termination of NRF2 degradation [85, 86].

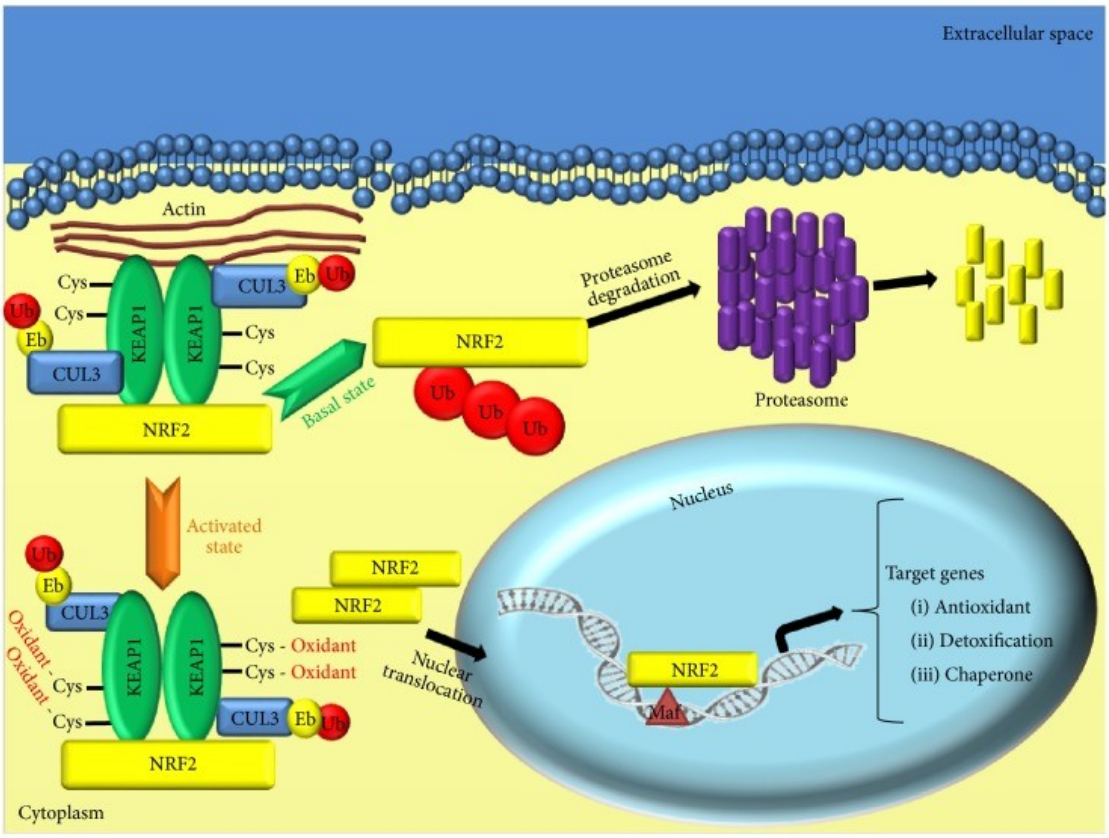

Figure 14. KEAP1/NRF2 axis in lung cancer. Under basal conditions (green arrow), NRF2 is sequestered in the cytoplasm by the KEAP1-CUL3 complex and rapidly degraded in a ubiquitin-proteasome-dependent manner. This KEAP1-mediated degradation activity requires two reactive cysteine residues of KEAP1, located in the IVR domain. Upon stress condition (orange arrow), modification of these cysteine residues of KEAP1 inhibits ubiquitin conjugation to NRF2 by the KEAP1-CUL3 complex, thereby provoking NRF2-KEAP1 impairment and resulting in the nuclear accumulation of de novo synthesized NRF2 protein and enhancement of target genes transcription [83].

2.3 THE NOTCH SIGNALING

The *NOTCH* genes encode highly conserved cell surface receptors from Drosophila to humans that drive a complex signaling pathway including a large number of ligands, negative and positive modifiers, and transcription factors. In mammals, a critical role is played by four NOTCH receptors (NOTCH1 to

NOTCH4) and two families of NOTCH ligands (Jagged1 and Jagged2 and Delta-like-1, Delta-like-3, and Delta-like-4) in modulating cell-cell dependent communications [87].

The activation of NOTCH intracellular signaling can occur through canonical or non-canonical pathways which are described in **Figure 15**. Canonical NOTCH pathway is activated via interaction of the NOTCH protein by cell ligand-binding. Upon interaction, NOTCH results cleaved, firstly by ADAM 10/17 protease and then by γ- secretase cleavage. Furthermore, NOTCH activated (NICD) translocates into the nucleus and interacts with CSL protein (also known binding factor RBPJ), where, upon interaction, the proteins complex switches into a transcriptional activator of targets genes. Non-canonical NOTCH pathways may be divided into dependently or independently activation following ligand interaction and may be γ-secretase dependent or independent. Non-canonical NOTCH signaling interacts with mTORC2, AKT, Wnt, HIF-1α, NFκB, and PI3K pathways at either the cytoplasmic or nuclear levels. The regulatory region of the *NOTCH1* transcript has been shown to have a functional ARE through which NRF2 can regulate *NOTCH1* gene expression.

In the activated state (orange arrow, transient upon stress stimuli or constitutive activation due to mutations in tumor cells as shown in the figure below), *de novo* synthesized NRF2 protein accumulates into the nucleus, where it promotes the activation of the transcription of several ARE-genes, including *NOTCH1*. In the basal state (green arrow as illustrated in the figure below), KEAP1 binds NRF2 and induces its ubiquitination through which NRF2 is degraded by ubiquitin-proteasome complex [83].

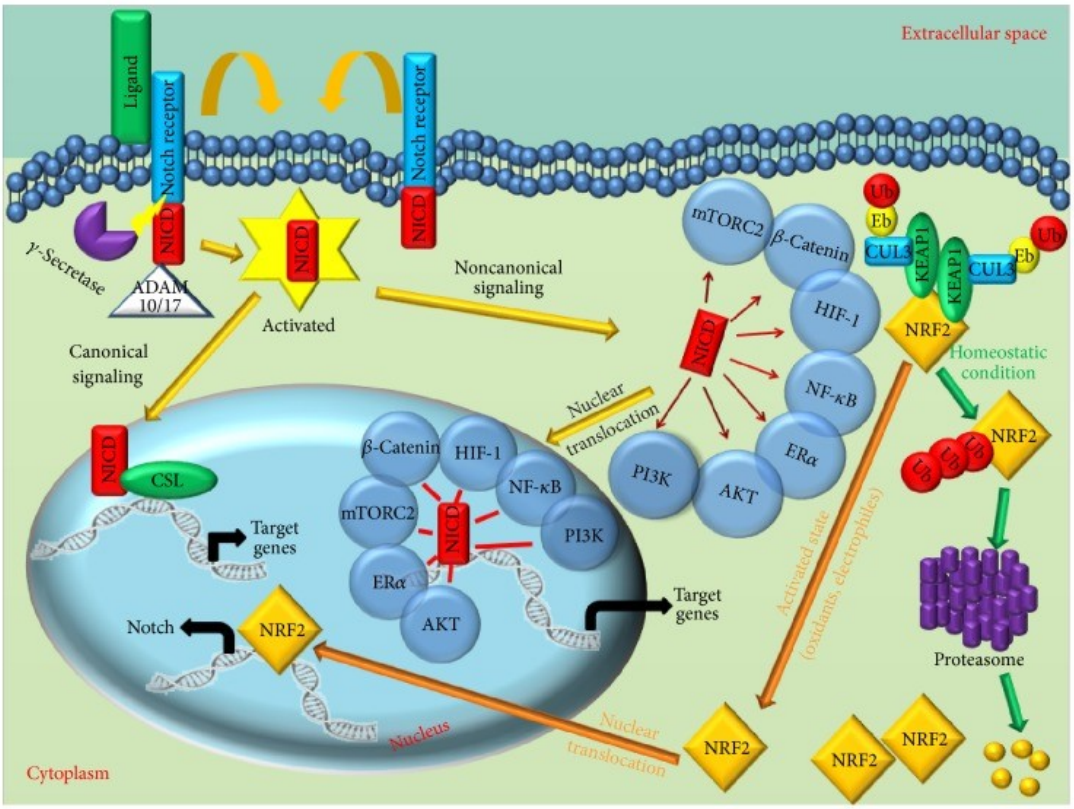

Figure 15. Canonical and noncanonical NOTCH signaling pathways [83].

Generally, NOTCH signaling in tumorigenesis can be either oncogenic or anti-proliferative cell function and can orchestrate a large number of events regarding embryonic and postnatal development, proliferation, apoptosis, border formation, and cell fate decisions. Different human malignancies, including lung, skin, pancreas, breast, and colon cancers have been implicated in the aberrant expression of NOTCH receptors and its target genes [88]. In lung tumors, NOTCH family activity is often deregulated and activates several oncogenic pathways via direct or indirect induction, differently by subtype or specific molecular profiles [89]. It has also been reported that NOTCH1 signaling acts as a key regulator of the cell growth in lung adenocarcinoma through the interaction with ADAM metalloproteases and promotes escape from apoptosis due to negative modulation of the P53 protein. These findings could explain the observed relationship between NOTCH1 activation and poor prognosis in NSCLC patients without *TP53* mutations [90]. Few data have been discussed until now about the role of *NOTCH1* in lung adenocarcinoma harboring

mutations in other lung cancer driver genes, such as *PIK3CA* or *EGFR* (Epidermal Growth Factor Receptor). In NSCLC cell lines, it has been preliminary demonstrated that the expression of *NOTCH1* cleaved form (NICD1) can lead to increased proliferation activity, in addition to malignant transformation, and tumor growth in presence of EGF (Epidermal Growth Factor). In light of these results, the *EGFR* activation may be essential for NOTCH-mediated malignant transformation and tumor growth. Moreover, the concomitant expression of *MYC* can contribute to the development and progression of cancer with metastatic spread, indicating a synergistic effect between NOTCH1 and other oncogenes [91]. The NOTCH1 signaling has been observed to also interact either as a negative or as a positive regulator of Phosphatase and Tensin Homologue gene (PTEN) of transcription process [92]. NOTCH1 coordinates the PTEN downregulation through the activation of the transcription factor hair and enhancer of SPLIT (HES1), in contrast to PTEN up-regulation that comes from the inhibition of the binding protein suppressor of hairless (RBPJ), also known as CBF-1. The activation of PTEN transcription by NOTCH1 up-regulation has been observed to interact with pro-survival phosphatidylinositol 3-kinase (PI3K)/Akt/mammalian target of rapamycin (mTOR) signaling pathway as important event in NSCLC and malignant mesothelioma cells [93, 94]. It has been described that NOTCH1 has an impact on clinical outcome in many types of cancer. In this respect, NOTCH1 also represents an independent prognostic factor in surgically resected adenocarcinoma patients with important results obtained from the combination with VEGF-A (Vascular Epidermal Growth Factor-Alpha) overexpression [95]. The usefulness of targeting NOTCH signaling in a specific subpopulation of NSCLC patients will be clarified by future investigations [96]. Specifically, in SCLC NOTCH signaling has an inhibitory effect on cell function, in the context of cell invasion and metastasis. The stable expression of the active form of NOTCH1 in SCLC cells has been verified by the inhibition of cell proliferation and its consequence on the decreased expression level in several neuroendocrine markers was observed [97]. Moreover, the alteration of NOTCH-ASCL1-RB-p53 axis has been recently described as a major driver that mediates the development of phenotypic neuroendocrine transformation from NSCLC to SCLC. These findings provide a novel cellular mechanism for lung histology transition and

suggest NOTCH signaling reactivation as a possible therapeutic strategy for SCLC patients [98].

2.4 NOTCH, ITS RECEPTORS AND LIGANDS

NOTCH receptors are single-pass transmembrane proteins that consist of distinct protein modules. The extracellular region of NOTCH receptors is composed of a series of N-terminal EGF repeats followed by a juxtamembrane negative regulatory region (NRR). The latter one is comprised of three Lin12/NOTCH repeats (LNRs) and a heterodimerization domain. The EGF-like repeats of an extracellular portion of NOTCH are essential for ligand binding [99]. The bond between ligands and extracellular NOTCH domains activates the intracellular portion and promotes intracellular sequential proteolytic cleavages by ADAM metalloproteases family [100]. The intracellular region of NOTCH receptors contains a protein-binding RPBJ-associated molecule (RAM) region, seven ankyrin repeat domains, a transcriptional activation domain, and a C-terminal degron domain which is rich in the amino acids proline, glutamate, serine, and threonine (PEST), (**Figure 16a**). In mammalian cells, this has mainly focused on possible interactions involving NICD with downstream effectors other than RBPJ, thus enhancing the expression of several target genes encoding for Hairy Enhancer of Split (HES) family proteins, HES-related proteins (HEY), and p21cip1/waf1, cyclin D1 and 3, c-myc, and HER2, in a cell-context-dependent manner [87]. The core components of this complex include the DNA-binding transcription factor CSL (C-promoter-binding factor (in mammals; also known as RBP-J) and the activation of transcription at CSL binding sites may constitute the main link between the core NOTCH-containing complex and the general transcription machinery [99]. On the basis of the possibility of non-canonical NOTCH signaling mechanisms, in fact, different evidence has been generated suggesting that NICD physically interacts with β-catenin [101], SMAD proteins [102], and HIF-1α [103] thereby ensuring direct crosstalk between NOTCH and the Wnt, TGF-β, and hypoxia-dependent signaling pathways, respectively.

Four different NOTCH receptors, NOTCH 1–4, encoded by a different gene, are expressed in mammals. These receptors contain from 29 to 36 EGF repeats and this fact explains the structural divergence in their C-terminal intracellular regions. NOTCH1 and NOTCH2 receptors contain 36 EGF repeats, whereas NOTCH3 contains 34 repeats and NOTCH4 contains 29 repeats. The other difference concerns the transactivation domain (TAD). NOTCH1 and NOTCH2 are expressed widely in many tissues of adult mammals throughout development. By contrast, NOTCH3 is most abundant in vascular smooth muscle and pericytes and NOTCH4 most highly expressed in endothelium [104]. In line with these expression patterns, NOTCH1 and NOTCH2 knockouts in mice are implicated in embryonic lethality in association with developmental defects in many organs, whereas NOTCH3 and NOTCH4 knockout mice are susceptible to have a subtle phenotype which is localized at the blood vessels [105-107]. There are four functional NOTCH ligands in mammals (**Figure 16b**), all of which are also single-pass transmembrane proteins: DLL1 and DLL4, which are part of the Delta family of ligands, and Jag1 and Jag2, which are members of the Serrate family of ligands. Last but not least, there is a *DLL3* gene that appears to encode a decoy ligand, as phenotypes observed in DLL3-deficient mice are consistent with *NOTCH* gain of function [108].

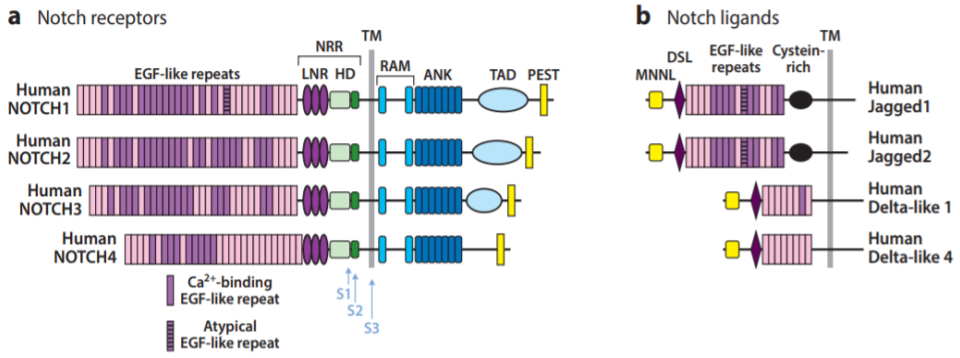

Figure 16. Structure of human **(a)** NOTCH receptors and **(b)** NOTCH ligands. Abbreviations: ANK, ankyrin repeat domain; DSL, Delta-Serrate-Lag2 domain; HD, heterodimerization domain; LNR, Lin-12/NOTCH repeat; MNNL, N-terminal domain of NOTCH ligand; NRR, negative regulatory region; PEST, proline, glutamate, serine, and threonine; RAM, RPBJ-associated molecule; TAD, transcriptional activation domain; TM, transmembrane domain [104].

2.5 NRF2 AND ITS REGULATED GENES

Several NRF2 target genes have provided so far, and their number is steadily increasing through the recent technical advances. The interplay between the NRF2 and its target genes is evaluated in the context of oncogenesis, cell proliferation, apoptosis, and tumor cell growth and the major cytoprotective functions of NRF2 have a significant impact on the ability to activate its targets expression [109]. NRF2 controls the expression of key components of the glutathione (GSH) and thioredoxin (TXN) antioxidant system, as well as enzymes involved in NADPH regeneration, ROS, and xenobiotic detoxification, heme metabolism. The **Figure 17** illustrates the main cytoprotective defense system in maintaining the redox homeostasis of the cell [110].

NRF2-mediated response to xenobiotic and oxidative stress by the regulation of GSH levels and the direct control of the expression of the two subunits: the catalytic subunit (Gclc) and the modifier subunit (Gclm), which constitute the glutamate-cysteine ligase (Gcl) complex [111]. In addition to GSH synthesis that derives from the catalyzation of Gcl, NRF2 plays an intriguing role in GSH maintenance. NRF2 regulates the transcription of numerous ROS-detoxifying enzymes such as glutathione peroxidase 2 (Gpx2) and several glutathione S-transferases (Gsts such as Gsta1, Gsta2, Gsta3, Gsta5, Gstm1, Gstm2, Gstm3 and Gstp1), [112]. These enzymes are able to use GSH in ROS inactivation and generate oxidized glutathione (GSSG). GSSG is reduced back to GSH by glutathione reductase 1 (Gsr1), another NRF2 target, in an NADPH-dependent manner [113]. In addition to the regulation of GSH levels within the cells, NRF2 plays a key role in the control of the thioredoxin (Txnrd1)-based antioxidant system [114]. NRF2 also regulates the expression of sulfiredoxin (Srxn1), [115] which are fundamental for the reduction of oxidized protein thiols. NADPH acts in drug metabolizing enzymes as an obligatory cofactor and antioxidant systems, such as cytochromes p450 (Cyp) enzymes and the NRF2 target Nqo1 [116]. It is notable that NRF2 supports NADPH production through the positive regulation of the principal NADPH-generating enzymes: glucose-6-phosphate dehydrogenase (G6pd), 6-phosphogluconate dehydrogenase (Pgd), isocitrate dehydrogenase 1 (Idh1), and malic enzyme 1 (Me1), as demonstrated in primary cortical astrocytes [117] and lung cancer cells [118]. Another remarkable

enzyme regulated by NRF2 is heme oxygenase (Hmox1), which exhibits cytoprotective effects since the excess of free heme sensitizes cells to undergo apoptosis [119]. Additionally, NRF2 can also affect the cellular elimination of xenobiotics by monitoring the expression of many phases I and phase II drug-metabolizing enzymes [116], as well as the multi-drug-resistance-associated transporters (Mrps), [120]. In summary, NRF2 increases the cellular defense mechanisms against xenobiotic and oxidative stress through the coordinated expression of numerous antioxidant and detoxification genes.

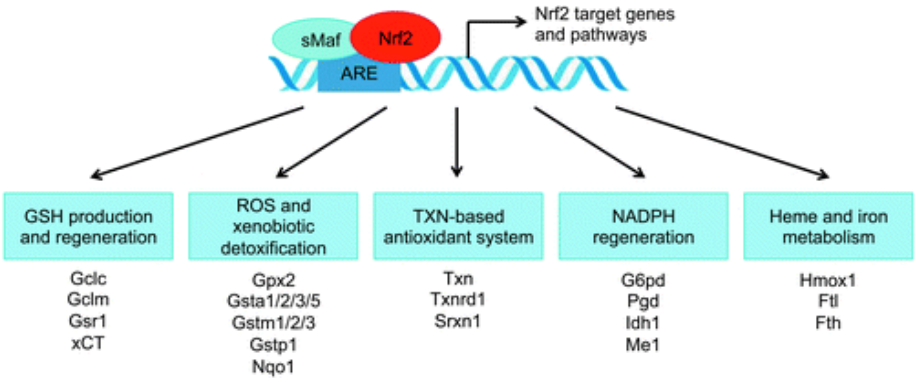

Figure 17. The NRF2-regulated cytoprotective defense system. Through the coordinated regulation of GSH and TXN production, utilization and regeneration, NADPH regeneration, heme and iron metabolism, ROS and xenobiotic detoxification, NRF2 provides the main cytoprotective defense system in the cell. GSH, glutathione; HMOX1, heme oxygenase 1; Idh1, isocitrate dehydrogenase 1; NAPDH, nicotinamide adenine dinucleotide phosphate; Nqo1, NADPH quinone dehydrogenase 1; Pgd, 6-phosphogluconate dehydrogenase; ROS, reactive oxygen species; TXN, thioredoxin [110].

2.6 MECHANISMS OF NOTCH AND NRF2 DEREGULATIONS IN CANCER

NOTCH and NRF2 are both transcription factors and their related pathways were discovered independently. However, recent data demonstrated the existence of a NRF2/NOTCH crosstalk which supports cytoprotection and improves maintenance

of cellular homeostasis and tissue organization by modulating cell proliferation kinetics, and stem cell self-renewal in several organs [121]. NOTCH receptors have been found deregulated in many tumors, and although the prevalence and location of mutations within each NOTCH receptor they exhibit subtle difference according to the tumor type [122]. Many identified mutations are heterozygous and the correlation with haploinsufficiency in tissue patterns suggests that the process of tumorigenesis is due to the loss of a single copy that functionally could impact on NOTCH signaling. In general, *NOTCH1* gene mutations are more frequently searched than in the other NOTCH receptor genes. This reason is related to the greater number of tumors with *NOTCH1* sequencing data. In fact, *NOTCH1* mutations were relatively recurrent (5–15%) and clustered at or near identified important domains in head and neck cancer (HNSCC) and lung and breast cancers [83].

As described by Singh et al., the first molecular impairment of KEAP1/NRF2 axis has been then extensively proven in NSCLC cell lines and tissues with different mutation clusters to specific histological subtypes. The genetic and epigenetic alterations in *KEAP1* and *NFE2L2* genes led to the overexpression of nuclear NRF2 and the subsequent activation of defense machinery and an increase in the expression pattern of several antioxidant enzymes [123]. Somatic mutations of the *KEAP1* gene frequently impair the DC domain and reduced the KEAP1-dependent NRF2 ubiquitination by CUL3 and the nuclear export of NRF2 by KEAP1/CUL3 complexes. In both cases, under cellular stress condition, NRF2 escapes degradation and translocates into the nucleus to boost the expression of its target genes [124]. It was found that *NFE2L2* mutations could induce a constitutive activation and have been found to mainly cluster within the DLG and ETGE motifs, which are hotspot sites for NRF2 binding to the KEAP1 DC binding domain [125]. A network of NOTCH interactions and responses to NRF2 is presented in **Figure 18**.

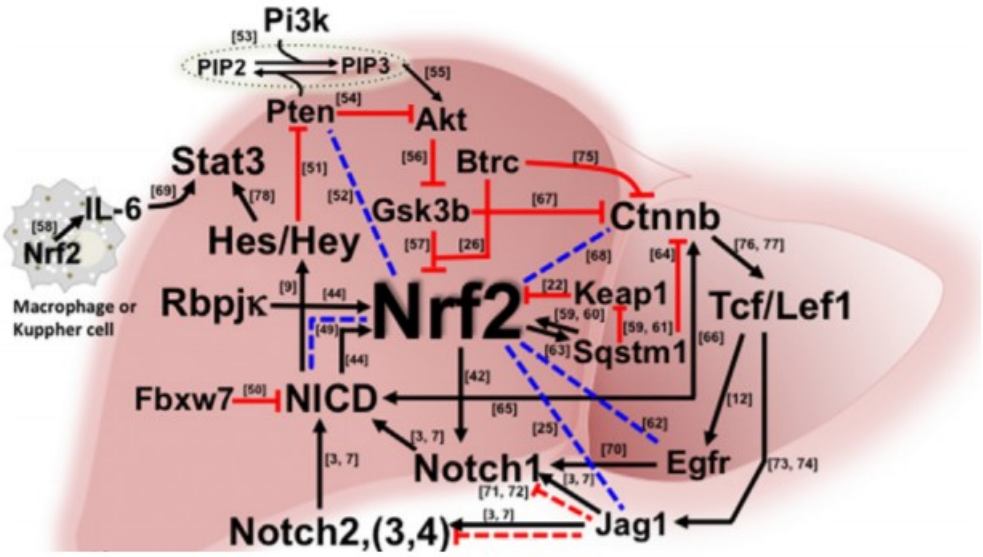

Figure 18. An integrated network of NRF2/NOTCH crosstalk signaling. Published (solid lines) and hypothetical (broken lines) elements of NRF2 interaction with other signaling networks. Arrows indicate induction and "T" indicates repression [121].

2.7 MOLECULAR MECHANISMS UNDERLYING THE DYSREGULATION OF THE NRF2/NOTCH PATHWAYS CROSSTALK IN LUNG CANCER

NRF2, *KEAP1*, and *NOTCH1* genes were deemed to be significant in both the combined sets of tumors and individual tumor types. This observation led to the speculative notion that the outcome from the impairment of aberrant molecular NRF2/NOTCH crosstalk might have a critical role in tumorigenesis and progression of cancer [121].

In lung cancer, the deregulation of the NOTCH pathway is mainly ascribable to missense mutations that affect the ligand-binding domain (EGF repeats 11 and 12) or the ankyrin domains which lead to a ligand-independent activation [126]. *NOTCH1* activating mutations have been defined as a common event in human NSCLC and have been correlated to poor prognosis and response to therapy in lung patients without *p53* mutations [127]. In SqCC, *NOTCH1* appeared to be more mutated than

in pulmonary adenocarcinoma, and their typical location next to the ligand-binding domain suggests important speculation that *NOTCH1* is more likely to function as a tumor suppressor in SqCC than in the adenocarcinoma histology [122]. By contrast, mutations affecting the *NOTCH* family genes have been largely studied as one of the most mutated pathways driving neuroendocrine features of lung tumor and SCLC. Different frequency of missense changes in *NOTCH1–NOTCH4* genes has been reported in the different histologies of lung neuroendocrine tumors [128]. In SCLC, the mutations that have been identified in the extracellular domain with an incidence of about 25%, suggesting that NOTCH plays a tumor suppressor role, leading to growth inhibition and neuroendocrine markers reduction [43, 129]. To corroborate the idea of the crucial role of NOTCH in lung neuroendocrine development, mutations in *NOTCH1–NOTCH4* family genes (28%) have also been recently reported by genomic analysis in Large Cell Neuroendocrine Cancer (LCNEC). This represents an additional and strong evidence of how many mutations are located in the extracellular EGF-like domain and mainly associated with NSCLC-like subgroup that differs from the typical mutation pattern of lung adenocarcinoma [130]. Alternative mechanisms of NOTCH deregulation have been also reported in lung cancers. In particular, molecular profiling of alternative splicing variants in lung adenocarcinoma was performed in primary breast and colon cancers and has suggested the occurrence of some deregulated events that affecting the *NUMB* gene, a negative regulator of NOTCH signaling. These abnormal isoforms promote the inhibition of NUMB protein expression and the activation of the NOTCH signaling pathway, thereby enhancing cell proliferation [131]. Few evidences of an epigenetic modulation of NOTCH expression have been provided so far in lung cancer. Some of these focus on pharmacological induction of miR-34a that determines a decreased in the expression of *NOTCH1* and its downstream targets including *HES-1*, *Cyclin D1*, *Survivin*, and *BCL-2*. This may lead to an impairment of NOTCH signaling, cell proliferation, and invasion and inducing apoptosis in NSCLC cells [132].

Mutations in *NFE2L2* gene were also widely described in lung tumors, suggesting a strong link between molecular abnormalities of the NRF2 pathway and response to oxidative stress [133]. Mutations and copy number alterations of *NFE2L2* and *KEAP1* and/or deletion or mutation of *CUL3* were observed in 25–34%

of SqCC patients with a smoking history related to the histological subtype of lung cancer [134, 135]. Instead, a low incidence of *KEAP1* mutations has been reported in advanced stage ADC patients with different ethnicity (3–19%) and a lower incidence of *EGFR* mutations [136], except for papillary adenocarcinoma tumors subtypes (60%), [137]. In addition, TCGA analysis of lung adenocarcinomas has shown a direct relationship between those patients that harboring *KEAP1* mutation which increased more than six-fold and loss of *LKB1* expression. LKB1-deficient tumors are susceptible to oxidative stress because they are unable to activate the adaptive responses mechanisms underlying metabolism and biosynthesis. The high level of overlap in loss of function of *KEAP1* and *LKB1* genes may suggest that selective pressure exists for the activation of NRF2 as a secondary protective mechanism to compensate for *LKB1* loss [138].

Despite the assumption of NRF2 function as a transcription factor for classic cytoprotective genes, recent evidence can be found exploring the possibility of miRNA transcript regulation by NRF2 [77]. miR-144 recently emerged as having a central role in the modulation of cellular stress response in blood malignancies and solid tumors [139] and some of these were experimentally proven to directly target and repress the NRF2 activity such as miR-28 in MCF-7 breast cancer cells [140]. A direct effect of miR-93 on nuclear accumulation of NRF2 was well described by *Singh et al.* in which was observed a significant reduction in carcinogenesis-associated phenotypes [141]. More recently, a mutual regulation between NRF2 and microRNAs, especially in the mechanisms of tumor chemoresistance such as miR-200a reactivation in resistant lung tumor cell lines was demonstrated [142].

By looking at *KEAP1* alterations, it has been discovered an important molecular feature of neuroendocrine tumors by Fernandez-Cuesta et al. They have demonstrated that it is possible to distinguish an LCNEC SCLC-like group, carrying *MYCL1* amplifications and mutations in both *RB1* and *TP53* genes from an AD/SQ-like group, harboring *CDKN2A* deletions, *TTF1* amplifications, and frequent mutations in *KEAP1* and *STK11*. On the basis of a different genetic background, this represents a dynamic and evolutionary picture that makes a distinction between SCLC and AD/SQ [143]. These data have been confirmed by Rekhtman et al., who reported an incidence of 31% of *KEAP1* mutations in LCNEC NSCLC-like subset

[44]. In addition to somatic mutations, other mechanisms affecting *NRF2* expression in lung tumors have been reported, even though this field still remains mostly unexplored. For instance, there are compelling evidences that epigenetic regulation by promoter methylation might play a key role in modulating KEAP1/NRF2 axis in lung cancer cells [70, 144]. More recently, the discovery of hypermethylation of the *KEAP1* promoter linked to cell-detoxifying network added a new important dimension in the complex regulation of the KEAP1/NRF2 system [77]. The methylation of the *KEAP1* promoter region was firstly described by Wang et al. as a pivotal mechanism in the regulation of the *KEAP1* mRNA expression in cell lines and primary lung tumors that could be rescued by 5-Aza treatment [145]. These results were validated from our group on a cohort of primary resected NSCLCs and proved that the epigenetic inactivation of *KEAP1* by promoter hypermethylation as the main mechanism which leads to reduced or absent KEAP1 protein expression previously reported by *Wang et al.* in NSCLC. Most importantly, another intriguing data that comes out from genetic and epigenetic analyses of this cohort is the *KEAP1* biallelic inactivation as molecular marker of worst prognosis [146]. Finally, it has been recently demonstrated by *in vitro* analysis that the methylation status of *KEAP1* can also predict the tumor cells sensitivity to radiation in combination with the angiogenesis inhibitor, Genestein. Results suggest that an increase of ROS levels and cell apoptosis may affect the overexpression of NRF2, GSS, and Ho-1 in lung adenocarcinoma cells [147].

2.8 THERAPEUTIC TARGETING OF NOTCH AND NRF2 PATHWAYS

The anticancer effects of different classes of compounds inhibiting NOTCH signaling activation such as siRNAs, GSIs, and mAbs have been tested in numerous preclinical models [148]. But importantly, encouraging results came from clinical implementation in combination with either chemotherapy or targeted agents. Among these, the oral GSI PF-0308414 showed clinical activity in a phase I study in patients with advanced stage solid tumors [149]. In this context, the investigation of NOTCH

pathway inhibition is currently considered as a novel therapeutic strategy in SCLC. For instance, the fully human IgG2 antibody Tarextumab (TRXT, OMP59R5) plus chemotherapy has been shown to significantly reduce the risk of tumor recurrence in patient-derived SCLC xenografts by targeting NOTCH2/NOTCH3 [150]. A phase I/II study of Tarextumab in combination with six cycles of cisplatin and etoposide in ES-SCLC, followed by Tarextumab maintenance (PINNACLE, NCT01859741) is currently ongoing to support and improve the SCLC patients' outcome [151].

Alternative approaches for targeting NOTCH signaling in lung cancer may include several natural agents, such as curcumin (3,3′-diindolylmethane, DIM), resveratrol 3,5-bis (2,4-difluoro benzylidene)-4-piperidone (DiFiD), and epigallocatechin-3-gallate (EGCG) whose anticancer activity has been demonstrated in both *in vitro* and *in vivo* models of other solid tumors [152].

Similarly, the pharmacological inhibition of NRF2 signaling may represent a further therapeutic option for cancer treatment, especially in those patients with increased levels of NRF2. Indeed, recent reports have shown that the NRF2 that appeared higher are significantly associated to chemo- and radioresistance, making the development of novel NRF2 inhibitors particularly intriguing [153]. For example, it has been demonstrated that all-trans retinoic acid (ATRA) and retinoic acid receptor-α (RARα) agonists can directly sequester NRF2 and prevent its binding to the ARE, leading to the global downregulation of NRF2-dependent gene expression [154]. On the strength of these results, similar outcomes have been reported about the physical blocking of NRF2 by other nuclear receptors, such as peroxisome proliferator-activated receptor-γ (PPARγ), estrogen receptor-α (ERα), estrogen-related receptor-β (ERRβ), and glucocorticoid receptor (GR), [155]. A growing number of natural compounds are also known to confer a strong effect on NRF2, thus corroborating the idea of the interplay with the NOTCH pathway. Among these, sulforaphane induces activation of the KEAP1/NRF2 cellular detoxification cascade once reacts with thiols of KEAP1 DGR domain [156] and resveratrol restores cigarette smoke exposure- (CSE-) depleted GSS (glutathione synthetase) levels by triggering GCL expression (γ-glutamate cysteine ligase) and successively reducing CSE-mediated NRF2 modifications [157].

To date, the lack of a few selective inhibitors for NRF2 and related pathway and the high risk of off-target toxic effects represent some important limitations. In conclusion, the therapeutic NRF2 targeting has documented a promising beneficial option as an adjuvant strategy in combination with any category of chemotherapeutics, both ROS generating and non-ROS generating agents.

CHAPTER III

3. MATERIAL AND METHODS

3.1 SCLC CELL LINES

SCLC Hcc33, H1963, N417, H2107, H1184, H209, H69V cell lines were purchased from the American Type Culture Collection (ATCC, Manassas, Virginia, United States) whereas GLC1, GLC2, GLC3, GLC8, GLC14 cell lines were obtained in collaboration with the UMCG, Department of Genetics, Groningen, the Netherland (Dr. Klaas Kok, PhD). Cells were cultured in RPMI 1640 medium supplemented with 10% or 20% fetal bovine serum (FBS), 100 U/mL penicillin and 100 U/mL streptomycin, and maintained at 37°C in a 5% CO_2 incubator. All the cell culture products were purchased from Euroclone, Milan, Italy.

3.2 DNA AND RNA EXTRACTIONS FROM CELL LINES

Cells from 1 well of 12-multiwell were treated with 180 ul of Te9 solution (1 ml 1M Tris-HCl, pH 9.0, 0.5ml 0.5M EDTA, pH 8.0; 1.25 ml 5M NaCl; 97.25 ml dH_2O), 30 ul of Proteinase K 10mg/ml, 60 ul of Proteinase K/SDS 10% (100 mg proteinase K, 10 ml 10% SDS) for the DNA extraction. Cells were disrupted and incubated at 48°C. After 60', 300 ul of Phenol/chloroform was added to cell lysates. After, lysates were shaken and centrifuged for 20' at 4°C at 18000 g. Supernatants were collected and 300 ul of Phenol/Chloroform was added. Supernatants were centrifuged at 18000 g for 20' at 4°C. After discarding the supernatants, the pellets were suspended in 900 ul of cold 100% Ethanol solution and 100 ul of Ammonium Acetate pH 7.5 After, the sample were centrifuged at 18000g for 20' at 4°C. After discarding supernatant, DNA pellets were washed in 70% Ethanol and centrifuged at 7500 g for 10'. Finally, DNA pellets were suspended in LOTE solution (3 mM Tris-HCl (pH 8.0)/0.2 mM EDTA, pH 8.0).

To extract RNA, cells from 1 well of 12-multiwell were treated with 200 ul of cold Trizol reagent (Invitrogen). Cells were disrupted and 50 ul of chloroform were added to lysates. After 1' of vortexing, lysates were shaken for 20' at 4°C. After, lysates were centrifuged for 20' at 4°C at 18000 g. The supernatant was collected and 110 ul of isopropanol was added to the supernatant. After 10' of shaking at 4°C, supernatants were centrifuged at 18000 g for 20' at 4°C. After discarding the supernatants, the pellet was washed in 500 ul of cold 70% Ethanol solution. After washing, the pellet was centrifuged at 7500 g for 10' at 4°C. After discarding supernatant (70% ethanol), the RNA pellet was suspended in 20-25 ul of H_2O DEPC (Diethylpyrocarbonate water). Both DNA and RNA concentrations were estimated by NanoDrop Spectrophotometer ND-1000 (Thermo Scientific).

3.3 POINT MUTATION DETECTION

Exon/intron gene structure has been obtained from NCBI/Genbank databases and primers set used for genetic screening has been designed in order to cover the entire region of the DGR domain of the *KEAP1* gene, the exon 2 of *NFE2LE* gene and *NOTCH1* coding region [158]. PCR amplification of each fragment was performed by using Gene Amp PCR System 9700 thermal cycler (Applied Biosystem, Foster City, CA). PCR products were purified using GFX PCR DNA and the Gel Band Purification Kit (GE Healthcare, Buckinghamshire, UK) and sequenced by using the Big Dye Terminator Ready Reaction mix v. 1.1 on an ABI 3100 sequence detection system with the Sequencing Analysis software v.3.7 (Applied Biosystems), [159].

3.4 CNV AND LOH ANALYSIS

KEAP1 Copy number variation (CNV) for SCLC cell lines using genomic DNA from tumor cell lines for four microsatellite markers flanking the *KEAP1* gene (D19S865, DM1, D19S906, D19S840) were assessed by extracting data from SNP Array combined with data sourced from http://cancer.sanger.ac.uk/cancergenome/projects/cosmic/ and http://www.ncbi.nlm.nih.gov/geo/.

3.5 METHYLATION ANALYSIS

3.5.1 DNA SODIUM BISULFITE CONVERSION AND QUANTITATIVE METHYLATION SPECIFIC PCR (QMSP)

Bisulfite conversion of DNA and QMSP investigations required one microgram of DNA extracted from cell lines and tissue samples that were subjected to bisulfite treatment and DNA purification using the Epitect Bisulfite kit (Qiagen Sci, MD, USA) according to manufacturer's instruction. Bisulfite-modified DNA was used as a template for QMSP to detect converted DNA. Calibration curves for both target and reference genes were constructed using serial dilutions (90–0.009 ng) of commercially available fully methylated DNA (CpGenome Universal Methylated DNA, Millipore, Chemicon, cat#S7821). Amplification reactions were carried out in triplicate in 384-well plates and in a volume of 10 ul that contained 50 ng of bisulfite-modified DNA on an ABI PRISM 7900 Sequence detection system and were analyzed by SDS 2.1.1 software (Thermo Fisher Inc., Applied Biosystems Division). PCR primers were used to amplify DNA target region and were *in silico* designed through MethPrimer both for *ACTB* and *KEAP1*, a program that from an original and modified sequence of interest (extrapolated from UCSC database) simulates the modification with sodium metabisulfite and executes an algorithm for potential CpG islands prediction. Primer/probe sets for the *KEAP1* promoter region and for the unmethylated promoter region of the *ACTB* as reference gene are previously described and reported in **Table 4**. Each plate included calibration curves for the *ACTB* and *KEAP1* genes, patients' DNA samples, a positive control CpGenome Universal Methylated DNA, and multiple water blanks. The Cp (cross point) values of each QMSP reaction were calculated using the second derivative maximum method. The QMSP standard curves of the *KEAP1* and *ACTB* genes for the normalization of the input DNA were established with CpGenome Universal Methylated DNA. Methylation levels were finally calculated as the ratio of *KEAP1* to *ACTB* and then multiplied by 1000 for easier tabulation (average value of triplicates of *KEAP1*/average value of triplicates of *ACTB* × 1000), [158].

Table 4. Primers sequence and probes used for *KEAP1* and *ACTB* for QMSP analysis.

Primer/Probe Name	primer sequence (5′ → 3′)	Annealing Temperature (°C)
KEAP1-meth_forw	TGCGGTCGTCGGATTACGAGGTCG	66
KEAP1-meth_rev	CTTCCATCTCCCGATTTCGTTAC	
KEAP1-meth_probe	FAM-GTGGCGCGTAGTTTCGCGAG-TAMRA	
ACTB-forw	TGGTGATGGAGGAGGTTTAGTAAGT	55
ACTB-rev	AACCAATAAAACCTACTCCTCCCTTAA	
ACTB-probe	FAM-ACCACCACCCAACACACAATAACAAACACA TAMRA	

3.5.2 PYROSEQUENCING

Fifty ng of bisulfite-treated genomic DNA was amplified by PCR process. Amplification primers used for the *KEAP1* promoter region were as follows: forward: 5′-GTTTGAGGTTAGGAGTTTAAGGTTG-3′, reverse: 5′-CACAACCAAACCCCCCTT-3′. The reverse primer contained biotin at the 5′ position. Two assays were designed and run on this template using two sequencing primers: 5′-GAGGTAGATGATTTTTTTTAGAT-3′ (assay for CpGs 1-7) and TAAAAGGAGAATAGTAGATGGTG (assay for CpGs 8–13). For the pyrosequencing reaction, single-stranded DNA templates were immobilized on streptavidin-coated sepharose beads (Qiagen, Hilden, Germany) using the PSQ Vacuum Prep Tool and Vacuum Prep Worktable (Qiagen, Hilden, Germany), according to the manufacturer instructions, then incubated at 80°C for 2'. Pyrosequencing was performed using PyroMark Q24 (Qiagen, Hilden, Germany). The proportion of DNA methylation at each CpG site was automatically calculated by the PyroMark Q24 Software 2.0 and given as a percentage. The % methylated fraction (C/T ratio) is displayed in a small colored box just above each CpG site in the analyzed sequence [147].

3.6 GENE EXPRESSION ASSAY WITH TAQMAN PROBE BY REAL-TIME PCR

PCR fragments for *KEAP1*, *NFE2L2*, *NOTCH1*, *HES1*, *DLL3*, *NQO1*, *TXNRD1*, and *RPLPO* were amplified by the TaqMan assay listed in **Table 5** and were cloned into the StrataClone™ PCR Cloning Vector pSC-A (Stratagene, Milan, Italy). Mini-prep cultures were grown in 5 ml of LB-Ampicillin broth. Plasmid DNA from the selected transformed cells was isolated using the QIAprep® Spin Miniprep Kit (Qiagen). Five plasmid dilutions in the range of 1×10^6 copies to 1×10^2 copies were used to construct the standard curves for real-time PCR. First strand cDNA synthesis from 1 µg of total RNA extracted from SCLC cell lines was carried out with SuperScript III First-Strand Synthesis (Thermo Fisher, Invitrogen Division, Carlsbad, CA, USA) using a gene expression amplification mixture containing 2.5 × TaqMan® Universal PCR Master Mix (Thermo Fisher, Life Technologies division), 250 nM of TaqMan™ Gene Expression Assay with TaqMan probe and 1 µl of template cDNA or plasmid product (serial dilutions). Reactions were run on ABI PRISM 7900HT Sequence Detection System (Thermo Fisher, Life Technologies Division). Protocol conditions were as follows: 10' at 95°C, 40 cycles at 95°C for 15'' and 60°C for 60''. Each assay was carried out in triplicate and the transcription level was normalized using *RPLPO* as a reference gene. Calibration curves for all genes (used as calculation method) were constructed and sample concentration was calculated using the plasmid standard curve, resulting in plasmid concentrations expressed as copy number of corresponding standard molecules. The relative sample amount was expressed as ratio marker ([Target/Housekeeping]*1000 for an easier tabulation).

Table 5. Probes set used for RT-qPCR analysis.

Gene	TaqMan gene expression
KEAP1	Hs00202227_m1*
NFE2L2	Hs00975961_g1*
NOTCH1	Hs01062014_m1*
HES1	Hs00172878_m1*
DLL3	Hs01085096_m1*
NQO1	Hs02512143_s1*
TXNRD1	Hs01555214_g1*
RPLPO	4326314E

*Taqman gene expression assay from Life Technologies, Thermo Fisher Inc.

3.7 CELL CULTURE AND 5-AZACYTIDINE (5-AZA-dC) TREATMENT

The H69V SCLC cell line was seeded in a 6 well dish. The 5-aza-2'-deoxycytidine (DAC), an inhibitor of DNA methyltransferase, was added in a concentration of 5µM (Sigma-Aldrich) with fresh medium for 24h, 48h, and 72h. At each time points (24h, 48h, and 72h) cells were harvested for DNA and RNA isolation to interrogate the induction of the DNA demethylation and analyze the *KEAP1* expression level [158, 159].

3.8 PROTEIN EXTRACTION AND WESTERN BLOT

Cells cultures were solubilized in at least ten volumes of RIPA buffer (25 mM Tris–HCl, pH 7,6; 150 mM NaCl; 1% Triton X-100; 1% sodium deoxycholate; 0,1% SDS) added with a cocktail of protease inhibitors (https://lifescience.roche.com). The lysis was performed on ice for 60' and the samples were then centrifuged at 22,000 g for 45'. The protein content of the supernatant was measured with bicinchoninic acid (BCA) Protein Assay Kit (http://www.thermoscientific.com). Equal amounts of protein samples were separated by 12% Tris-Glycine-SDS-PAGE and transferred to polyvinylidene fluoride (PVDF) membranes (http://www.merckmillipore.com/). Membranes were saturated with 5% fats free Milk and were incubated with primary antibodies overnight at 4°C, washed, and incubated with peroxidase-conjugated secondary antibodies for 60' at Room Temperature. Reactive proteins were revealed with an enhanced chemiluminescent detection system (ECL Plus, ThermoScientific, USA) and visualized on a Chemidoc XRS imaging system.

3.9 *KEAP1* SILENCING

KEAP1 siRNA duplexes specific for human *KEAP1* were purchased from Thermo Scientific (USA), (Silencer Select). A scrambled siRNA was used as a negative control (CTRL siRNA) and was purchased from Thermo Scientific. The

selected siRNA sequences were submitted to a BLAST search to avoid the targeting of other homologous genes. RNA interference (RNAi) experiments in H69V, H1184, and N417 cells were performed by transient transfection for 48h. The RNAiMAX Lipofectamine (Invitrogen, Milan, Italy) transfection protocol was used. Cells were analyzed for KEAP1 expression by Western blot analysis after 48 hours.

3.10 IMMUNOFLUORESCENCE

Cells cultures were plated on coverslips and fixed in 4% paraformaldehyde, washed in phosphate buffered saline (PBS), and permeabilized with 0.3% Triton X-100 in PBS. After blocking with 1% BSA in PBS, cells were incubated with primary antibodies for 120' at RT. After washings in PBS, cells were incubated for 60' at RT with Alexa conjugated secondary antibodies and Phalloidin 647 (Alexa Fluor, Thermo Scientific) to stain the cytoskeleton. Coverslips were mounted on slides, using a mounting medium (PBS, 50% Glycerol, 0.1% N-Propyl-Gallate) and examined by using a confocal microscope (TCS SP8, Leica). Nuclei were stained with DAPI. Once captured, the auto contrast function was applied to all the whole images using Adobe Photoshop CS5 in order to create a more accurate tonal and color correction workflow.

3.11 ANTIBODIES

The primary antibodies used are: anti-KEAP1 polyclonal (1:800, Proteintech, USA), anti-AKR1C1 monoclonal (1:1000, Proteintech, USA), anti-TXNRD1 polyclonal (1:1000, Proteintech, USA), anti-NRF2 polyclonal (1:500, Proteintech, USA), anti-NOTCH1 monoclonal (1:1000, CST, USA), anti-E-Cadherin (1:1000, CST, USA), anti-HES1 (1:1000, CST, USA), anti- cMyc (1:1000, CST, USA), anti-Caspase 3 full length (1:1000, CST, USA), anti-Caspase 3 cleaved (1:1000, CST, USA), anti-BCL2 (1:500, DAKO), anti-β-Actin (1:10000, Sigma-Aldrich). The secondary antibodies used are the following: horseradish peroxidase (HRP) conjugated donkey anti-goat and donkey anti-mouse IgG (http://www.scbt.com) for Western blot.

3.12 PHARMACOLOGICAL TREATMENTS

3.12.1 ETOPOSIDE

Etoposide is a semisynthetic derivative of podophyllotoxin from the rhizome of the wild mandrake (Podophyllum peltatum). More specifically, it is a glycoside of podophyllotoxin with a D-glucose derivative. Etoposide has a molecular weight of 588,6 g/mol, melting point at 236-251°C and is poorly soluble in water but soluble in organic solvents such as ethanol, methanol, and DMSO. Etoposide acts primarily in the G2 and S phases of the cell cycle. Metabolic activation of etoposide by oxidation into the O-quinone derivative may play a significant role in its activity against DNA. This drug binds to and inhibits topoisomerase II, an enzyme elevated in tumor cells. This results in the accumulation of double-strand DNA breaks, the inhibition of DNA replication and transcription and the induction of apoptotic cell death [160].

3.12.2 CISPLATIN

Cisplatin, also called cis-diamminedichloroplatinum (II), is a metallic (platinum) coordination compound with a square planar geometry. It is a white or deep yellow to yellow-orange crystalline powder at room temperature. It is slightly soluble in water and soluble in dimethylprimanide and N, N-dimethylformamide. Cisplatin is stable under normal temperatures and pressures but may transform slowly over time to the trans-isomer. Cisplatin has a molecular weight of 301.1 gm/mol, a density of 3.74 g/cm3 , a melting point of 270° C, a log Kow of -2.19 and a water solubility of 2.53 g/L at 25° C [161]. The main cellular target for cisplatin is genomic DNA and this compound binds to DNA in order to form intra-strand crosslinks and adducts. DNA adducts generated by cisplatin action inhibit DNA replication and/or transcription and activate several signal transduction pathways. Cisplatin binds to DNA in two steps: firstly the bond with N7 guanine is formed, and then it binds with guanine or adenine in the same or opposite strand. The N7 atoms of guanine and adenine are the most accessible ones and cisplatin forms a broad spectrum of intra-

and inter-strand crosslinks and all of them cause the distortion of the DNA [162, 163].

3.12.3 DAPT [N-(N-[3,5-DIFLUOROPHENACETYL]-L-ALANYL)-S-PHENYLGLYCINE T-BUTYL ESTER]

An early generation non-transition state analog is DAPT, N-[N-(3,5-difluorophenacetyl)-L-alanyl]-S-phenylglycine t-butyl ester, a dipeptide inhibitor of the benzodiazepine type, also known as a γ-secretase inhibitor (GSI) IX and Compound 3. It is the most widely used in the laboratory setting and represented in **Figure 19** [164]. DAPT (GSI-IX) inhibits GSI production with IC50 of 20 nM in HEK 293 cells and potentiated the apoptotic effects of the DNA-damaging alkylating agent in MCF-7 breast cancer cells [165]. In addition, DAPT also induces caspase-dependent and caspase-independent apoptosis in lung squamous cell carcinoma cells by inhibiting NOTCH receptor signaling pathway [166]. In cell lines with chromosomal translocations, DAPT inhibits the proliferation of truncated NOTCH-1 expressing an ADAM cleavage site but not of truncated NOTCH-2 which was without the cleavage site [167].

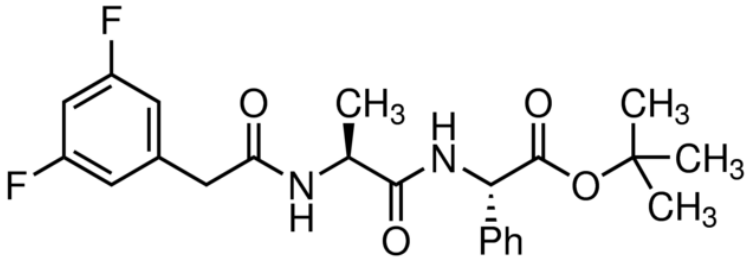

Figure 19. Chemical representation of DAPT compound from PubChem Open Chemistry database.

3.13 CELL VIABILITY ASSAY

To determinate the IC50 per each pharmacological compounds, cell lines were analyzed by means of PrestoBlue assay. PrestoBlue™ Cell Viability Reagent is a ready-to-use reagent for rapidly evaluating the viability and proliferation of a wide range of cell types. PrestoBlue™ reagent is quickly reduced by metabolically active

cells, providing a quantitative measure of viability and cytotoxicity. Cell lines were cultured into a 96 multi-well plate and the day after, PrestoBlue was added directly to the culture medium (10% v/v) of each sample. After 120’ of incubation at 37°C, fluorescence measurement (560 nm/590 nm) was performed using Biotek Synergy HT.

3.14 STATISTICAL ANALYSIS

Data are expressed as mean±SE of the number of experiments (n) indicated in the figure legends proposed in the project. In all the assays "n" is referred to the number of independent experiments performed on different cell preparations. For each experiment, at least three to seven different wells were analyzed. Statistically significant differences were computed using a t-test, the significance level being set at $P<0,05$. All graphs showed, were performed by GraphPad Prism 5.

CHAPTER IV

4. AIM AND SCOPE OF THE PROJECT

The KEAP1/NRF2 pathway is the master regulator of antioxidants and cellular stress responses implicated in resistance of tumor cells against chemotherapeutic drugs. Additionally, tumor growth and progression of lung tumors have been proved to involve the molecular crosstalk among KEAP1/NRF2 and several pathways also implicated in cell invasion and metastasis, with relevant implications in antioxidant protection, survival of cancer cells and drug resistance to therapies.

At present, the data concerning the role and impact of KEAP1/NRF2 modulation and its deregulation mechanisms in small cell lung cancer are mostly uninvestigated, whereas the implication of NOTCH pathway modulation is well known in this context.

To increase the knowledge about this aspect, we firstly aim in the present project to evaluate the molecular background for NRF2 and NOTCH pathways dysfunctions in a collection of SCLC cell lines by performing genetic and epigenetic profiling. Data from this profiling will be then used to verify and better understand the features of KEAP1-NRF2/NOTCH interaction and to clarify its role in SCLC tumorigenesis. Finally, we will evaluate by *in vitro* functional studies the putative role of KEAP1 and NRF2 proteins related to response to NOTCH inhibitors and conventional therapies.

CHAPTER V

5. RESULTS

5.1 *KEAP1, NRF2, NOTCH1* GENETIC AND EPIGENETIC PROFILING IN SCLC CELL LINES

The molecular alterations of KEAP1/NRF2 pathway in solid tumors are well studied and appear to depend on several main factors such as the existence of activating mutations in *NFE2L2* gene and/or loss of function mutations and methylation in the *KEAP1* gene. In SCLC, point mutations in *KEAP1* and *NFE2L2* genes appear a rare events; by contrast, the *NOTCH1* gene appears in the list as the more frequently mutated in this type of lung tumor.

A collection of 12 SCLC cell lines were investigated at the molecular level: Hcc33, H1963, N417, H2107, GLC1, GLC2, GLC3, GLC8, GLC14, H1184, H209, H69V. A comprehensive *KEAP1* molecular profile was performed and data from point mutation screening, promoter hypermethylation, LOH at gene locus and CNV analyses. *NFE2L2* and *NOTCH1* genes point-mutation screening were also performed and data collected.

An aberrant promoter hypermethylation of the CpGs located into the P1 promoter region of the *KEAP1* gene by QMSP analysis was found in 5/12 (42%) of SCLC cell lines (GLC3, GLC8, H1963, H209, H69V) while LOH at the *KEAP1* locus (19p13.2) was demonstrated in 4/12 (34%) of SCLC cell lines (N417, GLC2, Hcc33, H69V). A CNV>2 was detected at *NFE2L2* gene locus (2q31.1) in 3/10 of cell lines, thus suggesting a possible genomic amplification involving the *NFE2L2* gene locus (2q31.1) in these cell lines (**Table 6a**). Fluorescent *in situ* hybridization analysis confirmed the copy number gains (>2 no. of spots/probe) at *NFE2L2* locus in H209 and GLC2 cell lines. H1184 and H69V showed signals only on the two homologs normal chromosome 2. NRF2 mRNA expression level was assessed in a set of four SCLC cell lines with different values of CNV. Expression in H209 (CNV=4) was significantly higher than the mean of the expression levels observed in Hcc33 and H1184 (CNV=2) and was significantly higher than the expression level in H69V

(CNV=1), (p=0.0058 and p=0,0022 respectively, data not shown), suggesting the NRF2 gene CNV as an alternative mechanism of the NRF2 deregulation.

We observed in H1184 cells only one just described point mutation in the Kelch-Repeat 2 of the *KEAP1* gene. This mutation induces the aminoacidic change p.G364C in the DGR domain of the KEAP1 protein. It was already known that this non-synonymous modification alters the efficiency of protein capability to interact with the NRF2 transcription factor, thus leading to an increase in its nuclear accumulation in cells. By contrast, no mutations were found in the *NFE2L2* and *NOTCH1* genes (**Table 6b**). These genetic results confirm the already published evidence of a rarity of point mutations linked to the KEAP1/NRF2 pathway deregulation in SCLC [43].

Table 6a. Epigenetic and genomic amplification profiles of the *KEAP1* gene.

SCLC cell lines	*KEAP1* methylation (KEAP1/ACTB*1000) by QMSP analysis	*KEAP1* LOH (19p13.2)	*NFE2L2* LOH (2q31.1)
Acc33	**0**	**Yes**	**No**
H1963	**15**	**No**	**No**
N417	**0**	**Yes**	**No**
H2107	**0**	**No**	**Yes**
GLC1	**0**	**No**	**No**
GLC2	**0**	**Yes**	**Yes**
GLC3	**644**	**No**	**No**
GLC8	**219**	**Yes**	**No**
GLC14	**0**	**No**	**No**
H1184	**0**	**No**	**No**
H209	**51**	**No**	**Yes**
H69V	**330**	**Yes**	**No**

Table 6b. *KEAP1*, *NFE2L2* and *NOTCH1* genetic profiles in SCLC cell lines.

SCLC cell lines	*KEAP1* nucleotide and aa change	*NFE2L2* nucleotide and aa change	*NOTCH1* nucleotide and aa change
Acc33	**wt**	**wt**	**wt**
H1963	**wt**	**wt**	**wt**
N417	**wt**	**wt**	**wt**
H2107	**wt**	**wt**	**wt**
GLC1	**wt**	**wt**	**wt**
GLC2	**wt**	**wt**	**wt**
GLC3	**wt**	**wt**	**wt**
GLC8	**wt**	**wt**	**wt**
GLC14	**wt**	**wt**	**wt**
H1184	**c.1090G>T (p.G364C)**	**wt**	**wt**
H209	**wt**	**wt**	**wt**
H69V	**wt**	**wt**	**wt**

Wt, wild-type; aa, amino acid.

In the present study, the CpG methylation status at *KEAP1* promoter region was firstly assessed by QMSP. To estimate the rate of methylation of each CpG sites (13 in total) located in the P1 region [145], we then performed pyrosequencing analysis on two methylated (H69V, H209) and two unmethylated (H1184, N417) cell lines.

As shown in **Figure 20**, two sequencing primers were used for the pyrosequencing reaction, with the first reaction examining seven CpG sites (1–7), while the second reaction examining six additional CpG sites (8–13) with their respective sequence to analyze (TTTGYGGTYGTYGGATTAYGAGGTYGGYGTTGTGYG; GYGYGTAGTTTYGYGAGGAGATATTTAGTAAYGAAATYGGGA). The mean of *KEAP1* methylation level observed was significantly higher in both H69V (78,5%) and H209 (27,4%) than H1184 and N417 cell lines, that resulted unmethylated. Universal Methylated Human DNA bisulfite-converted showed a methylation level of about 96% in all CpG sites examined (a good indicator of cellular 5-methylcytosine level), in contrast to Universal Unmethylated Human DNA, that shows a methylation level under 3%. The mean of methylation levels in cell lines at the 13 CpG sites within the CpG island of the *KEAP1* promoter was shown in **Table 7**.

Table 7. The methylation data for each CpG site within all tested region of the *KEAP1* promoter.

Sample	Methylated CpG Site (%)													
	1	**2**	**3**	**4**	**5**	**6**	**7**	**8**	**9**	**10**	**11**	**12**	**13**	**Mean %**
H69V	92	92	96	76	93	89	78	92	91	77	64	43	38	**78,5**
H209	55	47	54	23	40	37	22	21	28	15	7	4	3	**27,4**
H1184	14	9	13	4	7	5	6	8	9	8	2	2	2	**6,9**
N417	21	19	19	7	11	15	10	12	12	6	3	1	2	**10,6**
MET	96	100	100	92	100	94	92	97	94	98	93	90	97	**95,6**
UNMETH	5	4	3	3	4	2	3	4	4	5	2	2	3	**3,4**
BLANK	-	-	-	-	-	-	-	-	-	-	-	-	-	-

A

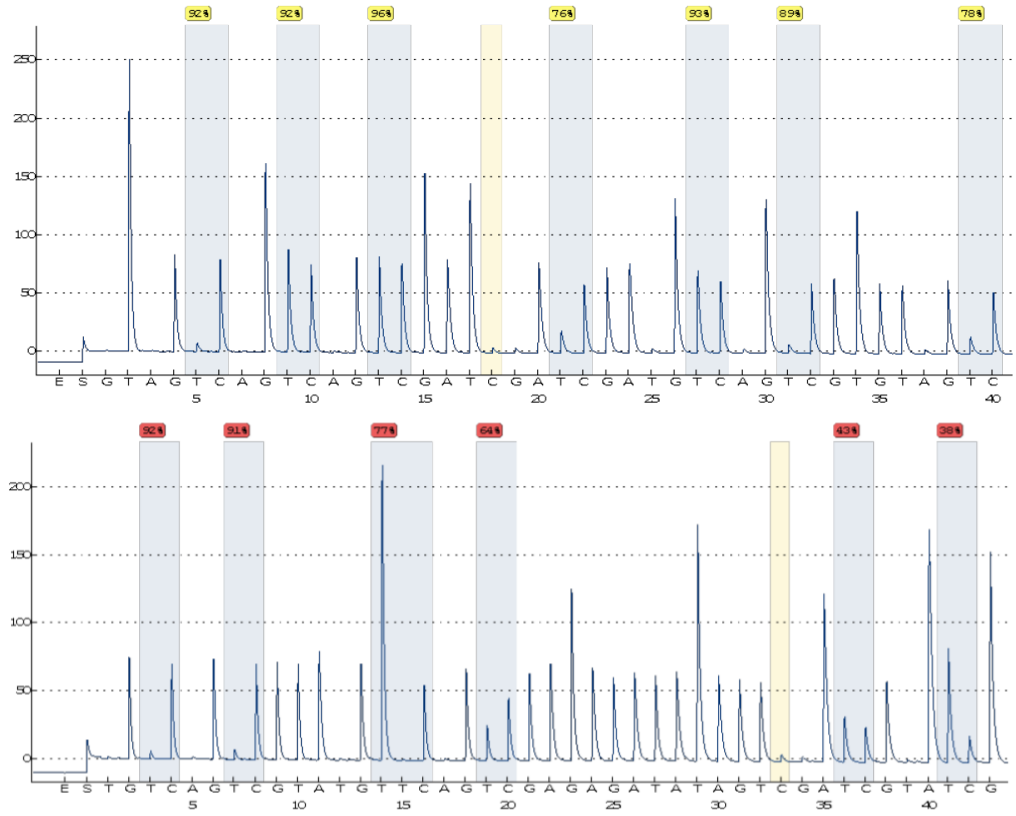

B

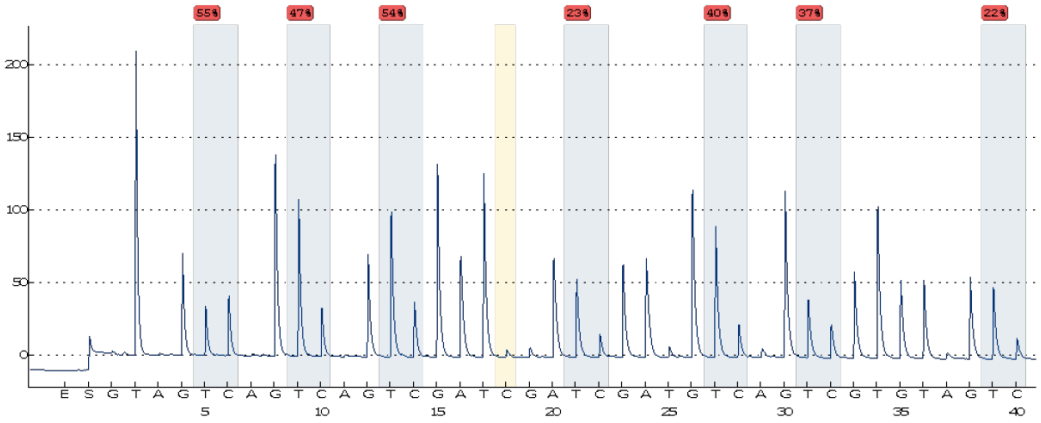
55%
47%
54%
23%
40%
37%
22%
200
150
100
50
0
E S G T A G T C A G T C A G T C G A T C G A T C G A T G T C A G T C G T G T A G T C
5
10
15
20
25
30
35
40

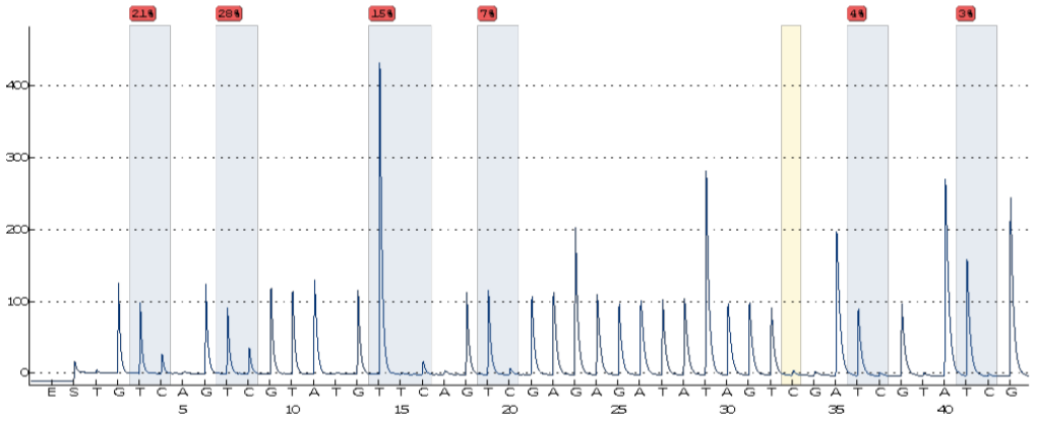
21%
28%
15%
7%
4%
3%
400
300
200
100
0
E S T G T C A G T C G T A T G T T C A G T C G A G A G A T A T A G T C G A T C G T A T C G
5
10
15
20
25
30
35
40

C

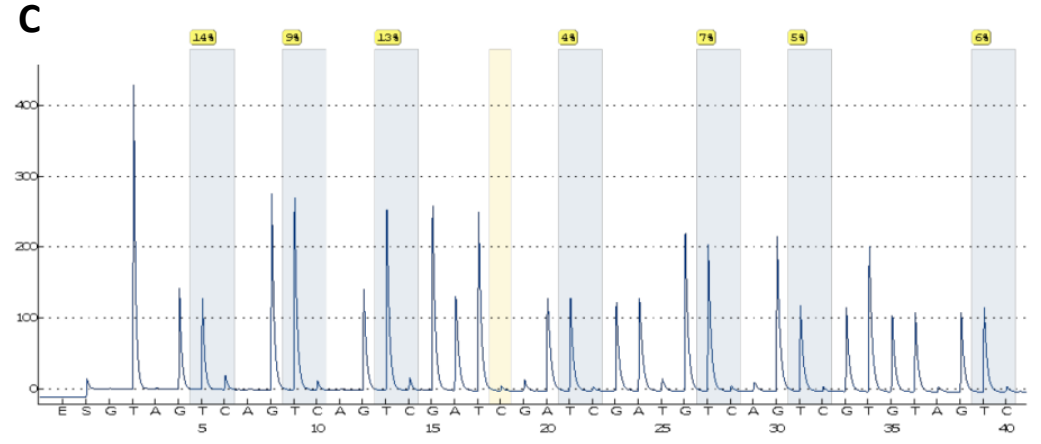
14%
9%
13%
4%
7%
5%
6%
400
300
200
100
0
E S G T A G T C A G T C A G T C G A T C G A T C G A T G T C A G T C G T G T A G T C
5
10
15
20
25
30
35
40

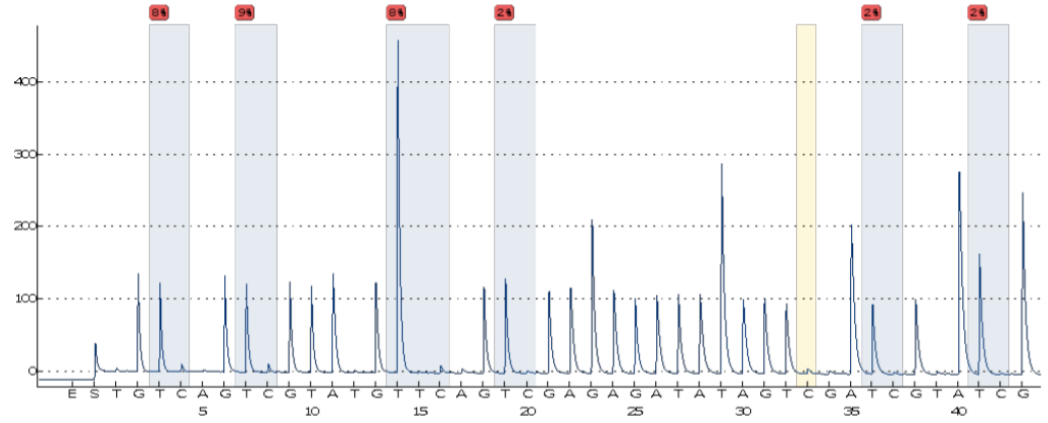
8%
9%
8%
2%
2%
2%
400
300
200
100
0
E S T G T C A G T C G T A T G T T C A G T C G A G A G A T A T A G T C G A T C G T A T C G
5
10
15
20
25
30
35
40

D

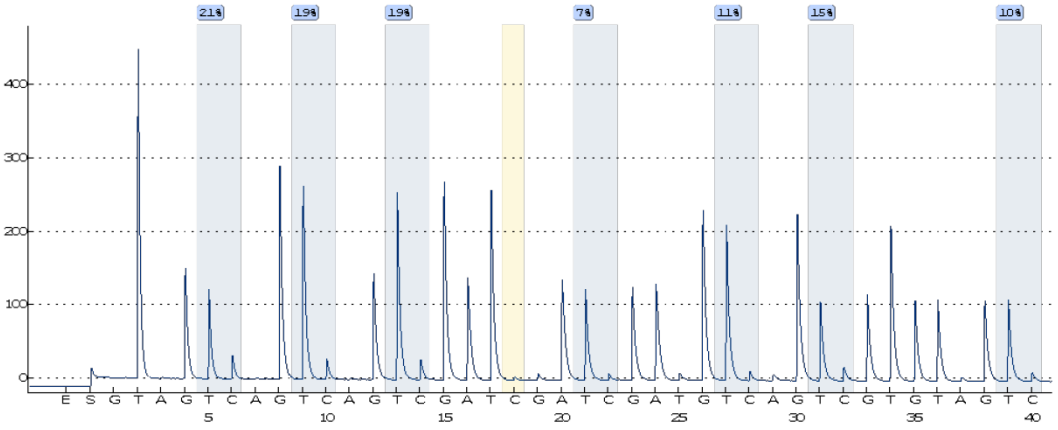
21%
19%
19%
7%
11%
15%
10%
400
300
200
100
0
E S G T A G T C A G T C A G T C G A T C G A T C G A T G T C A G T C G T G T A G T C
5
10
15
20
25
30
35
40

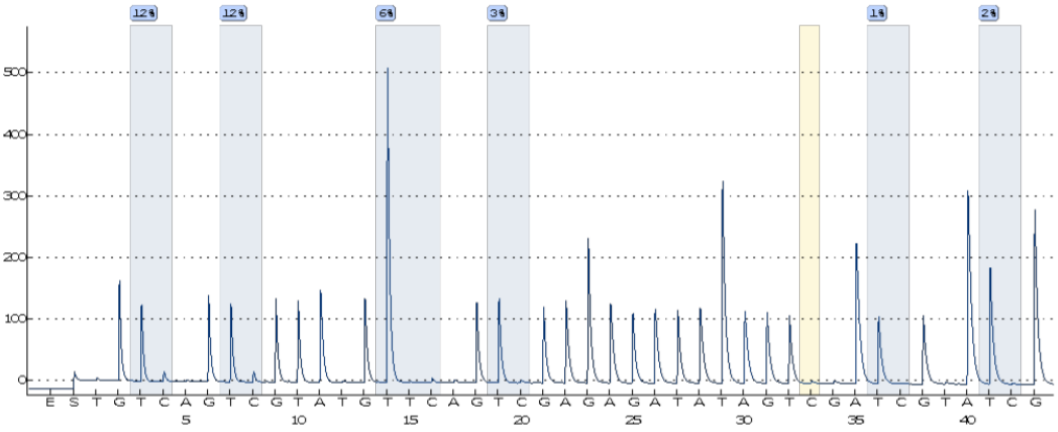
12%
12%
6%
3%
1%
2%
500
400
300
200
100
0
E S T G T C A G T C G T A T G T T C A G T C G A G A G A T A T A G T C G A T C G T A T C G
5
10
15
20
25
30
35
40

E

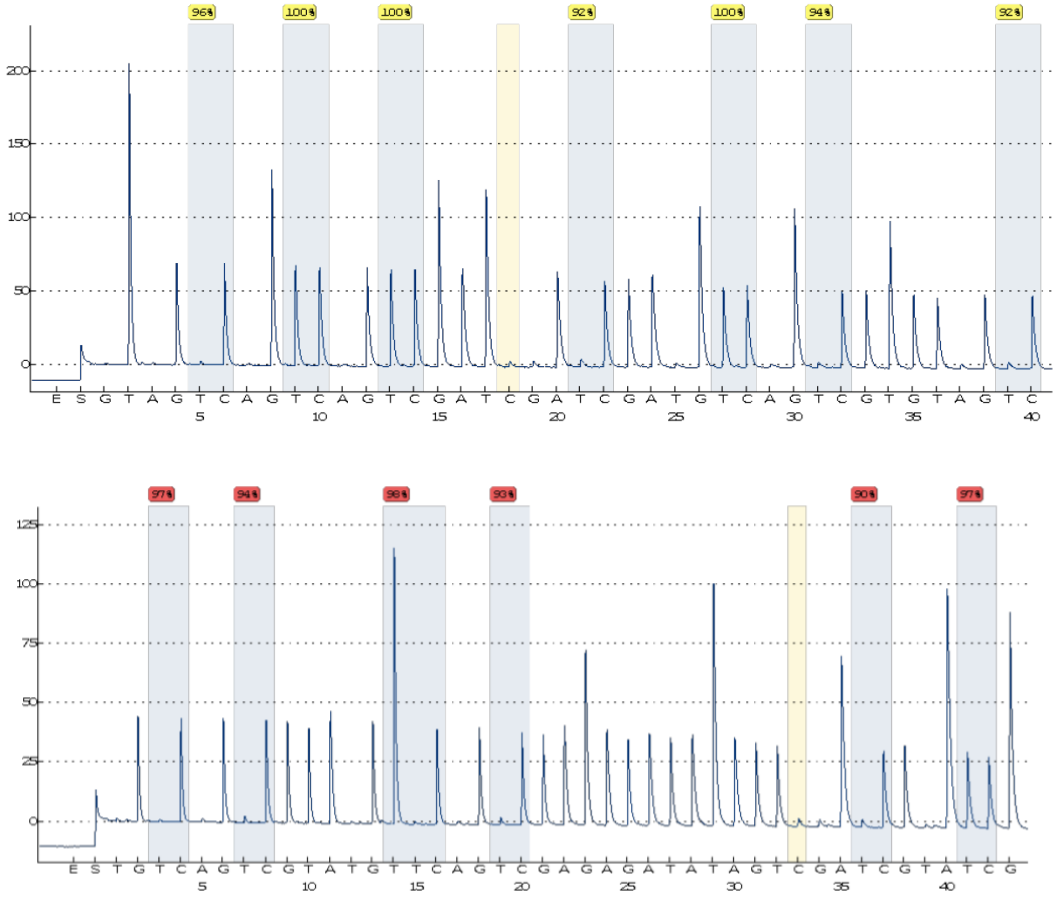

F

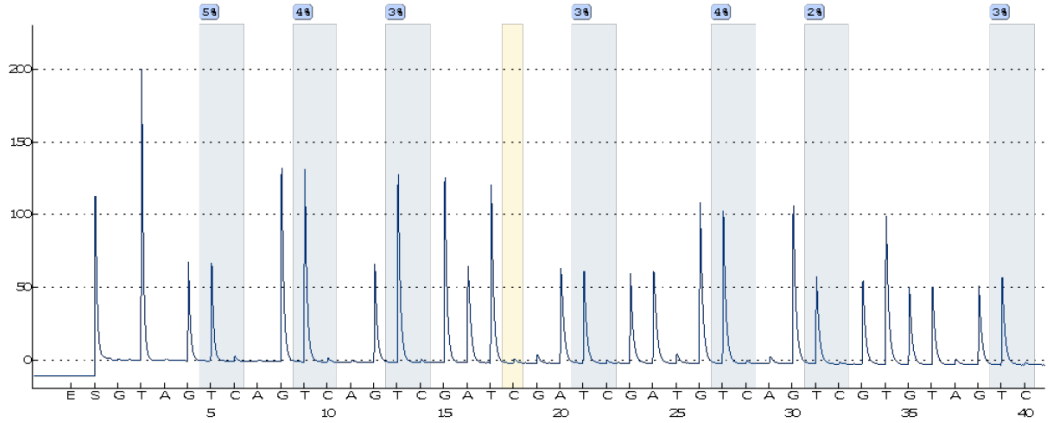

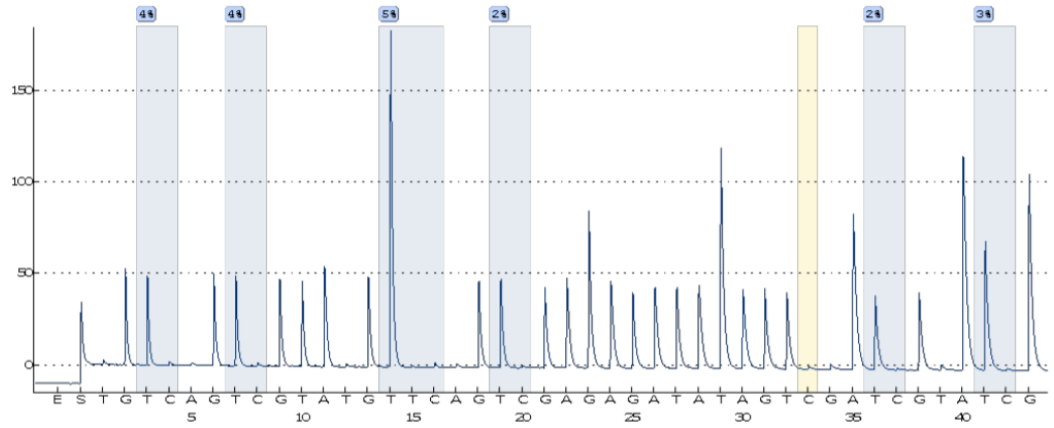

Figure 20. Representative DNA methylation pyrograms obtained with the first and second reactions of *KEAP1* primers (1–7 and 8–13 CpG sites, respectively) are shown in the following pyrograms: **A)** H69V; **B)** H209; **C)** H1184; **D)** N417; **E)** Universal Methylated Human DNA; **F)** Universal Unmethylated Human DNA. X axis shows the dispensation order; the pyrosequencing assay used to measure the *KEAP1* methylation level in a subset of SCLC cell lines. Percentages (blue bars) indicate the proportion of cytosine (C) Nucleotides at each CpG site after bisulfite conversion. From these proportions, we can measure the methylation levels at these sites. Overall *KEAP1* methylation level is calculated as the average proportion of cytosines (%) at the four CpG sites. The arrow indicates the absence of residual cytosines at non-CpG sites, indicating complete bisulfite conversion.

Pyrosequencing data showed, in general, a differential CpG promoter hypermethylation pattern in the promoter region of *KEAP1* containing 1-7 and 8-13 CpGs groups of the P1 region. The first seven single CpG sites appeared more methylated than the others and could represent the critical sub-region closer to the transcription start site that exerts a more strong regulation impact on *KEAP1* promoter region and its transcript levels. Specifically, P1 region should contains specific consensus protein binding sites, such as GC-box, and E-box, as well as AP2-, Sp1-, and Ets-binding motifs [145].

5.2 FUNCTIONAL EFFECTS OF *KEAP1* ALTERATIONS OF NRF2 AXIS IN SCLC CELL LINES

To investigate the effects of the genetic and epigenetic alterations found in SCLC cell lines a preliminary analysis of KEAP1 transcript level was assessed by RT-qPCR. The *KEAP1* mRNA resulted to be significantly down-regulated in the four cancer cell lines H1184, H69V, H209, and H1963 showing a mutation/hypermethylated for the *KEAP1* gene (**Figure 21**) in comparison with the expression in N417, GLC1 and GLC2 (p=0.0007, t-test) with no genetic or epigenetic alterations. This first result suggests a correlation between the molecular deregulation of the *KEAP1* gene and the mRNA expression level in SCLC cells.

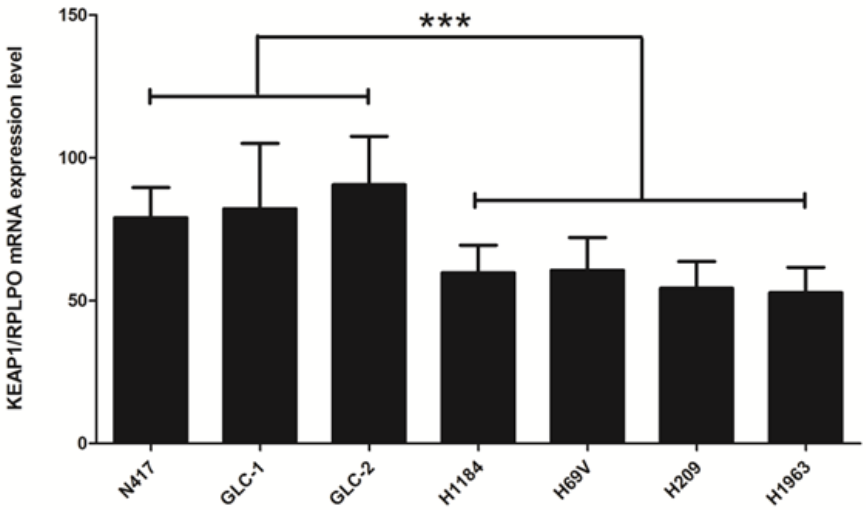

Figure 21. Expression level analysis (± standard error mean) of the *KEAP1* gene determined by RT-qPCR. The relative quantification was expressed as ratio marker (*KEAP1*/*RPLPO*).****p<0.001*.

The potential effects of the genetic and epigenetic alterations on the *KEAP1* gene were also investigated in SCLC cell lines by evaluating their effects on protein levels of KEAP1, NRF2, and NRF2 targets by western blot analysis. Specifically, we analyzed the AKR1C1 and TXNRD1, two proteins involved in the NRF2-cell mechanism defense system. As results, a significant lower KEAP1 protein level was

observed in cell lines with genetic/epigenetic deregulation of KEAP1 (**Figure 22A and 22B**) in comparison with N417 wild type cell line. Additionally, in the H209 cells, an protein abundance of AKR1C1 NRF2-dependent target gene was observed (**Figure 22C**). Finally, a significant abundance of transcripts of *AKR1C1* gene in KEAP1 genetic/epigenetic deregulated cell lines was underlined (**Figure 23A, 23B, 23C**).

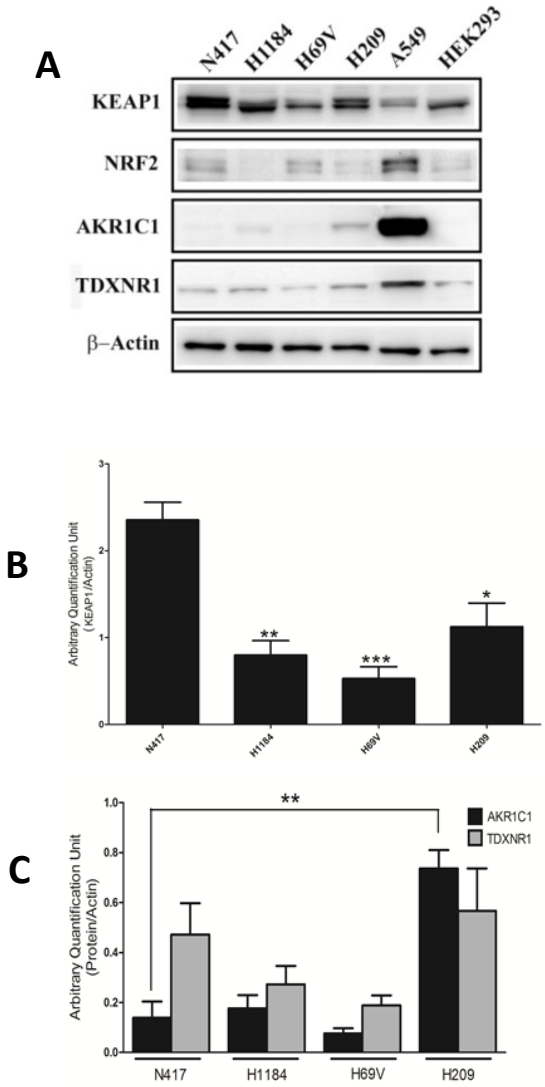

Figure 22. **(A)** Representative western blots analysis showing a comparison between the expression levels of the KEAP1, NRF2, AKR1C1 and TXNRD1 proteins in N417, H1184, H69V H209. A549 and HEK293 were used as a positive control for NRF2 and KEAP1. **(B-C)** Histograms showing the expression levels of the proteins normalized to actin. N=4). *$p<0.05$, **$p<0.01$, ***$p<0.001$.

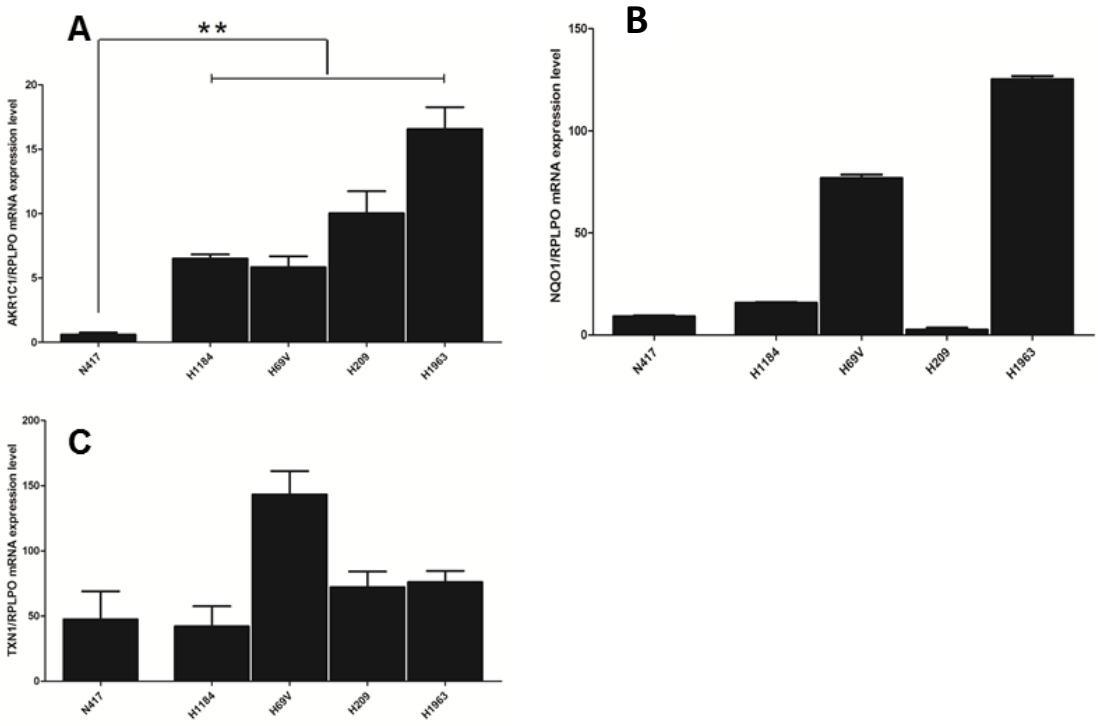

Figure 23. Comparison of mRNA expression level (± standard error mean) of *NRF2*-target enzymes **(A)** *AKR1C1*, *NQO1* **(B)** and *TXNRD1* **(C)** between SCLC cells with genetic/epigenetic alterations and the other SCLC lines. ***p<0.01*.

Moreover, the *NRF2* mRNA expression level was assessed in the set of four SCLC cell lines showing different values of CNV at the gene locus (https://cancer.sanger.ac.uk/cosmic). Expression in H209 (CNV=4) was found to be significantly higher than the mean of the expression levels observed in Hcc33 and H1184 (CNV=2) and was significantly higher than the expression level in H69V (CNV=1), (p=0.0058 and p=0.0022 respectively, t-test), (**Figure 24**).

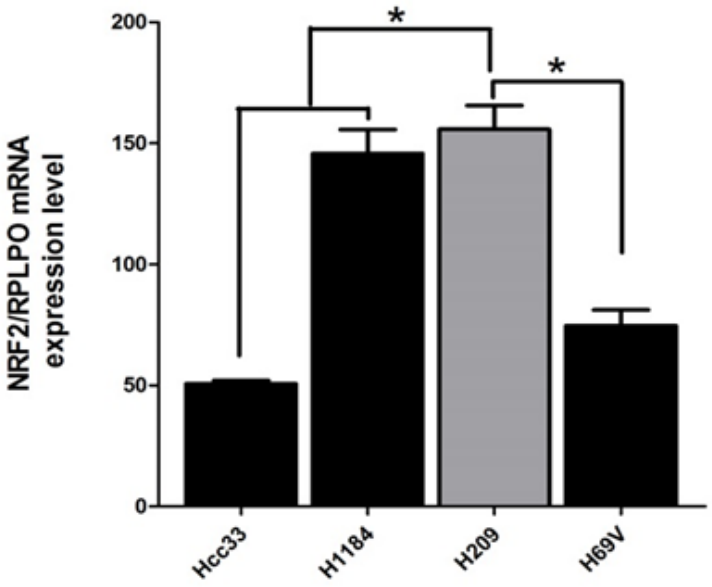

Figure 24. Expression level analysis (± standard error mean) of the *NFE2L2* gene determined by RT-qPCR. The relative quantification was expressed as ratio marker (*NFE2L2/RPLPO*).*$p<0.05$.

Finally, the cellular localization patterns of the KEAP1 and NRF2 proteins was also investigated in epigenetic H69V and H417 silenced cell lines by immunofluorescence analysis. In N417 cell line (having no alterations in *KEAP1* and *NFE2L2*) KEAP1 (green signal) and NRF2 (red signal) resulted mostly expressed in the cytosol (**Figure 25**), while in H69V cell line a predominantly nuclear localization of NRF2 was observed, suggesting an enhancement of its transcriptional activity on the ARE-genes.

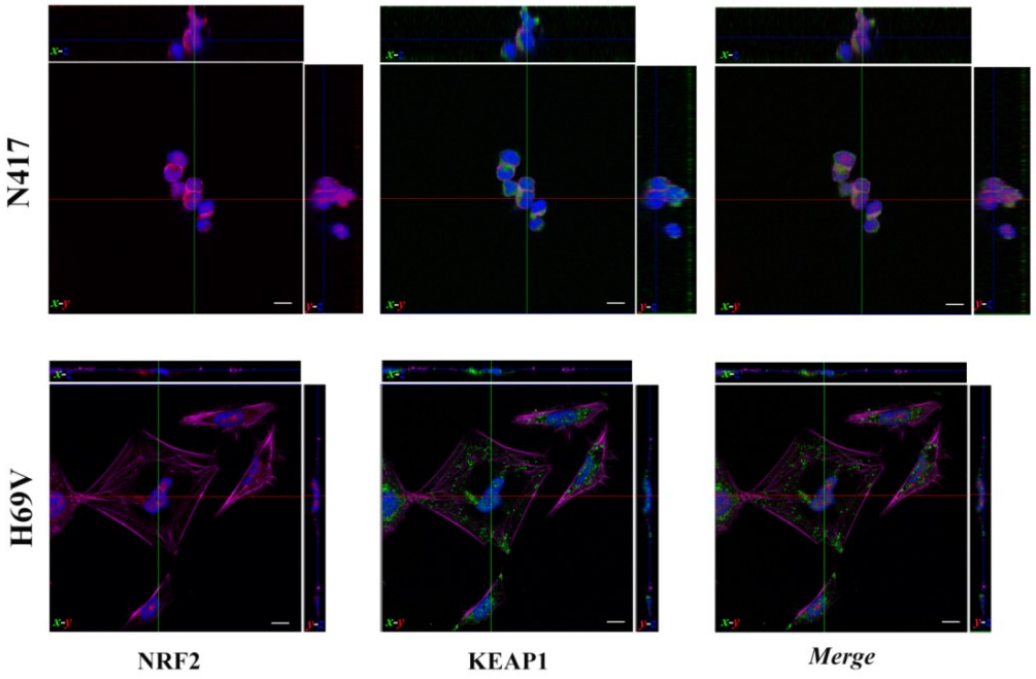

Figure 25. The proteins subcellular localizations were examined by immunostaining with anti-KEAP1 and anti-NRF2 antibody and examined with confocal microscopic. Blue= Nucleus. Magenta= Actin. Scale bar: 20µm.

The effects of epigenetic deregulation of *KEAP1* gene promoter on its transcript levels were clearly confirmed on H69V SCLC cell line by using 5-Aza-2'deoxycytidine (DAC) treatment ($p<0.05$, t-test). 5-aza-dC, an inhibitor of DNA methyltransferase, was added at a concentration of 5µM for 24h, 48h, and 72h. At each time points (24h, 48h, and 72h) cells were harvested for DNA and RNA isolation to interrogate the induction of the DNA demethylation and to analyze the *KEAP1* mRNA expression level. The results of qRT-PCR show a significant increase of *KEAP1* transcript during treatment (**Figure 26**).

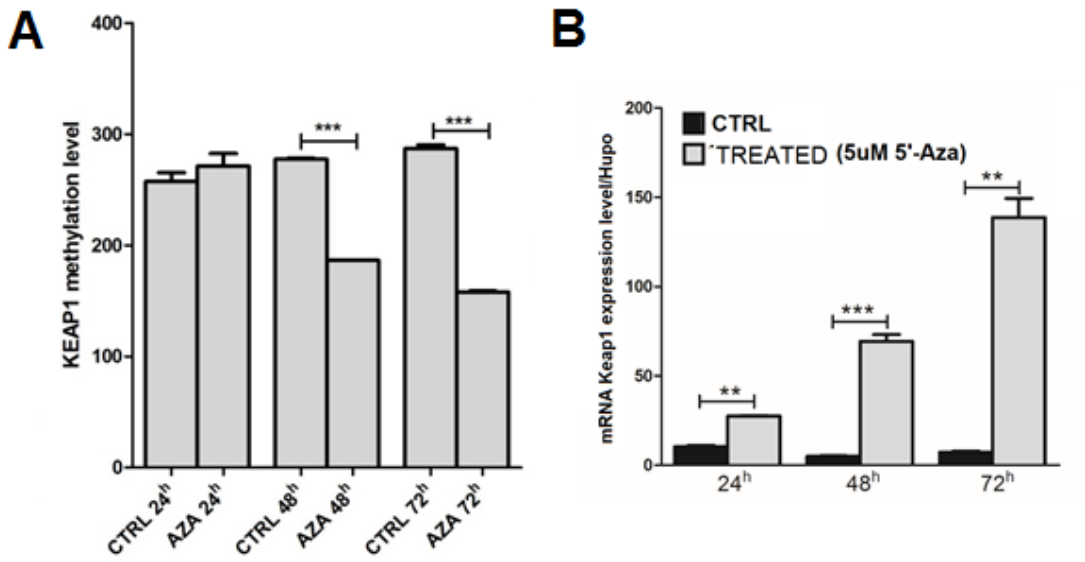

Figure 26. Changes in **A)** *KEAP1* promoter methylation levels and **B)** *KEAP1* mRNA transcript levels in the H69V cell line before and after treatment with 5-azacytidine at 24h, 48h, and 72h. Error bars indicate the standard deviation of three different experiments. *$p<0.05$,**$p<0.01$,***$p<0.001$.

5.3 EFFECTS OF *KEAP1* SILENCING IN SCLC CELL LINES ON NRF2 ACTIVITY

To a better evaluation and quantification of the effects of loss of expression/function of the *KEAP1* in SCLC on NRF2 modulation, a specific protocol of *KEAP1* genetic silencing using small interference RNA (siRNA) was optimized.

The efficiency of silencing was first evaluated using two different siRNAs having a complementary sequence to *KEAP1* exon4 (siRNA-1) and exon2 (siRNA-2). The most efficient *KEAP1* siRNA (siRNA-1) was then tested at different concentrations [15nM, 25nM, and 50 nM] and at different times of treatment (24h and 48h). The *KEAP1* siRNAs have been found to reduce the KEAP1 protein expression to approximately 35-70% of the total amount present at the control condition performed using a scrambled siRNA. In particular, it has been possible to observe a reduction of KEAP1 expression of 65%, 80% and 75% in N417, H1184, and H69V, respectively.

The *in vitro KEAP1* siRNA silencing procedure was assessed to evaluate the effects of *KEAP1* impairing on protein level modulation of KEAP1, NRF2, and its dependent targets genes (AKR1C1, TDXN1). Transcripts levels and protein levels were monitored in SCLC cell lines by RT-qPCR and Western blotting respectively (**Figure 27A, 27B, 27C**). In N417, H1184 and H69V cell lines were clearly observed that a variation of KEAP1 protein level produced a significant increase of NRF2 and its targets proteins levels ($p<0.05$, t-Test). By contrast, the variation of AKR1C1 was evident in the H1184 cell line, whereas the increase of TXNRD1 protein expression was observed in N417 and H69V. Our results indicate that *KEAP1* silencing affects the NRF2 targets expression levels in SCLC lines and whereby suggests that the impairment of KEAP1 activity is able to modulate the expression of some cytoprotective enzymes also in SCLC cells.

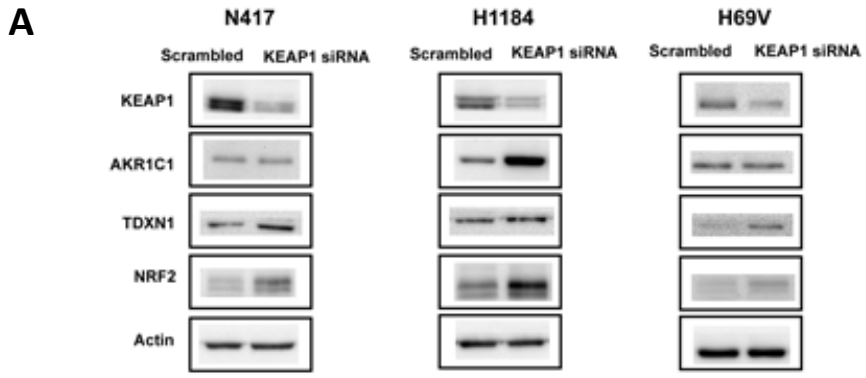

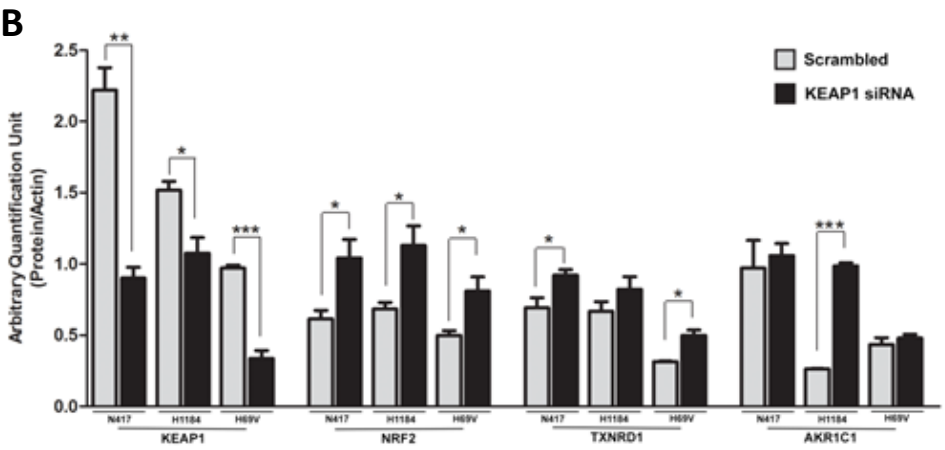

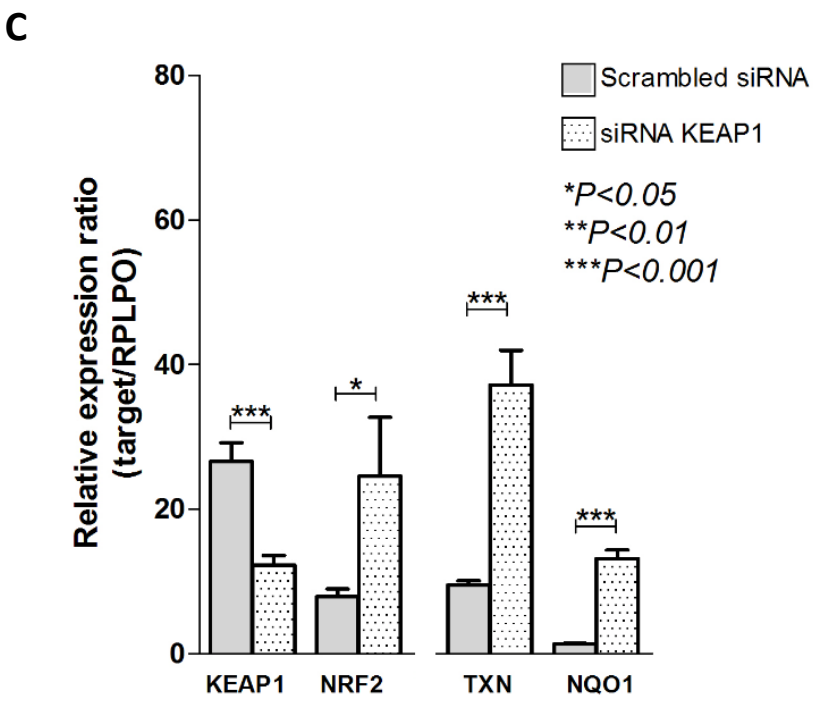

Figure 27. **(A)** Representative Western blots analysis showing the expression levels of KEAP1, NRF2, AKR1C1 and TXNRD1 proteins in N417, H1184 and H69V cell lines respectively. **(B)** Histograms showing the expression levels of the proteins normalized to actin (N=4). **(C)** Transcript levels variation of KEAP1, NRF2, TXN and NQO1 in H69V cell line under KEAP1 silencing. **p<0.05,**p<0.01,***p<0.001*.

5.4 ROLE OF KEAP1/NRF2 PATHWAY IN PHARMACOLOGICAL RESPONSE OF SCLC CELL LINES

Taking into account the well-known role of the KEAP1/NRF2 pathway in the chemotherapy resistance of many solid tumors, pharmacological tests were carried out to assess if this pathway was also implicated in the SCLC cell lines response to two agents currently used in the SCLC clinical setting: cisplatin and etoposide. Etoposide works by blocking the Topoisomerase 2 which is necessary for cancer cells division. If this enzyme is blocked, the cell's DNA gets tangled up and the cell cannot divide. Cisplatin works by interfering with DNA replication too and killing the fastest proliferating cell.

To establish the best concentration of chemotherapic (IC50) to use in the *KEAP1* silencing experiments under drugs treatments, the H69V and H1184 cell lines were firstly treated with increasing concentrations of etoposide and cisplatin. A significant effect on cell viability of H69V was observed already after 0.1uM of Cisplatin with an IC50 at 20uM. By contrast, Etoposide showed its effect on H69V viability at 5uM and an IC50 at 40uM. The H1184 cell line showed higher pharmacological resistance than H69V, in fact, range concentration compounds are wider than H69V. It was possible to observe Cisplatin effects on H1184 viability after 0.5uM and an IC50 of 100uM, whereas Etoposide induces viability impairing after 5uM of treatment and IC50 is 100mM (**Figure 28**).

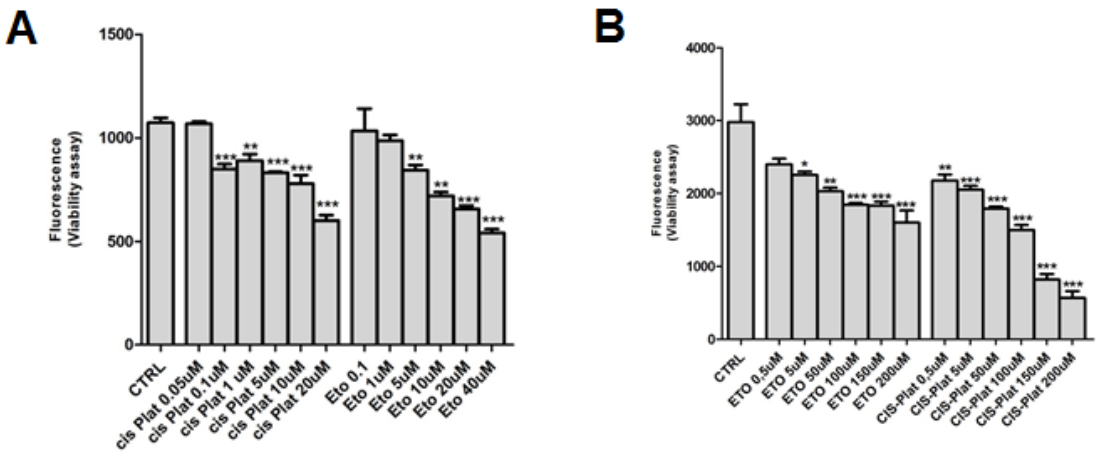

Figure 28. **A)** Cisplatin and Etoposide significantly inhibit the viability of H69V cell line. The cell was treated with six different concentrations of pharmacological compounds for 24h. **B)** Cisplatin and Etoposide significantly inhibit the viability of H1184 cell line. Cells were treated with six different concentrations of pharmacological compounds for 24h. The data represented means ± S.E of five treatments. *$p<0.05$,**$p<0.01$,***$p<0.001$.

To further assess the possible role of *KEAP1* silencing in SCLC resistance to cisplatin and etoposide treatments, we decide to use the H69V cell line as the first instance to test drugs effect alone and in combination (20uM and 10 uM). We

evaluated the effects of *KEAP1* silencing in terms of cellular apoptosis and cell viability. Western blot analysis showed that both BCL2 and cleaved CAS-3 decreased in cell treated with etoposide (40uM, 24h) and cisplatin (20uM, 24h) under KEAP1 silencing (**Figures 29A, 29B and 29C**) in statistically significant manner respect of treated non-silenced control. Our first results support the idea that *KEAP1* can modulate the chemoresistance of SCLC via NRF2 interaction by decreasing the effect of chemotherapies. Anyhow, additional through monitoring caspase 7 levels and by performing proliferation assays are demanded to confirm our hypothesis.

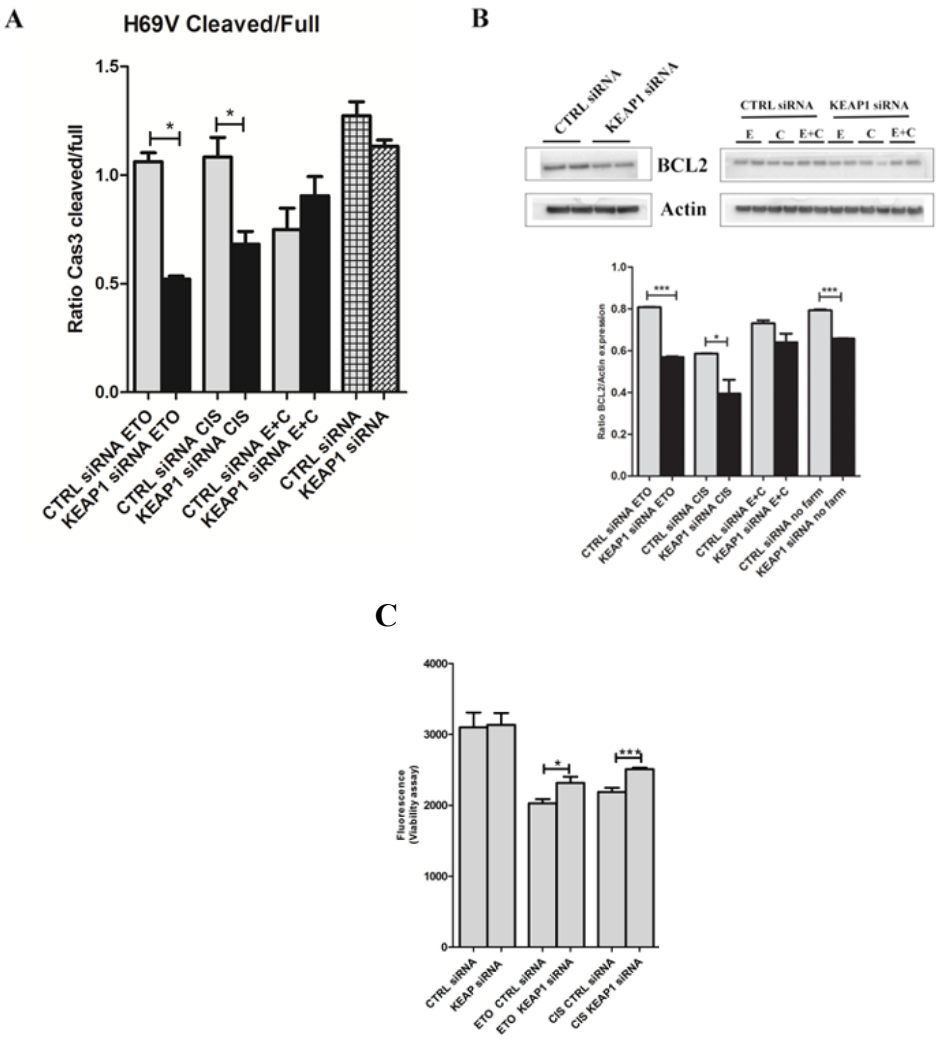

Figure 29. A-B) KEAP1 RNAi experiments in H69V cell line. Representative immunoblot analysis of caspase 3 and BCL2 expression in H69V after silencing and pharmacological treatment. Actin was revealed in parallel for each sample and used as a non-targeted internal control housekeeping gene for the densitometric analysis. E, Etoposide. C, Cis-Platin. E+C, Combination.KEAP1 and NRF2 protein expression levels in H69V cell line. The histogram shows the analysis of 3 independent experiments performed 48 after transfection with the siRNAs *(*p<0.05*). Statistically significant differences were computed using Student-t-test. **C)** The viability of H69V cell line after *KEAP1* silencing under cisplatin and etoposide treatment. The cell was treated with specific concentrations of pharmacological compounds for 24h. The data represented means ± S.E of five treatments. C-E means Cisplatin/Etoposide.**p<0.05,**p<0.01,***p<0.001*.

5.5 EFFECTS OF *KEAP1* SILENCING ON NOTCH-KEAP1/NRF2 PATHWAYS INTERPLAY

To investigate the existence of a crosstalk between NOTCH and KEAP1/NRF2 pathways and clarify its role in SCLC tumorigenesis, we firstly evaluated by Western Blot analysis the NOTCH1 protein levels in a collection of available SCLC cell lines. Results show an elevated NOTCH1 protein level in H69V cell line (**Figure 30**), thus suggesting this specific cell line as the most suitable one for NRF2/NOTCH crosstalk and pharmacological investigation under *KEAP1* silencing in SCLC.

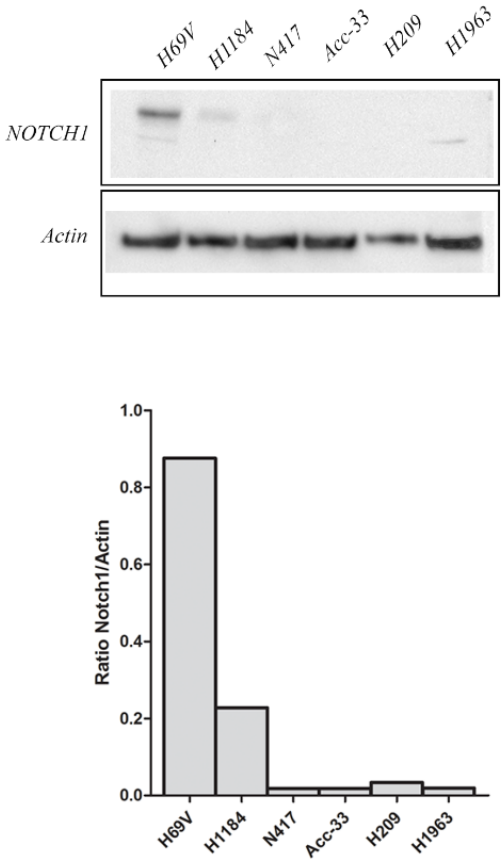

Figure 30. Representative Western blot analysis showing the expression levels of NOTCH1 protein on a collection of SCLC cell lines. After densitometric analysis of the bands which was performed with ImageJ software, the amount of NOTCH1 signaling protein was normalized to actin.

The *in vitro KEAP1* siRNA silencing procedure was then re-assessed to evaluate the effects of *KEAP1* impairing on transcript and protein level modulation of

NOTCH and its dependent targets genes (HES1 and DLL3). Transcripts levels and protein levels were monitored in H69V cell line by RT-qPCR and Western blotting respectively (**Figure 31A, 31B)**. In H69V cell lines was clearly observed that KEAP1 silencing induced a significant increase of NOTCH1, HES1 and DLL3 transcripts levels (**Figure 31A**). By contrast, only HES1 resulted significantly increased at protein levels (**Figure 31B**). Our results globally indicate that *KEAP1* silencing affects some critical points of the NOTCH pathway both at transcript and protein level in SCLC cell lines.

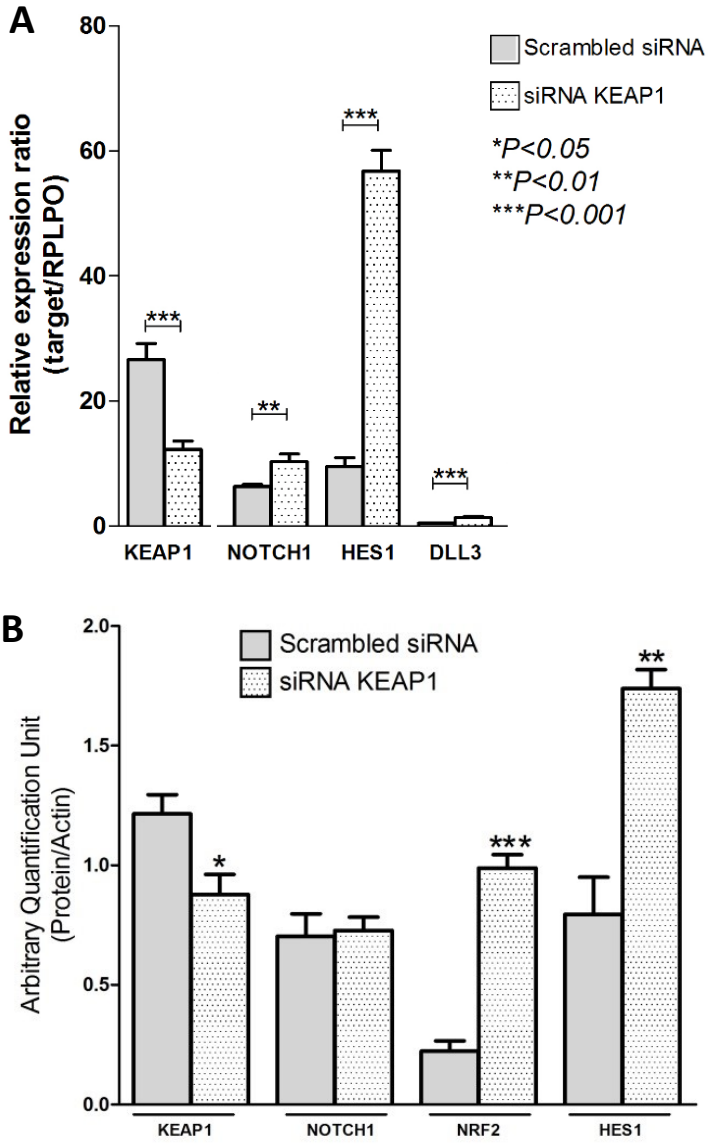

Figure 31. **A)** Transcript levels variation of KEAP1, NOTCH1, HES1, and DLL3 in H69V cell line under KEAP1 silencing **p<0.05,**p<0.01,***p<0.001*. **B)** Representative immunoblot analysis of KEAP1, NOTCH1, NRF2, and HES1 on H69V cell line under KEAP1 silencing. After densitometric analysis of the bands which was performed with ImageJ software, the amount of these proteins was normalized to actin. **p<0.05,**p<0.01,***p<0.001.*

5.6 EFFECTS OF THE *KEAP1* SILENCING THROUGH THE MODULATION OF NRF2/NOTCH CROSSTALK IN H69V CELL UNDER γ-SECRETASE INHIBITOR (DAPT) TREATMENT

To evaluate the role of *KEAP1* as a potential predictive marker of response to DAPT treatment in cell lines we firstly established on H69V the best concentration of DAPT to use in the *KEAP1* siRNA experiments. Specifically, the H69V cell line was firstly treated with increasing concentration of DAPT alone (50uM, 65uM 85uM, 100uM, 24h) that inhibited GSI production and potentiated the apoptotic effects by blocking the NOTCH signaling pathway. γ-secretase serves a key function in the NOTCH signal pathway: γ-secretase blockage may suppress the cleavage of Notch receptor and block signaling transduction. The inhibition of NOTCH1 signaling with small molecule inhibitors of the γ-secretase complex (GSI) induces cell cycle arrest and apoptosis in solid tumors [168]. Overexpression of NOTCH1 levels also resulted in increased expression of snail homolog 1, a transcription factor that induces EMT, and reduced expression of adhesion molecules, such as E-cadherin [169].

Western Blot analysis showed a statistically significant decrease of NOTCH1 expression levels under DAPT pharmacological effects (65 uM and 100 uM, 24h) on this cell line compared to control (**Figure 32**). According to *Cao and coworkers* [166] it was established the best concentration of γ-secretase inhibitor to use in *KEAP1* silencing experiments as 100 uM.

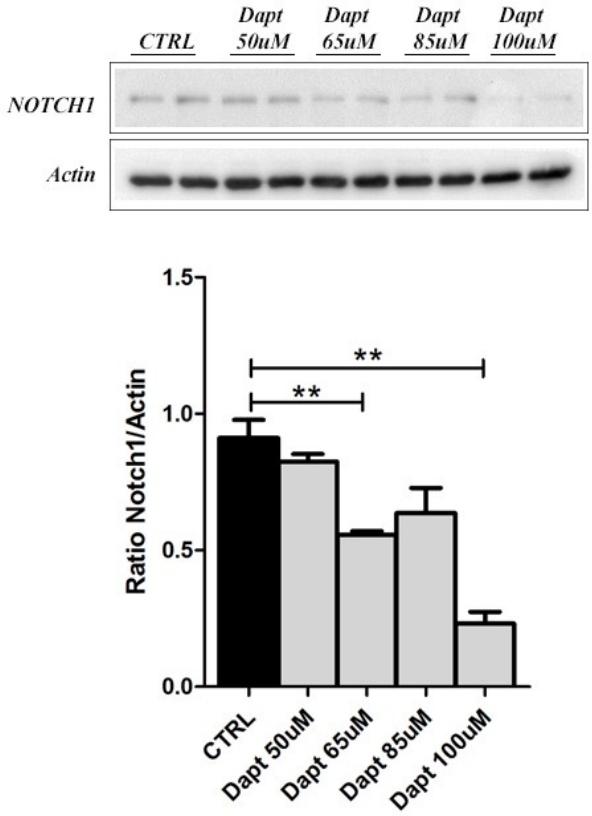

Figure 32. Representative Western blot analysis showing the expression levels of NOTCH1 protein on H69V cell line under DAPT treatment. The cell was treated with four different concentrations of DAPT compound for 24h. After densitometric analysis of the bands which was performed with ImageJ software, the amount of NOTCH1 signaling protein was normalized to actin.**p<0.01.*

The H69V has been seeded in 12 Multi-Well plate and transfected at the same time with Lipofectamine RNAiMAX and siRNA Scrambled (CTRL) and *KEAP1* siRNA. Each experiment was performed in triplicates. After 48 hours of transfection, cell line has been treated with DAPT and after an additional 24 hours, cell lines have been harvested and used to extract RNA and proteins, respectively. Gene expression levels were evaluated as the first instance at transcript level for *KEAP1*, *NRF2,* some of the NRF2 targets (*NQO1, TXNRD1),* NOTCH1 and some of NOTCH target genes (*HES1* and *DLL3*), **(Figure 33)**. Additionally, western blot analysis was performed to

assess the effect of *KEAP1* silencing on protein levels (KEAP1, NRF2, NOTCH, HES1, E-cadherin, c-MYC) and normalized to actin **(Figure 34)**.

As expected results showed that *KEAP1* silencing results in a significant decrease of *KEAP1* transcript levels, following by a significant increase in the mRNA levels of NRF2, NOTCH1, DLL3, and HES1. These variations were concordant both in experiments without DAPT and under DAPT treatment in H69V cell line. By contrast, no significant variations at protein levels were observed for NOTCH1 and HES1 proteins levels, whereas a significant increase in E-cadherin and decrease in c-MYC levels were observed in treated and non-treated cells (**Figure 33, 34**).

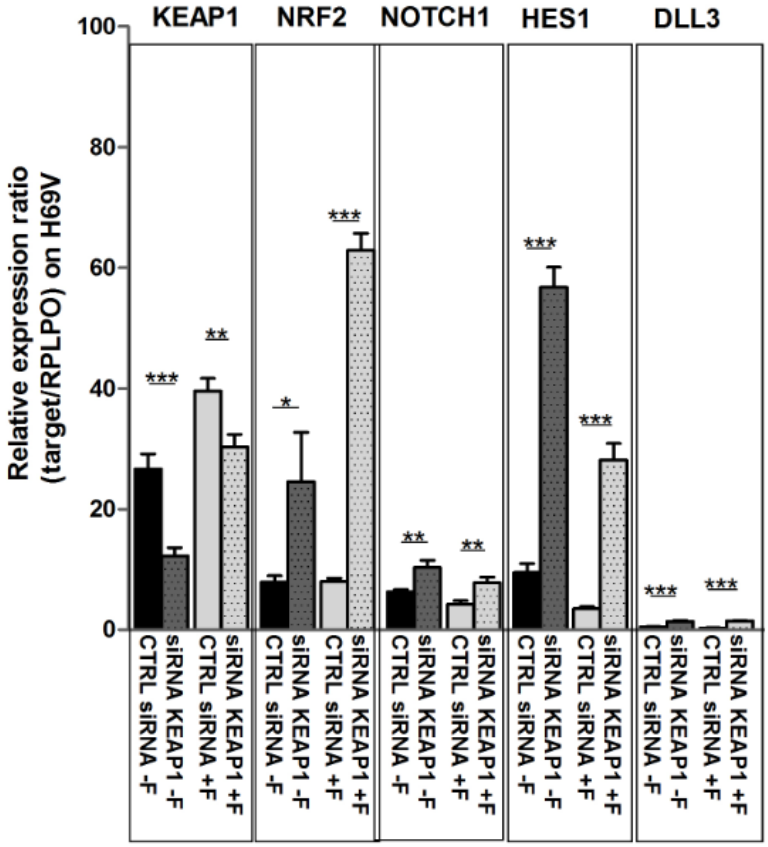

Figure 33. Comparison of mRNA expression level (± standard error mean) of *KEAP1, NRF2, NOTCH1, HES1, DLL3*. Changes in mRNA transcript levels on H69V cell line *KEAP1* silenced treated with DAPT at 24h. Relative expression was obtained from the ratio between each target and *RPLPO*. Error bars indicate the standard deviation of three different experiments. *$p<0.05$, **$p<0.01$, ***$p<0.001$.

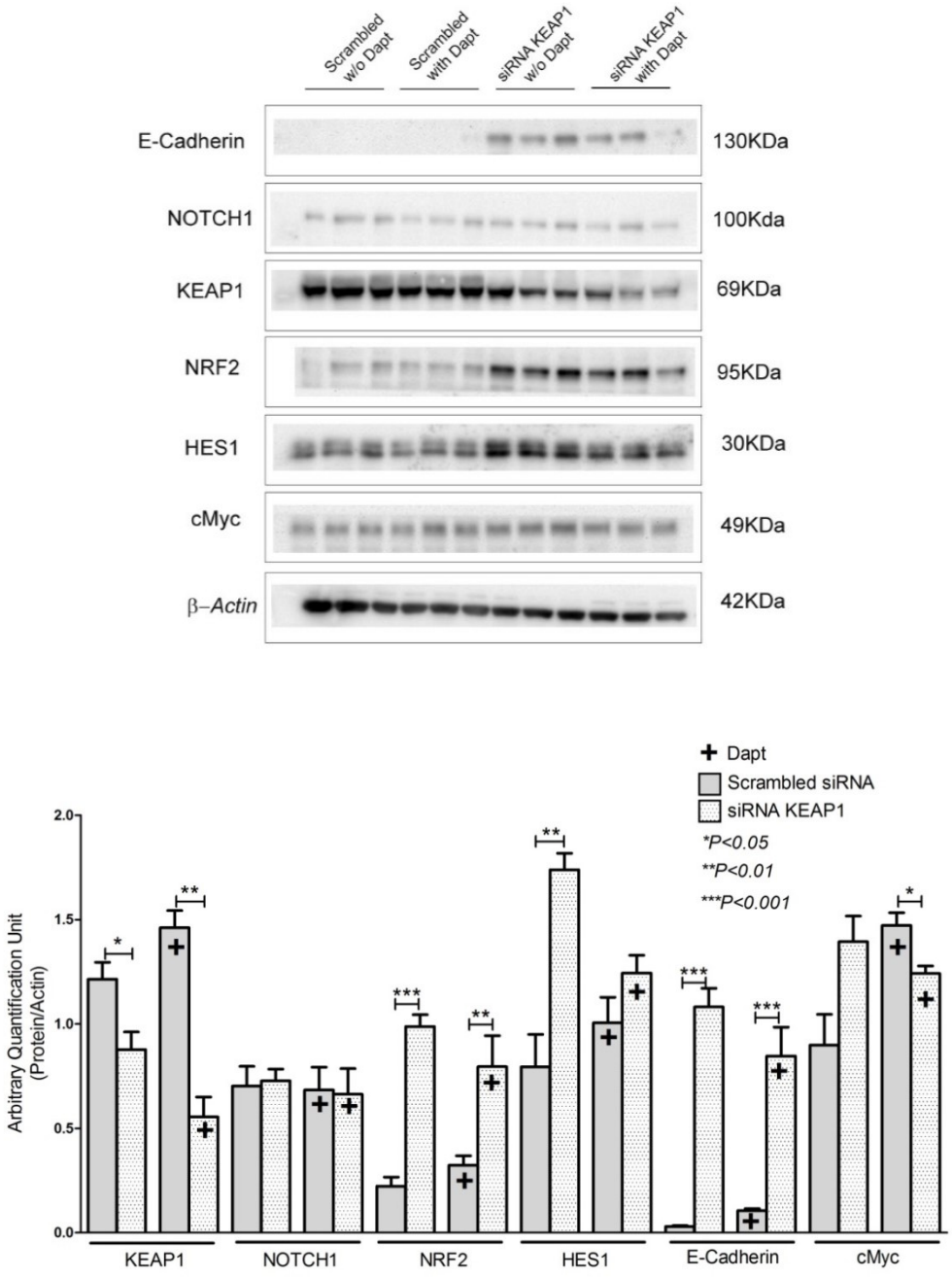

Figure 34. Representative Western blot analysis showing the expression levels of NOTCH1, KEAP1, NRF2, HES1, E-Cadherin, cMyc proteins on H69V after *KEAP1* silencing and pharmacological DAPT treatment. The cell was treated with four different concentrations of DAPT compound for 24h. A scrambled siRNA was used as a control. Actin was revealed in parallel for each sample and used as a non-targeted internal control housekeeping gene for the densitometric analysis. After densitometric analysis of the bands which was performed with ImageJ software, the amount of these proteins was normalized to actin. *$p<0.05$, **$p<0.01$, ***$p<0.001$.

A viability assay was also performed by Presto Blue to assess the effect on viability after KEAP1 reduction and DAPT treatment at the same time. A statistically significant increase in cell viability after *KEAP1* silencing without compound (36h) was observed. By contrast, no significant variations were noticed under DAPT treatment (**Figure 35**).

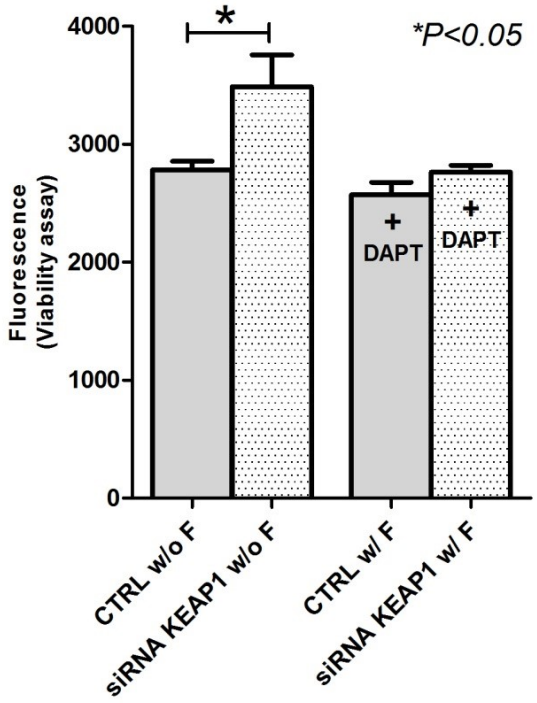

Figure 35. The viability of H69V cell line after *KEAP1* silencing and DAPT treatment. Histograms show the cells not treated and treated with specific concentrations of pharmacological compound for 36h. **p<0.05*.

CHAPTER VI

6. DISCUSSION

Lung cancer is the leading cause of cancer-related death worldwide [170, 171]. Among its different histologies, SCLC represents the most aggressive pulmonary malignancy and accounts for approximately 20% of lung cancers. Despite an initial chemotherapy and radiation response, it recurs rapidly after primary treatment by the development of resistance, with only 6% of patients surviving 5 years from the first diagnosis [151].

In the last decade the efficacy of targeting key "growth drivers" in cancer treatment of a small subset of lung cancers are emerged and encouraged the investigation on new target proteins that are selectively expressed in cancer cells that should suggest a novel, additional pharmacological options [54].

NRF2 is a key regulator of the cell adaptive response to radical oxidant species and xenobiotics through and exerts its activity through the interaction with its negative regulator, the KEAP1. Several studies suggested that the activation of NRF2 protects against chronic such as cardiovascular diseases, lung inflammation, and fibrosis diabetes and nephropathy. However, in recent years the dark side of NRF2 has emerged and growing evidence suggests that NRF2 constitutive upregulation is associated with cancer development, progression and contributes to both intrinsic and acquired chemo- and radio-resistance resistance [172].

The NOTCH family (NOTCH1–4) are transmembrane proteins, which interact with ligands of the Delta and/or Jagged/Serrate family. NOTCH pathway is one of the most important cells signaling systems in cancers and its deregulation is well reported in SCLC [43, 173, 174]. In the context of tumorigenesis it can be either oncogenic or anti-proliferative and in SCLC has an inhibitory cell function, and modulate tumor cells invasion and metastasis [98]. Both NRF2 and NOTCH are transcription factors and their related pathways were discovered and described independently. However, recent emerging data showed that NRF2/NOTCH crosstalk influences cytoprotection and enhances maintenance of cellular homeostasis and tissue organization through actions on cell proliferation kinetics and cell fate

determinants of stem cell renewal and cell differentiation [121]. Interestingly, NRF2 and NOTCH signaling mutually regulate each other as shown by that *NOTCH1* is an *NRF2* target gene and *NRF2* is a downstream gene regulated by NOTCH signaling [83].

To date, while *NFE2L2* and *KEAP1* mutations are less investigated in SCLCs, *NOTCH1* appears in the list as frequently mutated genes in this tumor types. This observation led to the speculative notion that if an aberrant NRF2/NOTCH crosstalk exists in SCLC, it should be induced by genetic and epigenetic lesions in key genes of both pathways and, by consequence, should play a critical role in tumorigenesis and progression of the disease.

We propose to investigate the molecular basis of NRF2/NOTCH crosstalk deregulation in SCLC and its impact on the modulation of cellular defence systems, cell proliferation, and differentiation and to evaluate the impact of this impairing systems on response to conventional chemotherapies and NOTCH inhibitors.

Our genetic and epigenetic investigations on KEAP1/NRF2 and NOTCH on a collection of SCLC cell lines confirmed that *KEAP1* and NRF2 genes point mutations affect only marginally the SCLC histology and is typically related to non-small cell lung cancer (NSCLC), [175]. Only one just reported aminoacidic change in the DGR domain of the *KEAP1* gene has been in fact identified in H1184 cell line and is already reported to affect the KEAP1 ability to bind NRF2 and promotes its proteasomal degradation in the cytoplasmatic compartment of cells [176]. No mutations were found in the NRF2 gene and this result partially confirms the marginal contribution of point mutations of KEAP1/NRF2 pathway deregulation in SCLCs [43]. Despite these negative results, an unreported epigenetic alteration of the KEAP1/NRF2 axis has revealed and frequent aberrant promoter methylation of the *KEAP1* gene was described for the first time in 5 out of 12 SCLC cell lines (42%). Differential CpGs hypermethylation status in the promoter region of *KEAP1* scanned by pyrosequencing indicated that the first seven single CpG sites of the *KEAP1* promoter are more subjected to an epigenetic control by methylation than the other ones. Since they map among consensus sequencing for several transcription sites, we hypothesize that they are critical for the modulation of *KEAP1* transcription [145, 177] and suggest that these mechanisms should be a possible new modulation

mechanism of this pathway in SCLC. *In vitro* experiments on SCLC cell lines H69V with the demethylating agent 5-aza-2'-deoxycytidine corroborated this hypothesis and confirmed that epigenetic silencing in SCLC of the *KEAP1* gene was responsible to the modulation of the *KEAP1* at transcript and protein levels, induces nuclear accumulation of NRF2 and enhances transcriptional induction of xenobiotic metabolism enzymes. Additional short interfering RNA inhibition experiments of the *KEAP1* was also conducted to corroborate the idea that *KEAP1* silencing modulates NRF2 also in the SCLC. A significant variable increase in NRF2 and some of its targets (AKR1C1, TXN1, and NQO1) mRNA and protein levels in different cell lines was observed. AKR1C1 is a member of the AKR1C family and it is believed to be involved in carcinogen metabolism. It is highly expressed in lung tumor tissues and it is characterized by ARE in the promoter region which is regulated by NRF2 [178]. TXNRD1 is a seleno-protein that plays a role in enzyme catalysis at the active site of the protein and acts into the NRF2 pathway as a component of a redox-sensitive trigger [179]. NQO1, which is tested by gene expression, plays a critical factor for Quinone metabolism and toxicity and after the dissociation with KEAP1, activated NRF2 enriched in the nucleus and mediated NQO1 induction by binding to endogenous ARE [180]. Globally, these findings corroborated the idea of a strong modulation of NRF2 activity by KEAP1 protein also in SCLC cell line.

After proving evidence of KEAP1/NRF2 interplay in SCLC and taking into account the well-known role of the KEAP1/NRF2 pathway in chemotherapy resistance, pharmacological tests were performed to investigate if the *KEAP1* suppression should have an impact on SCLC as a molecular marker to predict tumor cell response to cisplatin and etoposide agents. Results from viability assays and measurements of BCL2 and CAS-3 in the H69V cell line suggested that *KEAP1* silencing should effectively impact on the drug response though contrasting their effects on tumor cells. Additional pharmacological evaluation is planned in this context to confirm our findings.

Accumulating data have demonstrated that NOTCH1 plays a critical role in cell fate decisions through cell-cell communication and its activity is linked to NRF2 modulation in solid tumors [83]. We showed in H69V cell line that *KEAP1* silencing controls NOTCH, HES-1 and DLL3 expression mainly at transcript levels and has an

only partial effect on their protein levels. So, it is not clear if the negative regulatory role of KEAP1 significantly modulates the NRF2/NOTCH interplay or it exists in SCLC independently from KEAP1 activity. Pharmacological treatment of H69V cell line using DAPT gives results also corroborate the idea that NRF2/NOTCH interplay in the context of resistance to treatment is poorly linked to KEAP1 expression. Under DAPT treatment, *KEAP1* silenced cells did not show in fact a significant variation in NOTCH and HES-1 in protein levels or changes in the viability of tumor cells.

In summary, we demonstrated that KEAP1/NRF2 axis is controlled by methylation in SCLC cell lines and that silencing of KEAP1 by siRNA induces upregulation of NRF2 with consequent increase of cells chemoresistance. KEAP1 modulation also interfered with NOTCH1, HES1, and DLL3 transcription, so we can suggest cooperation of these two pathways in tumorigenesis of SCLC. We plan to corroborate these data by performing additional NRF2 silencing experiments under different pharmacological treatment and by analyzing additional SCLC cell lines. The findings of this present study might help to guide the identification of new therapeutic targets of this aggressive histology of lung cancer.

BIBLIOGRAPHY

1. Thun MJ, L.M., Cerhan and H.C. JR, Schottenfeld D, *Cancer Epidemiology and Prevention*, O.U. Press, Editor. 2018: New York. p. 519-542.

2. Bray, F., et al., *Global cancer statistics 2018: GLOBOCAN estimates of incidence and mortality worldwide for 36 cancers in 185 countries.* CA Cancer J Clin, 2018 68(6): p. 394-424.

3. Lortet-Tieulent, J., et al., *Convergence of decreasing male and increasing female incidence rates in major tobacco-related cancers in Europe in 1988-2010.* Eur J Cancer, 2015. 51(9): p. 1144-63.

4. The, L., *GLOBOCAN 2018: counting the toll of cancer.* Lancet, 2018. 392(10152): p. 985.

5. Islami, F., et al., *Proportion and number of cancer cases and deaths attributable to potentially modifiable risk factors in the United States.* CA Cancer J Clin, 2017. 68(1): p. 31-54.

6. Hecht, S.S., *Tobacco smoke carcinogens and lung cancer.* J Natl Cancer Inst, 1999. 91(14): p. 1194-210.

7. Pleasance, E.D., et al., *A small-cell lung cancer genome with complex signatures of tobacco exposure.* Nature, 2009. 463(7278): p. 184-90.

8. Hecht, S.S. and E. Szabo, *Fifty years of tobacco carcinogenesis research: from mechanisms to early detection and prevention of lung cancer.* Cancer Prev Res (Phila), 2014. 7(1): p. 1-8.

9. Max, W., H.Y. Sung, and Y. Shi, *Deaths from secondhand smoke exposure in the United States: economic implications.* Am J Public Health, 2012. 102(11): p. 2173-80.

10. Vieira, A.R., et al., *Fruits, vegetables and lung cancer risk: a systematic review and meta-analysis.* Ann Oncol, 2016. 27(1): p. 81-96.

11. Xiong, W.M., et al., *The association between human papillomavirus infection and lung cancer: a system review and meta-analysis.* Oncotarget, 2016. 8(56): p. 96419-96432.

12. Yu, Y.H., et al., *Increased lung cancer risk among patients with pulmonary tuberculosis: a population cohort study.* J Thorac Oncol, 2011. 6(1): p. 32-7.

13. Field, R.W. and B.L. Withers, *Occupational and environmental causes of lung cancer.* Clin Chest Med, 2012. 33(4): p. 681-703.

14. Lu, G., et al., *Arsenic exposure is associated with DNA hypermethylation of the tumor suppressor gene p16.* J Occup Med Toxicol, 2014. 9(1): p. 42.

15. Markowitz, S.B., et al., *Asbestos, asbestosis, smoking, and lung cancer. New findings from the North American insulator cohort.* Am J Respir Crit Care Med, 2013. 188(1): p. 90-6.

16. Kanwal, M., X.J. Ding, and Y. Cao, *Familial risk for lung cancer.* Oncol Lett, 2017. 13(2): p. 535-542.

17. Moorthy, B., C. Chu, and D.J. Carlin, *Polycyclic aromatic hydrocarbons: from metabolism to lung cancer.* Toxicol Sci, 2015. 145(1): p. 5-15.

18. Stejskalova, L., Z. Dvorak, and P. Pavek, *Endogenous and exogenous ligands of aryl hydrocarbon receptor: current state of art.* Curr Drug Metab, 2016. 12(2): p. 198-212.

19. Liu, X., et al., *Meta-analysis of GSTM1 null genotype and lung cancer risk in Asians.* Med Sci Monit, 2014. 20: p. 1239-45.

20. Hecht, S.S., *Lung carcinogenesis by tobacco smoke.* Int J Cancer, 2012. 131(12): p. 2724-32.

21. Travis, W.D., et al., *The 2015 World Health Organization Classification of Lung Tumors: Impact of Genetic, Clinical and Radiologic Advances Since the 2004 Classification.* J Thorac Oncol, 2015. 10(9): p. 1243-1260.

22. Rossi, R.E., et al., *Chromogranin A as a predictor of radiological disease progression in neuroendocrine tumours.* Ann Transl Med, 2015. 3(9): p. 118.

23. Sholl, L.M., *The Molecular Pathology of Lung Cancer.* Surg Pathol Clin, 2016. 9(3): p. 353-78.

24. Lantuejoul, S., et al., *[New WHO classification of lung adenocarcinoma and preneoplasia].* Ann Pathol, 2016. 36(1): p. 5-14.

25. Caplin, M.E., et al., *Pulmonary neuroendocrine (carcinoid) tumors: European Neuroendocrine Tumor Society expert consensus and recommendations for best practice for typical and atypical pulmonary carcinoids.* Ann Oncol, 2015. 26(8): p. 1604-20.

26. Hendifar, A.E., A.M. Marchevsky, and R. Tuli, *Neuroendocrine Tumors of the Lung: Current Challenges and Advances in the Diagnosis and Management of Well-Differentiated Disease.* J Thorac Oncol, 2017. 12(3): p. 425-436.

27. Pelosi, G., et al., *Large cell carcinoma of the lung: a tumor in search of an author. A clinically oriented critical reappraisal.* Lung Cancer, 2015. 87(3): p. 226-31.

28. Travis, W.D., *Pathology and diagnosis of neuroendocrine tumors: lung neuroendocrine.* Thorac Surg Clin, 2014. 24(3): p. 257-66.

29. Pelosi, G., et al., *Classification of pulmonary neuroendocrine tumors: new insights.* Transl Lung Cancer Res, 2017. 6(5): p. 513-529.

30. Bernhardt, E.B. and S.I. Jalal, *Small Cell Lung Cancer.* Cancer Treat Res, 2016. 170: p. 301-22.

31. Thunnissen, E., et al., *The Use of Immunohistochemistry Improves the Diagnosis of Small Cell Lung Cancer and Its Differential Diagnosis. An International Reproducibility Study in a Demanding Set of Cases.* J Thorac Oncol, 2017. 12(2): p. 334-346.

32. van Meerbeeck, J.P. and D. Ball, *Small-cell lung cancer: local therapy for a systemic disease?* Lancet, 2011. 385(9962): p. 9-10.

33. Kay, F.U., et al., *Revisions to the Tumor, Node, Metastasis staging of lung cancer (8(th) edition): Rationale, radiologic findings and clinical implications.* World J Radiol, 2017. 9(6): p. 269-279.

34. Detterbeck, F.C., et al., *The Eighth Edition Lung Cancer Stage Classification.* Chest, 2017. 151(1): p. 193-203.

35. Rusch, V.W., et al., *The IASLC lung cancer staging project: a proposal for a new international lymph node map in the forthcoming seventh edition of the TNM classification for lung cancer.* J Thorac Oncol, 2009. 4(5): p. 568-77.

36. Stinchcombe, T.E., *Current Treatments for Surgically Resectable, Limited-Stage, and Extensive-Stage Small Cell Lung Cancer.* Oncologist, 2017. 22(12): p. 1510-1517.

37. Goldstraw, P., et al., *The IASLC Lung Cancer Staging Project: Proposals for Revision of the TNM Stage Groupings in the Forthcoming (Eighth) Edition of the TNM Classification for Lung Cancer.* J Thorac Oncol, 2016. 11(1): p. 39-51.

38. Schmid, S. and M. Fruh, *Immune checkpoint inhibitors and small cell lung cancer: what's new?* J Thorac Dis, 2018. 10(Suppl 13): p. S1503-S1508.

39. Peifer, M., et al., *Integrative genome analyses identify key somatic driver mutations of small-cell lung cancer.* Nat Genet, 2016. 44(10): p. 1104-10.

40. Santarpia, M., et al., *Targeted drugs in small-cell lung cancer.* Transl Lung Cancer Res, 2016. 5(1): p. 51-70.

41. Umemura, S., et al., *Therapeutic priority of the PI3K/AKT/mTOR pathway in small cell lung cancers as revealed by a comprehensive genomic analysis.* J Thorac Oncol, 2014. 9(9): p. 1324-31.

42. Kaiser, U., et al., *Expression of bcl-2--protein in small cell lung cancer.* Lung Cancer, 1996. 15(1): p. 31-40.

43. George, J., et al., *Comprehensive genomic profiles of small cell lung cancer.* Nature, 2015. 524(7563): p. 47-53.

44. Rekhtman, N., et al., *Next-Generation Sequencing of Pulmonary Large Cell Neuroendocrine Carcinoma Reveals Small Cell Carcinoma-like and Non-Small Cell Carcinoma-like Subsets.* Clin Cancer Res, 2016. 22(14): p. 3618-29.

45. Saunders, L.R., et al., *A DLL3-targeted antibody-drug conjugate eradicates high-grade pulmonary neuroendocrine tumor-initiating cells in vivo.* Sci Transl Med, 2015. 7(302): p. 302ra136.

46. Byers, L.A., et al., *Proteomic profiling identifies dysregulated pathways in small cell lung cancer and novel therapeutic targets including PARP1.* Cancer Discov, 2012. 2(9): p. 798-811.

47. Rudin, C.M., et al., *Comprehensive genomic analysis identifies SOX2 as a frequently amplified gene in small-cell lung cancer.* Nat Genet, 2012. 44(10): p. 1111-6.

48. Kalari, S., et al., *The DNA methylation landscape of small cell lung cancer suggests a differentiation defect of neuroendocrine cells.* Oncogene, 2013. 32(30): p. 3559-68.

49. Poirier, J.T., et al., *DNA methylation in small cell lung cancer defines distinct disease subtypes and correlates with high expression of EZH2.* Oncogene, 2015. 34(48): p. 5869-78.

50. Karlsson, A., et al., *Genome-wide DNA methylation analysis of lung carcinoma reveals one neuroendocrine and four adenocarcinoma epitypes associated with patient outcome.* Clin Cancer Res, 2014. 20(23): p. 6127-40.

51. Saito, Y., et al., *Prognostic significance of CpG island methylator phenotype in surgically resected small cell lung carcinoma.* Cancer Sci, 2016. 107(3): p. 320-5.

52. Alvarado-Luna, G. and D. Morales-Espinosa, *Treatment for small cell lung cancer, where are we now?-a review.* Transl Lung Cancer Res, 2016. 5(1): p. 26-38.

53. Sabari, J.K., et al., *Unravelling the biology of SCLC: implications for therapy.* Nat Rev Clin Oncol, 2017. 14(9): p. 549-561.

54. Byers, L.A. and C.M. Rudin, *Small cell lung cancer: where do we go from here?* Cancer, 2015. 121(5): p. 664-72.

55. Koinis, F., A. Kotsakis, and V. Georgoulias, *Small cell lung cancer (SCLC): no treatment advances in recent years.* Transl Lung Cancer Res, 2016. 5(1): p. 39-50.

56. Arcaro, A., *Targeted therapies for small cell lung cancer: Where do we stand?* Crit Rev Oncol Hematol, 2015. 95(2): p. 154-64.

57. Liu, T.C., et al., *Role of epidermal growth factor receptor in lung cancer and targeted therapies.* Am J Cancer Res, 2017. 7(2): p. 187-202.

58. Montero, J. and A. Letai, *Why do BCL-2 inhibitors work and where should we use them in the clinic?* Cell Death Differ, 2017. 25(1): p. 56-64.

59. Pietanza, M.C. and C.M. Rudin, *Novel therapeutic approaches for small cell lung cancer: the future has arrived.* Curr Probl Cancer, 2012. 36(3): p. 156-73.

60. Karachaliou, N., et al., *Cellular and molecular biology of small cell lung cancer: an overview.* Transl Lung Cancer Res, 2016. 5(1): p. 2-15.

61. Seeber, A., et al., *What's new in small cell lung cancer - extensive disease? An overview on advances of systemic treatment in 2016.* Future Oncol, 2017. 13(16): p. 1427-1435.

62. Rudin, C.M., et al., *Rovalpituzumab tesirine, a DLL3-targeted antibody-drug conjugate, in recurrent small-cell lung cancer: a first-in-human, first-in-class, open-label, phase 1 study.* Lancet Oncol, 2017. 18(1): p. 42-51.

63. Tan, W.L., et al., *Novel therapeutic targets on the horizon for lung cancer.* Lancet Oncol, 2016. 17(8): p. e347-e362.

64. Dayem, A.A., et al., *Role of oxidative stress in stem, cancer, and cancer stem cells.* Cancers (Basel), 2010. 2(2): p. 859-84.

65. Zhang, J., et al., *ROS and ROS-Mediated Cellular Signaling.* Oxid Med Cell Longev, 2016. 2016: p. 4350965.

66. Pandey, P., et al., *The see-saw of Keap1-Nrf2 pathway in cancer.* Crit Rev Oncol Hematol, 2017. 116: p. 89-98.

67. Jaiswal, A.K., *Nrf2 signaling in coordinated activation of antioxidant gene expression.* Free Radic Biol Med, 2004. 36(10): p. 1199-207.

68. Kryston, T.B., et al., *Role of oxidative stress and DNA damage in human carcinogenesis.* Mutat Res, 2011. 711(1-2): p. 193-201.

69. Kaspar, J.W., S.K. Niture, and A.K. Jaiswal, *Nrf2:INrf2 (Keap1) signaling in oxidative stress.* Free Radic Biol Med, 2009. 47(9): p. 1304-9.

70. Guo, Y., et al., *Epigenetic regulation of Keap1-Nrf2 signaling.* Free Radic Biol Med, 2015. 88(Pt B): p. 337-349.

71. Zipper, L.M. and R.T. Mulcahy, *The Keap1 BTB/POZ dimerization function is required to sequester Nrf2 in cytoplasm.* J Biol Chem, 2002. 277(39): p. 36544-52.

72. Adams, J., R. Kelso, and L. Cooley, *The kelch repeat superfamily of proteins: propellers of cell function.* Trends Cell Biol, 2000. 10(1): p. 17-24.

73. Tong, K.I., et al., *Keap1 recruits Neh2 through binding to ETGE and DLG motifs: characterization of the two-site molecular recognition model.* Mol Cell Biol, 2006. 26(8): p. 2887-900.

74. Suzuki, T., H. Motohashi, and M. Yamamoto, *Toward clinical application of the Keap1-Nrf2 pathway.* Trends Pharmacol Sci, 2013. 34(6): p. 340-6.

75. Shen, G. and A.N. Kong, *Nrf2 plays an important role in coordinated regulation of Phase II drug metabolism enzymes and Phase III drug transporters.* Biopharm Drug Dispos, 2009. 30(7): p. 345-55.

76. Itoh, K., et al., *Keap1 represses nuclear activation of antioxidant responsive elements by Nrf2 through binding to the amino-terminal Neh2 domain.* Genes Dev, 1999. 13(1): p. 76-86.

77. Fabrizio, F.P., et al., *Epigenetic versus Genetic Deregulation of the KEAP1/NRF2 Axis in Solid Tumors: Focus on Methylation and Noncoding RNAs.* Oxid Med Cell Longev, 2018. 2018: p. 2492063.

78. Menegon, S., A. Columbano, and S. Giordano, *The Dual Roles of NRF2 in Cancer.* Trends Mol Med, 2016. 22(7): p. 578-593.

79. Kobayashi, A., et al., *Oxidative stress sensor Keap1 functions as an adaptor for Cul3-based E3 ligase to regulate proteasomal degradation of Nrf2.* Mol Cell Biol, 2004. 24(16): p. 7130-9.

80. Tong, K.I., et al., *Two-site substrate recognition model for the Keap1-Nrf2 system: a hinge and latch mechanism.* Biol Chem, 2006. 387(10-11): p. 1311-20.

81. Hayes, J.D. and M. McMahon, *NRF2 and KEAP1 mutations: permanent activation of an adaptive response in cancer.* Trends Biochem Sci, 2009. 34(4): p. 176-88.

82. Kobayashi, A., et al., *Oxidative and electrophilic stresses activate Nrf2 through inhibition of ubiquitination activity of Keap1.* Mol Cell Biol, 2006. 26(1): p. 221-9.

83. Sparaneo, A., F.P. Fabrizio, and L.A. Muscarella, *Nrf2 and Notch Signaling in Lung Cancer: Near the Crossroad.* Oxid Med Cell Longev, 2016. 2016: p. 7316492.

84. Rachakonda, G., et al., *Covalent modification at Cys151 dissociates the electrophile sensor Keap1 from the ubiquitin ligase CUL3.* Chem Res Toxicol, 2008. 21(3): p. 705-10.

85. Eggler, A.L., et al., *Cul3-mediated Nrf2 ubiquitination and antioxidant response element (ARE) activation are dependent on the partial molar volume at position 151 of Keap1.* Biochem J, 2009. 422(1): p. 171-80.

86. Zhang, D.D. and M. Hannink, *Distinct cysteine residues in Keap1 are required for Keap1-dependent ubiquitination of Nrf2 and for stabilization of Nrf2 by chemopreventive agents and oxidative stress.* Mol Cell Biol, 2003. 23(22): p. 8137-51.

87. Yamamoto, S., K.L. Schulze, and H.J. Bellen, *Introduction to Notch signaling.* Methods Mol Biol, 2014. 1187: p. 1-14.

88. Bertrand, F.E., et al., *Developmental pathways in colon cancer: crosstalk between WNT, BMP, Hedgehog and Notch.* Cell Cycle, 2012. 11(23): p. 4344-51.

89. Li, Y., et al., *Distinct expression profiles of Notch-1 protein in human solid tumors: Implications for development of targeted therapeutic monoclonal antibodies.* Biologics, 2010. 4: p. 163-71.

90. Baumgart, A., et al., *ADAM17 regulates epidermal growth factor receptor expression through the activation of Notch1 in non-small cell lung cancer.* Cancer Res, 2010. 70(13): p. 5368-78.

91. Yuan, X., et al., *Notch signaling: an emerging therapeutic target for cancer treatment.* Cancer Lett, 2015. 369(1): p. 20-7.

92. Di Cristofano, A. and P.P. Pandolfi, *The multiple roles of PTEN in tumor suppression.* Cell, 2000. 100(4): p. 387-90.

93. Chappell, W.H., et al., *Increased protein expression of the PTEN tumor suppressor in the presence of constitutively active Notch-1.* Cell Cycle, 2005. 4(10): p. 1389-95.

94. Palomero, T., et al., *Mutational loss of PTEN induces resistance to NOTCH1 inhibition in T-cell leukemia.* Nat Med, 2007. 13(10): p. 1203-10.

95. Donnem, T., et al., *Prognostic impact of Notch ligands and receptors in nonsmall cell lung cancer: coexpression of Notch-1 and vascular endothelial growth factor-A predicts poor survival.* Cancer, 2010. 116(24): p. 5676-85.

96. Yuan, X., et al., *Meta-analysis reveals the correlation of Notch signaling with non-small cell lung cancer progression and prognosis.* Sci Rep, 2015. 5: p. 10338.

97. Hassan, W.A., et al., *Notch1 controls cell chemoresistance in small cell lung carcinoma cells.* Thorac Cancer, 2016. 7(1): p. 123-8.

98. Hassan, W.A., et al., *Notch1 controls cell invasion and metastasis in small cell lung carcinoma cell lines.* Lung Cancer, 2014. 86(3): p. 304-10.

99. Gordon, W.R., K.L. Arnett, and S.C. Blacklow, *The molecular logic of Notch signaling--a structural and biochemical perspective.* J Cell Sci, 2008. 121(Pt 19): p. 3109-19.

100. Bozkulak, E.C. and G. Weinmaster, *Selective use of ADAM10 and ADAM17 in activation of Notch1 signaling.* Mol Cell Biol, 2009. 29(21): p. 5679-95.

101. Jin, Y.H., et al., *Beta-catenin modulates the level and transcriptional activity of Notch1/NICD through its direct interaction.* Biochim Biophys Acta, 2009. 1793(2): p. 290-9.

102. Blokzijl, A., et al., *Cross-talk between the Notch and TGF-beta signaling pathways mediated by interaction of the Notch intracellular domain with Smad3.* J Cell Biol, 2003. 163(4): p. 723-8.

103. Gustafsson, M.V., et al., *Hypoxia requires notch signaling to maintain the undifferentiated cell state.* Dev Cell, 2005. 9(5): p. 617-28.

104. Aster, J.C., W.S. Pear, and S.C. Blacklow, *The Varied Roles of Notch in Cancer.* Annu Rev Pathol, 2016. 12: p. 245-275.

105. Domenga, V., et al., *Notch3 is required for arterial identity and maturation of vascular smooth muscle cells.* Genes Dev, 2004. 18(22): p. 2730-5.

106. Hamada, Y., et al., *Mutation in ankyrin repeats of the mouse Notch2 gene induces early embryonic lethality.* Development, 1999. 126(15): p. 3415-24.

107. Krebs, L.T., et al., *Notch signaling is essential for vascular morphogenesis in mice.* Genes Dev, 2000. 14(11): p. 1343-52.

108. Ladi, E., et al., *The divergent DSL ligand Dll3 does not activate Notch signaling but cell autonomously attenuates signaling induced by other DSL ligands.* J Cell Biol, 2005. 170(6): p. 983-92.

109. Chorley, B.N., et al., *Identification of novel NRF2-regulated genes by ChIP-Seq: influence on retinoid X receptor alpha.* Nucleic Acids Res, 2012. 40(15): p. 7416-29.

110. Gorrini, C., I.S. Harris, and T.W. Mak, *Modulation of oxidative stress as an anticancer strategy.* Nat Rev Drug Discov, 2013. 12(12): p. 931-47.

111. Moinova, H.R. and R.T. Mulcahy, *Up-regulation of the human gamma-glutamylcysteine synthetase regulatory subunit gene involves binding of Nrf-2 to an electrophile responsive element.* Biochem Biophys Res Commun, 1999. 261(3): p. 661-8.

112. Chanas, S.A., et al., *Loss of the Nrf2 transcription factor causes a marked reduction in constitutive and inducible expression of the glutathione S-transferase Gsta1, Gsta2, Gstm1, Gstm2, Gstm3 and Gstm4 genes in the livers of male and female mice.* Biochem J, 2002. 365(Pt 2): p. 405-16.

113. Harvey, C.J., et al., *Nrf2-regulated glutathione recycling independent of biosynthesis is critical for cell survival during oxidative stress.* Free Radic Biol Med, 2009. 46(4): p. 443-53.

114. Hawkes, H.J., T.C. Karlenius, and K.F. Tonissen, *Regulation of the human thioredoxin gene promoter and its key substrates: a study of functional and putative regulatory elements.* Biochim Biophys Acta, 2014. 1840(1): p. 303-14.

115. Abbas, K., et al., *Nitric oxide activates an Nrf2/sulfiredoxin antioxidant pathway in macrophages.* Free Radic Biol Med, 2011. 51(1): p. 107-14.

116. Hayes, J.D. and A.T. Dinkova-Kostova, *The Nrf2 regulatory network provides an interface between redox and intermediary metabolism.* Trends Biochem Sci, 2014. 39(4): p. 199-218.

117. Lee, J.M., et al., *Identification of the NF-E2-related factor-2-dependent genes conferring protection against oxidative stress in primary cortical astrocytes using oligonucleotide microarray analysis.* J Biol Chem, 2003. 278(14): p. 12029-38.

118. Mitsuishi, Y., et al., *Nrf2 redirects glucose and glutamine into anabolic pathways in metabolic reprogramming.* Cancer Cell, 2012. 22(1): p. 66-79.

119. Alam, J., et al., *Nrf2, a Cap'n'Collar transcription factor, regulates induction of the heme oxygenase-1 gene.* J Biol Chem, 1999. 274(37): p. 26071-8.

120. Maher, J.M., et al., *Oxidative and electrophilic stress induces multidrug resistance-associated protein transporters via the nuclear factor-E2-related factor-2 transcriptional pathway.* Hepatology, 2007. 46(5): p. 1597-610.

121. Wakabayashi, N., D.V. Chartoumpekis, and T.W. Kensler, *Crosstalk between Nrf2 and Notch signaling.* Free Radic Biol Med, 2015. 88(Pt B): p. 158-167.

122. Schwanbeck, R., *The role of epigenetic mechanisms in Notch signaling during development.* J Cell Physiol, 2015. 230(5): p. 969-81.

123. Singh, A., et al., *Dysfunctional KEAP1-NRF2 interaction in non-small-cell lung cancer.* PLoS Med, 2006. 3(10): p. e420.

124. Lee, O.H., et al., *An auto-regulatory loop between stress sensors INrf2 and Nrf2 controls their cellular abundance.* J Biol Chem, 2007. 282(50): p. 36412-20.

125. Shibata, T., et al., *Cancer related mutations in NRF2 impair its recognition by Keap1-Cul3 E3 ligase and promote malignancy.* Proc Natl Acad Sci U S A, 2008. 105(36): p. 13568-73.

126. Ding, X.Y., et al., *Cross-talk between endothelial cells and tumor via delta-like ligand 4/Notch/PTEN signaling inhibits lung cancer growth.* Oncogene, 2012. 31(23): p. 2899-906.

127. Westhoff, B., et al., *Alterations of the Notch pathway in lung cancer.* Proc Natl Acad Sci U S A, 2009. 106(52): p. 22293-8.

128. Meder, L., et al., *NOTCH, ASCL1, p53 and RB alterations define an alternative pathway driving neuroendocrine and small cell lung carcinomas.* Int J Cancer, 2016. 138(4): p. 927-38.

129. Kunnimalaiyaan, M. and H. Chen, *Tumor suppressor role of Notch-1 signaling in neuroendocrine tumors.* Oncologist, 2007. 12(5): p. 535-42.

130. Ball, D.W., *Achaete-scute homolog-1 and Notch in lung neuroendocrine development and cancer.* Cancer Lett, 2004. 204(2): p. 159-69.

131. Misquitta-Ali, C.M., et al., *Global profiling and molecular characterization of alternative splicing events misregulated in lung cancer.* Mol Cell Biol, 2011. 31(1): p. 138-50.

132. Ji, X., et al., *Delta-tocotrienol suppresses Notch-1 pathway by upregulating miR-34a in nonsmall cell lung cancer cells.* Int J Cancer, 2012. 131(11): p. 2668-77.

133. Mitsuishi, Y., H. Motohashi, and M. Yamamoto, *The Keap1-Nrf2 system in cancers: stress response and anabolic metabolism.* Front Oncol, 2012. 2: p. 200.

134. Network, T.C.G.A.R., *Comprehensive genomic characterization of squamous cell lung cancers.* Nature, 2012. 489(7417): p. 519-25.

135. Solis, L.M., et al., *Nrf2 and Keap1 abnormalities in non-small cell lung carcinoma and association with clinicopathologic features.* Clin Cancer Res, 2010. 16(14): p. 3743-53.

136. Kim, Y., et al., *Integrative and comparative genomic analysis of lung squamous cell carcinomas in East Asian patients.* J Clin Oncol, 2014. 32(2): p. 121-8.

137. Li, Q.K., et al., *KEAP1 gene mutations and NRF2 activation are common in pulmonary papillary adenocarcinoma.* J Hum Genet, 2011. 56(3): p. 230-4.

138. Kaufman, J.M., et al., *LKB1 Loss induces characteristic patterns of gene expression in human tumors associated with NRF2 activation and attenuation of PI3K-AKT.* J Thorac Oncol, 2014. 9(6): p. 794-804.

139. Zhou, C., et al., *MicroRNA-144 modulates oxidative stress tolerance in SH-SY5Y cells by regulating nuclear factor erythroid 2-related factor 2-glutathione axis.* Neurosci Lett, 2016. 655: p. 21-27.

140. Yang, M., et al., *MiR-28 regulates Nrf2 expression through a Keap1-independent mechanism.* Breast Cancer Res Treat, 2011. 129(3): p. 983-91.

141. Singh, B., et al., *MicroRNA-93 regulates NRF2 expression and is associated with breast carcinogenesis.* Carcinogenesis, 2013. 34(5): p. 1165-72.

142. Murray-Stewart, T., et al., *Histone deacetylase inhibition overcomes drug resistance through a miRNA-dependent mechanism.* Mol Cancer Ther, 2013. 12(10): p. 2088-99.

143. Fernandez-Cuesta, L., et al., *Frequent mutations in chromatin-remodelling genes in pulmonary carcinoids.* Nat Commun, 2014. 5: p. 3518.

144. Copple, I.M., *The Keap1-Nrf2 cell defense pathway--a promising therapeutic target?* Adv Pharmacol, 2016. 63: p. 43-79.

145. Wang, R., et al., *Hypermethylation of the Keap1 gene in human lung cancer cell lines and lung cancer tissues.* Biochem Biophys Res Commun, 2008. 373(1): p. 151-4.

146. Muscarella, L.A., et al., *Frequent epigenetics inactivation of KEAP1 gene in non-small cell lung cancer.* Epigenetics, 2011. 6(6): p. 710-9.

147. Liu, X., et al., *Genistein mediates the selective radiosensitizing effect in NSCLC A549 cells via inhibiting methylation of the keap1 gene promoter region.* Oncotarget, 2016. 7(19): p. 27267-79.

148. Wu, Y., et al., *Therapeutic antibody targeting of individual Notch receptors.* Nature, 2010. 464(7291): p. 1052-7.

149. Messersmith, W.A., et al., *A Phase I, dose-finding study in patients with advanced solid malignancies of the oral gamma-secretase inhibitor PF-03084014.* Clin Cancer Res, 2015. 21(1): p. 60-7.

150. Yen, W.C., et al., *Targeting Notch signaling with a Notch2/Notch3 antagonist (tarextumab) inhibits tumor growth and decreases tumor-initiating cell frequency.* Clin Cancer Res, 2015. 21(9): p. 2084-95.

151. Pietanza, M.C., et al., *Small cell lung cancer: will recent progress lead to improved outcomes?* Clin Cancer Res, 2015. 21(10): p. 2244-55.

152. Pinchot, S.N., et al., *Identification and validation of Notch pathway activating compounds through a novel high-throughput screening method.* Cancer, 2011. 117(7): p. 1386-98.

153. Jaramillo, M.C. and D.D. Zhang, *The emerging role of the Nrf2-Keap1 signaling pathway in cancer.* Genes Dev, 2013. 27(20): p. 2179-91.

154. Wang, X.J., et al., *Identification of retinoic acid as an inhibitor of transcription factor Nrf2 through activation of retinoic acid receptor alpha.* Proc Natl Acad Sci U S A, 2007. 104(49): p. 19589-94.

155. Ki, S.H., et al., *Glucocorticoid receptor (GR)-associated SMRT binding to C/EBPbeta TAD and Nrf2 Neh4/5: role of SMRT recruited to GR in GSTA2 gene repression.* Mol Cell Biol, 2005. 25(10): p. 4150-65.

156. Hong, F., M.L. Freeman, and D.C. Liebler, *Identification of sensor cysteines in human Keap1 modified by the cancer chemopreventive agent sulforaphane.* Chem Res Toxicol, 2005. 18(12): p. 1917-26.

157. Kode, A., et al., *Resveratrol induces glutathione synthesis by activation of Nrf2 and protects against cigarette smoke-mediated oxidative stress in human lung epithelial cells.* Am J Physiol Lung Cell Mol Physiol, 2008. 294(3): p. L478-88.

158. Fabrizio, F.P., et al., *Keap1/Nrf2 pathway in kidney cancer: frequent methylation of KEAP1 gene promoter in clear renal cell carcinoma.* Oncotarget, 2017. 8(7): p. 11187-11198.

159. Muscarella, L.A., et al., *Regulation of KEAP1 expression by promoter methylation in malignant gliomas and association with patient's outcome.* Epigenetics, 2011. 6(3): p. 317-25.

160. Hande, K.R., *Etoposide: four decades of development of a topoisomerase II inhibitor.* Eur J Cancer, 1998. 34(10): p. 1514-21.

161. Dasari, S. and P.B. Tchounwou, *Cisplatin in cancer therapy: molecular mechanisms of action.* Eur J Pharmacol, 2013. 740: p. 364-78.

162. Payet, D., et al., *Instability of the monofunctional adducts in cis-[Pt(NH3)2(N7-N-methyl-2-diazapyrenium)Cl](2+)-modified DNA: rates of cross-linking reactions in cis-platinum-modified DNA.* Nucleic Acids Res, 1993. 21(25): p. 5846-51.

163. Yen, H.C., et al., *Enhancement of cisplatin-induced apoptosis and caspase 3 activation by depletion of mitochondrial DNA in a human osteosarcoma cell line.* Ann N Y Acad Sci, 2005. 1042: p. 516-22.

164. Purow, B., *Notch inhibition as a promising new approach to cancer therapy.* Adv Exp Med Biol, 2012. 727: p. 305-19.

165. Meurette, O., et al., *Notch activation induces Akt signaling via an autocrine loop to prevent apoptosis in breast epithelial cells.* Cancer Res, 2009. 69(12): p. 5015-22.

166. Cao, H., et al., *Down-regulation of Notch receptor signaling pathway induces caspase-dependent and caspase-independent apoptosis in lung squamous cell carcinoma cells.* Apmis, 2012 120(6): p. 441-50.

167. Siemers, E., et al., *Safety, tolerability, and changes in amyloid beta concentrations after administration of a gamma-secretase inhibitor in volunteers.* Clin Neuropharmacol, 2005. 28(3): p. 126-32.

168. Palomero, T., et al., *NOTCH1 directly regulates c-MYC and activates a feed-forward-loop transcriptional network promoting leukemic cell growth.* Proc Natl Acad Sci U S A, 2006. 103(48): p. 18261-6.

169. Saad, S., et al., *Notch mediated epithelial to mesenchymal transformation is associated with increased expression of the Snail transcription factor.* Int J Biochem Cell Biol, 2010. 42(7): p. 1115-22.

170. Jemal, A., et al., *Cancer statistics, 2010.* CA Cancer J Clin, 2010. 60(5): p. 277-300.

171. Mountzios, G., et al., *Histopathologic and genetic alterations as predictors of response to treatment and survival in lung cancer: a review of published data.* Crit Rev Oncol Hematol, 2010. 75(2): p. 94-109.

172. Moon, E.J. and A. Giaccia, *Dual roles of NRF2 in tumor prevention and progression: possible implications in cancer treatment.* Free Radic Biol Med, 2015. 79: p. 292-9.

173. George, J., et al., *Integrative genomic profiling of large-cell neuroendocrine carcinomas reveals distinct subtypes of high-grade neuroendocrine lung tumors.* Nat Commun, 2018. 9(1): p. 1048.

174. Rossi, A., *Rovalpituzumab tesirine and DLL3: a new challenge for small-cell lung cancer.* Lancet Oncol, 2017. 18(1): p. 3-5.

175. (NGM), N.G.M., *A genomics-based classification of human lung tumors.* Sci Transl Med, 2013 5(209): p. 209ra153.

176. Padmanabhan, B., et al., *Structural basis for defects of Keap1 activity provoked by its point mutations in lung cancer.* Mol Cell, 2006. 21(5): p. 689-700.

177. Guo, D., et al., *A possible gene silencing mechanism: hypermethylation of the Keap1 promoter abrogates binding of the transcription factor Sp1 in lung cancer cells.* Biochem Biophys Res Commun, 2012. 428(1): p. 80-5.

178. Tian, H., et al., *High expression of AKR1C1 is associated with proliferation and migration of small-cell lung cancer cells.* Lung Cancer (Auckl), 2016. 7: p. 53-61.

179. Suvorova, E.S., et al., *Cytoprotective Nrf2 pathway is induced in chronically txnrd 1-deficient hepatocytes.* PLoS One, 2009. 4(7): p. e6158.

180. Li, L., et al., *Nrf2/ARE pathway activation, HO-1 and NQO1 induction by polychlorinated biphenyl quinone is associated with reactive oxygen species and PI3K/AKT signaling.* Chem Biol Interact, 2014. 209: p. 56-67.

ACKNOWLEDGEMENTS

Eccomi giunto alla fine di questo ciclo di dottorato al termine del quale credo di essere maturato sia scientificamente che umanamente e di aver affrontato con coraggio e determinazione le sfide che mi si sono presentate. Vorrei dedicare queste poche righe a tutti coloro che, con ruoli diversi ma ugualmente importanti, hanno sempre creduto in me e sostenuto nelle scelte più giuste da compiere.

Vorrei, innanzitutto, ringraziare la persona che è stata per me di grande aiuto per la sua costante presenza, pazienza e disponibilità: la dott.ssa Muscarella. A lei va un grazie immenso per la fiducia da subito dimostrata nei miei confronti e per avermi sempre saputo consigliare e indirizzare ogni qualvolta ne avessi avuto bisogno. Ringrazio, inoltre, il Prof. Fazio per il suo prezioso contributo ed interesse che mi ha permesso di realizzare questo lavoro.

Vorrei ringraziare i miei genitori perché mi hanno permesso di diventare la persona che sono oggi, per avermi sempre insegnato i valori della vita, per aver creduto in me, lasciandomi libero nelle mie scelte ma sostenendomi e aiutandomi sempre. A mio fratello e mia sorella va il mio grazie perché mi siete rimasti accanto nonostante le distanze universitarie e lavorative, incoraggiandomi a fare sempre del mio meglio.

Un grazie speciale alla mia ragazza che rappresenta un punto certo della mia vita, per aver saputo infondermi fiducia ed essere riuscita ad incoraggiarmi nei momenti più difficili ma soprattutto essermi stato sempre accanto.

Ringrazio i miei zii, cugini e nonni, vicini e 'lontani', che ancora si commuovono quando dico loro che ho partecipato o presentato un lavoro scientifico ad un congresso prestigioso, cosa che mi rende orgoglioso!

Ringrazio tutti i colleghi del laboratorio: chi con una collaborazione costante, chi con consigli e suggerimenti, chi con parole di incoraggiamento. Siete stati di supporto per il raggiungimento di questo mio traguardo.

Un altro contributo importante è stata la presenza degli amici di sempre per l'apporto e l'immancabile sostegno in questi anni.

Vorrei che questi ringraziamenti siano un punto di arrivo da una parte, ma anche di inizio dall'altra, perché non si finisce mai di aggiornarsi ma soprattutto di crescere

sperando di poter raggiungere tante altre soddisfazioni e traguardi nella vita con tutti voi ancora al mio fianco.

Questo lavoro è stato svolto non solo con passione e dedizione, ma anche e soprattutto con determinazione e costanza.

Grazie ancora,

Federico